Stability analysis and controller design for a system with hysteresis

Ouyang, Ruiyue

Stability Analysis and Controller Design For a System with Hysteresis

Ruiyue Ouyang

The research reported in this thesis is part of the research program of the Dutch Institute of Systems and Control (DISC). The author has successfully completed the educational program of the Graduate School DISC.

RIJKSUNIVERSITEIT GRONINGEN

Stability Analysis and Controller Design For a System with Hysteresis

Proefschrift

ter verkrijging van het doctoraat in de
Wiskunde en Natuurwetenschappen
aan de Rijksuniversiteit Groningen
op gezag van de
Rector Magnificus, dr. E. Sterken,
in het openbaar te verdedigen op
Maandag 30 September 2013
om 14.30 uur

door

Ruiyue Ouyang

geboren op 3 February 1982
te Jiangyou, China

Promotor(s):	Prof. dr. B. Jayawardhana Prof. dr. ir. J.M.A.Scherpen
Beoordelingscommissie:	Prof. dr. K. Morris Prof. dr. A. Van der Schaft Prof. dr. S. Tarbouriech

ISBN: 978-90-367-6306-6

To my parents: Lijun Song and Anping Ouyang

To my family: Ling Ji and Emma

Contents

Acknowledgments

This thesis is the result of my four-year research work, which is completed at the University of Groningen. During the past four years, I had learned technical skills and worked around nice colleagues. The most important is that this experience offers me the opportunity to grow as a person, both professionally and personally. There are many people I want to thank for their support during the time I spent on my research, without their help and support I would never have made it.

First of all, I would like to thank my supervisor Bayu Jayawardhana. I feel grateful that he give me the opportunity to pursue a Ph.D. degree. I want to thank him for the guidance, freedom, support, patience and criticism that he gave me during my research. I also thank him for creating such a nice research environment, where he was always there for discussions whenever I needed. It would not have been possible to conduct the research that presented here without his help, suggestions and ideas. I am also grateful to Prof. dr. Jacquelien M. A. Scherpen. I want to thank her for the suggestions and comments which she gave me during every discussion we had. She always had great ideas or suggestions which helped me to broaden my mind and improve my thinking. I also thank her for the time she took to read my work, for her comments and suggestions.

I want to thank the members of my reading committee Professors Arjan J. van der Schaft, Kirsten Morris and Sophie Tarbouriech who took the time to review this thesis. Their constructive comments helped me to improve the quality of the manuscript.

Now, it is time to thank my dear colleagues of the Discrete Technology and Production Automation group (DTPA). I will start with Shuo Zhang, a very nice friend in Groningen, I want to thank him for all the fruitful discussions. I want to thank my office mate Marko Seslija, who always had great ideas, philosophies and of course nice coffee, for all his help in mathematical problems and LaTex. I would like to

thank Ewoud Vos for his help with the Dutch translation of the summary. I am thankful to the former and present members, Daniel A. Dirksz, Thomas Voss, Ming Cao, Hui Liu, Chen Wang, Mauricio Muñoz Arias, Fan Zhang, Weiguo Xia, JianLei Zhang, Robert Huisman, S. Rao, Gunn Larsen, Matin Jafarian, Desti Alkano, Herman Kuis, Tao Liu, Hétor Garcia de Marina Peinado, Frederika Fokkens and Prof. Claudio de Persis, for their help and good times.

Finally, I want to thank my husband, Ling, for his love, understanding and support. He never complained a word for this long distance relationship and always gave me full support. Furthermore, I want to thank my parents whose love and encouragement was of great help in finding the force to finish my research. Also, many thanks to my parents-in-law, for all their help of taking care of my daughter when I was in Groningen. I have no words to express my gratitude to them.

List of symbols

List of Figures

List of Tables

Chapter 1

Introduction

1.1 Introduction to Hysteresis

Hysteresis is a nonlinear phenomenon that is present in many physical systems, such as piezo-actuator, magneto-rheological damper, ferromagnetic material and friction-induced mechanical systems. Due to the properties of the hysteresis and the complexity of its mathematical modeling, the existence of hysteresis in physical systems will affect the performance and even the stability of the system. Therefore, a proper handling by a controller is needed for a system that contains hysteresis.

The term "hysteresis" comes originally from $\ddot{\upsilon}\sigma\tau\epsilon\rho\acute{\epsilon}\omega$, an ancient Greek word meaning "to lag behind". It was first coined by the physicist Ewing in 1885, to

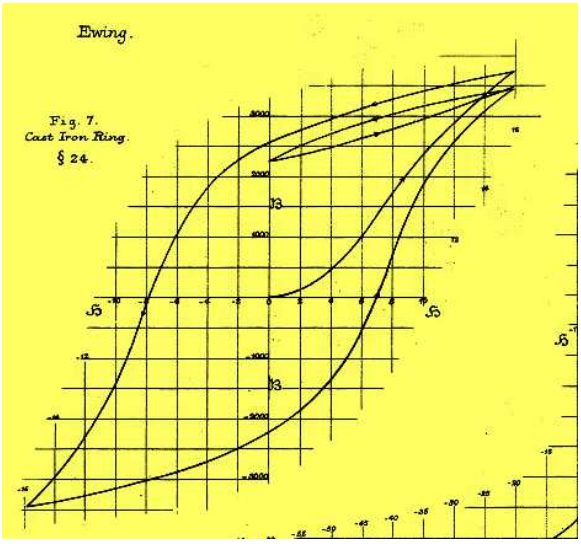

Figure 1.1: Magnetization of a cast-iron ring [11].

describe the changes of magnetism caused by gradual reversal and other cyclic changes of magnetising force [11], Figure 1.1 shows the magnetization curves of a cast-iron ring discovered by Ewing.

In [11], three important properties of hysteresis have been stated: lagging, memory and rate-independence, which are still regarded as the main characteristics of hysteresis.

> **Alfred Ewing (1885)** [11]: *When there are two quantities M and N, such that cyclic variations of N cause cyclic variation of M, then if the changes of M lag behind those of N, we may say that there is hysteresis in the relation of M and N. The value of M at any point of the operation depends not only on the actual value of N, but on all the preceding changes (and particularly on the immediately preceding changes) of N, and by properly manipulating those changes, any value of M within more or less wide limits may be found associated with a given value of N.*

The lagging property, the same as the meaning of the word "lagging", says that the output lags behind the input. The memory property of hysteresis means that the current output depends not only on the current input, but also on the history of the input. The rate-independence property means that the input-output map does not depend on the frequency of the input, but only on the amplitude of the input, i.e., the changes of the frequency in the input does not affect the phase plot from input to output.

In literature, there are a multitude of mathematical definitions of hysteresis. In [4], a hysteresis operator is defined as an operator which has the memory property and is rate-independent. In [35], hysteresis is defined as a nontrivial quasi-dc input-output closed curve, i.e. this nontrivial closed curve persists for an periodic input when the input frequency approaches zero. In [33], hysteresis is defined as a multi-branch nonlinearity generate by its input-output mapping and the branch-to-branch transitions occur after input extrema. The hysteresis operator used in this thesis will follow the definition given in [4], which has been used in many analysis for systems with hysteresis, see [31, 61].

Although the hysteresis phenomenon has been discovered in magnetism about 200 years ago, and later on in many physical systems, the first systematic mathematical modeling of hysteresis has been provided by the Russian scientist Krasnoselskii in 1970. After that, several hysteresis models have been proposed to describe hysteresis phenomenon in different systems, see, for example, [4], [32], [29], [3]. These includes: i). Prandtl operator and Preisach operator, which are normally called Preisach-type operator. This type of operator is constructed based on the superposition of individual relay operators; ii). the Duhem operator, the Dahl model,

the Coleman-Hodgdon model and the Bouc-Wen model, which are belong to the Duhem-type operator. This class operator is defined based on a discontinuous differential equation.

For the Preisach-type hysteresis operator, there are many results in literature that deal with the stability analysis and controller design. To name a few, I refer to the works by [13], [29], [33], [57] on the stability analysis involving these hysteresis operators. For the various control design, I refer to the works by [20], [19], [52].

In this thesis, I focus on the Duhem-type hysteresis operator which has not been studied extensively in the literature, despite the fact that they describe well the behavior of magnetic materials [25], friction [7] and piezo-electric materials [28]. Recent results on the Duhem operator in the control and systems literature are [35], [39] and [38], which focus on the semi-linear Duhem model and their properties, and [17] focus on the linear control for systems with Bouc-Wen model, which is a class of Duhem model.

1.2 Review of Related Work

There are a number of methodologies which have been proposed in literature to overcome or to compensate the effect of hysteresis in physical systems.

A well-known strategy is to use a feed-forward compensator, where an inverse hysteresis model is used to compensate for the hysteresis effect in the system such that the cascaded system (of the compensator and the hysteretic plant) becomes a linear system, where a linear controller can be designed to achieve the desired control objectives. For example, in [44], an inverse Preisach operator is used to compensate a hysteretic system; in [19], an inverse Prandtl model is used for hysteresis compensation in micro-positioning control; similarly, in [47], an inverse Preisach model is used to compensate hysteresis in piezoceramic actuator to achieve tracking control. However, these approaches have a major drawback since most of hysteresis models are not analytically invertible. As a result, approximate inverse hysteresis models are used [44, 12, 47] which introduce numerical errors and degrade the closed-loop feedback performance.

Another approach is to consider the hysteresis as an unknown nonlinearity with a certain structure so that an adaptive control law can be developed to guarantee the stability of the controlled system. These include, adaptive control design for compensating an unknown backlash-type hysteresis for systems with known plant [52]; an output feedback adaptive control scheme for a class of uncertain nonlinear system with unknown backlash-type hysteresis [63].

In the last approach, control design methods are proposed based on exploiting

specific "nice" properties of hysteresis, such as, monotonicity, sector-bound or dissipativity so that the use of inverse model can be avoided and a certain robustness against parameter uncertainties can be guaranteed. In [53, 54], the stability problem for a linear system with an backlash operator is solved by using generalized sector conditions of the backlash-type hysteresis and the stability conditions are given based on linear matrix inequalities (LMIs). In [14], the dissipativity of the Preisach operator is derived and a controller which is strictly passive is designed for the smart actuators.

In [29, 20], an integral/PID controller is proposed to control a linear system feedback interconnected to a hysteresis operator. In their approach, the Lipschitz condition of the hysteresis operator is used to derive a frequency-domain stability criteria for the closed-loop system.

In this thesis, I explore a natural input-output property of hysteresis as initially established by Ewing in 1885 [11]. When the output lags the input, the phase plot of the input and output signal undergoes a counter-clockwise behavior and this type of phenomena is called counterclockwise (CCW) input-output (I/O) behavior. For example, backlash model and Preisach model with positive weights generate CCW I/O behavior. On the other hand, when the output leads the input, the phase plot of the input and output signal undergoes a clockwise behavior and this type of phenomena is called clockwise (CW) input-output (I/O) behavior. For example, elastic-plastic model and Dahl model generate CW I/O behavior.

The CCW property of a dynamical system can also be interpreted by the classical passivity theory: the system is passive from the input to the time derivative of the output (instead of the output in the passivity theory), see in [1, 39]. Differs from the work by [14], i), this thesis is focused on the Duhem-type operator, where in [14] the Preisach-type operator is considered; ii), I provide the explicit representation of the storage function of the Duhem hysteresis operator, which can be considered as the Lyapunov function for stability analysis. iii). Using the CCW/CW properties, a new controller design methodology is proposed for stabilizing a linear system interconnected with a Duhem operator.

1.3 Contributions of this Thesis

The contributions appears in two main parts: 1. Dissipativity of the Duhem hysteresis operator and 2. Stability and control results for systems interconnected with Duhem hysteresis operator.

- I discussed the dissipativity property of counterclockwise Duhem operator. Sufficient conditions on the functions which define the Duhem operator are

given such that the Duhem operator has counterclockwise input-output dynamics. In particular, an explicit construction of the storage functions satisfying the counterclockwise dissipation inequality is given.
- See Chapter 4 and [22, 21].

- I investigated the dissipativity property of a certain class of Duhem hysteresis operators, which has clockwise (CW) input-output (I/O) behavior. In particular, I provide sufficient conditions on the Duhem operator such that it is CW and propose an explicit construction of the corresponding function satisfying dissipation inequality of CW systems.
  - See Chapter 4 and [36].

- I investigated the stability of positive and negative feedback interconnections between a linear system and a Duhem hysteresis operator. For solving this absolute stability problem, sufficient conditions are given based on the counterclockwise (CCW) or clockwise (CW) input-output property of each subsystem. Based on these results I introduce a control design methodology for stabilizing a linear plant with a hysteretic actuator or sensor.
  - See Chapter 5, Chapter 6 and [42, 37].

- I studied the robustness property of a second-order linear plant controlled by a proportional, integral and derivative (PID) controller with a hysteretic actuator. The hysteretic actuator is modeled by a Duhem model which exhibits: (i) clockwise (CW) input-output (I/O) dynamics (such as the Dahl model, LuGre model and Maxwell-Slip model, which describe hysteresis phenomena in mechanical friction); (ii) counter-clockwise(CCW) input-output (I/O) dynamics (such as the Jiles-Atherton model, the Coleman model, which describes the hysteresis phenomena in piezo-actuator). Based on our main result in Chapter 5, I provide sufficient conditions on the controller gains that depend on the plant parameters such that the origin of the plant and the state of the hysteresis is globally attractive. The robustness of the closed-loop system with respect to the measurement noise is also given, using the *integral* input-to-state stability (*i*ISS) concept.
  - See Chapter 6 and [43].

1.4 Organization of this Thesis

This thesis is organized in following manner. Chapter 2 provides some necessary theoretical backgrounds which are used throughout this thesis. Chapter 3 gives a

comprehensive introduction of the Duhem hysteresis operator: the general representation, the properties and the possible applications.

The dissipativity of the Duhem hysteresis operator is presented in Chapter 4, where I discussed the dissipativity property of the Duhem hysteresis operator in two categories: the Duhem hysteresis operator with CCW I/O behavior and the Duhem hysteresis operator with CW I/O behavior. Based on the dissipativity results, I investigated the absolute stability of a feedback interconnection between a linear system and a Duhem hysteresis operator in Chapter 5.

In Chapter 6, I proposed a controller design methodology for a linear system interconnected with a hysteretic actuator (sensor). As a special case, I studied the robustness property of a second-order linear plant controlled by a proportional, integral and derivative (PID) controller with a hysteretic actuator. To validate our approach, an experiment on the piezo-actuated stage is conducted and the detailed experimental results are also present. Finally the conclusion and future work are given in Chapter 7.

Chapter 2

Preliminaries

This chapter presents theoretical background which is used throughout this thesis. Firstly, the Lyapunov stability theory and *integral* input-to-state stability (*i*ISS) theory are provided, which will be used for the stability analysis results in Chapter 5 and for the controller design results in Chapter 6. Secondly, basic dissipativity theory is introduced in Section 2.2, which will be employed in Chapter 4. Furthermore, we give the definitions of the counter-clockwise and clockwise dynamics in Section 2.3, which are the basis of the main results in Chapter 4, 5 and 6. Finally, the definition of a hysteresis operator is given in Section 2.4.

A function $\alpha : \mathbb{R}_+ \to \mathbb{R}_+$ belongs to class $\mathcal{K}$ if it is continuous, strictly increasing and $\alpha(0) = 0$. A function α belongs to class $\mathcal{K}_\infty$ if $\alpha \in \mathcal{K}$ and $\lim_{s\to\infty} \alpha(s) = \infty$. A function $\beta : \mathbb{R}_+ \times \mathbb{R}_+ \to \mathbb{R}_+$ belongs to class $\mathcal{KL}$ if for each fixed $\varsigma \in \mathbb{R}_+$, $\beta(\cdot, \varsigma) \in \mathcal{K}$ and for each fixed $s \in \mathbb{R}_+$, $\beta(s, \cdot)$ is decreasing and $\lim_{\varsigma\to\infty} \beta(s, \varsigma) = 0$.

2.1 Basic Stability Theory

Consider an autonomous system

$$\dot{x} = f(x),\ x(0) = x_0, \tag{2.1}$$

where $f : \mathbb{R}^n \to \mathbb{R}^n$ is continuous. Suppose $x_e \in \mathbb{R}^n$ is an equilibrium point of (2.1), i.e. $f(x_e) = 0$.

Definition 2.1.1 *[46] The system* (2.1) *is*

1. ***stable at*** x_e*, if for each* $\epsilon > 0$*, there is* $\delta = \delta(\epsilon) > 0$ *such that* $\|x(0)\| < \delta \Rightarrow \|x(t)\| < \epsilon$*, for all* $t \geq 0$*.*

2. ***locally asymptotically stable at*** x_e ***(or*** x_e***-LAS)****, if it is stable and there exists a* $\delta > 0$ *such that, if* $\|x_0 - x_e\| < \delta$*, then* $\|x(t) - x_e\| = 0$*, as* $t \to \infty$*.*

3. ***globally asymptotically stable at*** x_e ***(or*** x_e***-GAS)****, if it is stable and for every* $x(t)$*, we have* $\|x(t) - x_e\| = 0$*, as* $t \to \infty$*.*

where $\|\cdot\|$ denotes the standard Euclidean norm.

Theorem 2.1.2 *(LaSalle)[46] Let $V : \mathbb{R}^n \to \mathbb{R}$ be a differentiable positive definite function $V(x) > 0$ for all $x \neq x_e$ such that on the compact set $\Omega_c = \{x \in \mathbb{R}^n : V(x) \leq c\}$ we have $\dot{V}(x) \leq 0$. Define $\mathcal{M} = \{x \in \Omega_c : \dot{V}(x) \leq 0\}$. Then the trajectory converges to the largest invariant set contained in $\mathcal{M}$ as $t \to \infty$.*

The concept of *integral* input-to-state stability is introduced for the stability analysis of nonautonomous nonlinear systems given a bounded-energy input signal in [49, 2]. It is an integral variant of the input-to-state stability (ISS) property and is closely related to the $\mathcal{L}^2$ stability of the nonlinear dynamical systems.

Consider a nonlinear system given by

$$\Sigma : \begin{cases} \dot{x} &= f(x,u) \\ y &= h(x,u), \end{cases} \tag{2.2}$$

where $h : \mathbb{R}^n \times \mathbb{R} \to \mathbb{R}^n$, $f : \mathbb{R}^n \times \mathbb{R} \to \mathbb{R}^n$ is continuous and locally Lipschitz on x for bounded u.

Definition 2.1.3 *[49] System* (2.2) *is integral input-to-state stable (iISS) if there exist functions $\alpha \in \mathcal{K}_\infty$, $\beta \in \mathcal{KL}$ and $\gamma \in \mathcal{K}$ such that, for every $x_0 \in \mathbb{R}^n$ and $u \in \mathcal{L}^\infty(\mathbb{R}^m)$, the unique maximal solution x is global and*

$$\alpha(\|x(t)\|) \leq \beta(\|x_0\|, t) + \int_0^t \gamma(\|u(s)\|)\mathrm{d}s \;\forall t \in \mathbb{R}_+, \tag{2.3}$$

where γ is referred to as iISS gain.

It is shown in [2] that system (2.2) is *integral* input-to-state stable (*i*ISS) if it is (a) 0-GAS and (b) dissipative with respect to supply rate $\sigma(u)$, where σ is class $\mathcal{K}$ function. The relation between the *i*ISS gain γ and the supply rate $\sigma(u)$ is then discussed in [23] and it is shown that for a class of dissipative systems, the supply rate $\sigma(u)$ is essentially the *i*ISS gain function.

In this thesis, a modified definition of the *i*ISS is used, which is called $\mathcal{A}$-*i*ISS. Compare to the standard *i*ISS, the solution x of the system converges to an invariant set $\mathcal{A}$ instead of the origin in the notion of $\mathcal{A}$-*i*ISS when a bounded-energy input signal is used. The definition of $\mathcal{A}$-*i*ISS is given as below.

Definition 2.1.4 *Consider the nonlinear system given in* (2.2)*. Let $\mathcal{A} \subset \mathbb{R}^n$ be a nonempty and closed set. It is said to be integral input-to-state stable with respect to $\mathcal{A}$ ($\mathcal{A}$-iISS) if*

there exist functions $\alpha \in \mathcal{K}_\infty$, $\beta \in \mathcal{KL}$ and $\gamma \in \mathcal{K}$ such that, for every $x_0 \in \mathbb{R}^n$ and $u \in L^\infty(\mathbb{R}^m)$, the unique maximal solution x is global and

$$\alpha(\|x(t)\|_{\mathcal{A}}) \leq \beta(\|x_0\|_{\mathcal{A}}, t) + \int_0^t \gamma(\|u(s)\|)\mathrm{d}s \quad \forall t \in \mathbb{R}_+, \tag{2.4}$$

where $\|\cdot\|_{\mathcal{A}}$ denotes the distance to the invariant set $\mathcal{A}$, γ is referred to as $\mathcal{A}$-iISS gain.

2.2 Dissipative System

The dissipativity theory introduced by Willems in [62] is a generalization of the concept of the passivity. The physical interpretation of dissipative system is that the stored energy in the system is less or equal to the total external supplied energy.

Consider the nonlinear system in (2.2) and let $s : (u, y) \to s(u, y)$ define the supply function.

Definition 2.2.1 *[59] The system Σ in* (2.2) *is said to be* dissipative *with respect to the supply rate s if there exists a function $S : \mathbb{R}^n \to \mathbb{R}_+$, called the* storage function, *such that for all $x_0 \in \mathbb{R}$, all $t_1 \geq t_0$ and all input signals u, the following dissipation inequality*

$$S(x(t_1)) \leq S(x(t_0)) + \int_{t_0}^{t_1} s(u(t), y(t))\mathrm{d}t \tag{2.5}$$

holds where $x(t_0) = x_0$, and $x(t_1)$ is the state of Σ at time t_1 resulting from initial condition x_0 and input function $u(\cdot)$. If (2.5) *holds with equality for all x_0, $t_1 \geq t_0$ and all $u(\cdot)$, then Σ is lossless with respect to s.*

The inequality (2.5) is called the *dissipation inequality*. The storage function associated with a dissipative dynamical system, is bounded from below by the *available* storage and from above by the *required* supply, as shown in the following theorems

Theorem 2.2.2 *[59] Consider the system* (2.2) *with supply rate function s. Then the system is dissipative with respect to s if and only if*

$$S_a(x) = \sup_{\substack{T \geq 0 \\ u(\cdot)}} -\int_0^T s(u(t), y(t))\mathrm{d}t, \ x(0) = x, \tag{2.6}$$

is finite for all $x \in \mathbb{R}^n$. Furthermore, if S_a is finite for all $x \in \mathbb{R}^n$ then S_a is a storage function, and all other possible storage function S satisfy

$$S_a(x) \leq S(x), \quad \forall x \in \mathbb{R}^n. \tag{2.7}$$

The quantity $S_a(x_0)$ can be interpreted as the maximal energy which can be extracted from the system (2.2) starting at initial condition x_0. The function S_a is called the *available storage*.

Theorem 2.2.3 *[59] Assume that the system* (2.2) *is reachable from $x^* \in \mathbb{R}$. Define the "required supply" from x^* by*

$$S_r(x) = \inf_{\substack{T\geq 0 \\ u(\cdot)}} \int_{-T}^{0} s(u(t), y(t))\mathrm{d}t,\ x(-T) = x^*, x(0) = x. \tag{2.8}$$

Then $S_r(x)$ satisfies the dissipation inequality (2.5)*. Furthermore, the system* (2.2) *is dissipative if and only if there exists $K > -\infty$ such that $S_r(x) \geq K$ for all $x \in \mathbb{R}^n$. Moreover, if S is a storage function for* (2.2)*, then*

$$S(x) \leq S_r(x) + S(x^*)\ \forall x \in \mathbb{R}^n,$$

and $S_r(x) + S(x^*)$ is itself a storage function.

The dissipativity theory is applied in Chapter 4, where we show the dissipativity of the Duhem-type operator by constructing an explicit storage function. The relations between the constructed storage function and the available/required storage function for hysteresis operator is also discussed.

2.3 Counter-clockwise and Clockwise Dynamics

In this section we give the definitions of the counter-clockwise (CCW) and clockwise (CW) dynamics, which are introduced by Angeli [1] and Padthe [39].

2.3.1 Counter-clockwise Dynamics

Consider an input-output pair (u, y) of a second-order linear system with a periodic input $u(t) \in \mathbb{R}$ and the corresponding output $y(t) \in \mathbb{R}$, as shown in Figure 2.1.

The arrows in the figure indicates that the output y lags the input u, i.e. the curves generated by the chosen input-output pair has a CCW orientation. The area $\mathbb{A}$ enclosed by the curve is given in yellow. To interpret this input-output behavior, let us recall the classical Green's theorem [50].

Theorem 2.3.1 *Let $\mathcal{C}$ be a positive oriented, piecewise-smooth, simple curve in the plane and let $\mathbf{R}$ be the region enclosed by $\mathcal{C}$. If $M(u, y)$ and $N(u, y)$ have continuous partial derivatives on an open region that contains $\mathbf{R}$ with $u, y \in \mathbb{R}$, then*

$$\int_{\mathcal{C}} M\mathrm{d}y + N\mathrm{d}u = \int\int_{\mathbf{R}} \frac{\mathrm{d}N}{\mathrm{d}y} - \frac{\mathrm{d}M}{\mathrm{d}u}\mathrm{d}\mathbb{A}, \tag{2.9}$$

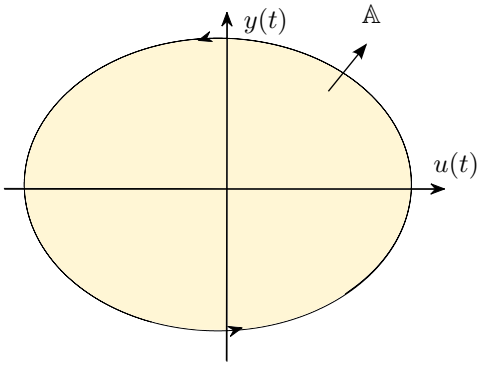

Figure 2.1: A graphical illustration of counter-clockwise (CCW) input-output behavior from a pair of (u, y).

where the left hand side is a line integral along the closed curve $\mathcal{C}$ and the right hand side is a surface integral over the enclosed region $\mathbf{R}$.

In the Green's theorem, the positive orientation of $\mathcal{C}$ indicates the counterclockwise traversal. The signed area $\mathbb{A}$ is positive when the closed curve $\mathcal{C}$ has counterclockwise orientation. The definition of the signed area $\mathbb{A}$ is given as follows

Definition 2.3.2 *[39] Consider a closed curve $\mathcal{C}$, then the signed area $\mathbb{A}$ enclosed by $\mathcal{C}$ is given by* $\mathbb{A} = \frac{1}{2}\int_{\mathcal{C}} u\mathrm{d}y - y\mathrm{d}u$

Now let us consider the second-order linear system given in Figure 2.1 and denote $\mathcal{C}$ the closed-curve given by (u, y). Let the input signal u be a continuous differentiable periodic signal such that for the time period $[0, T], T > 0$, $u(0) = u(T)$, the input signal u has exactly one local minimum and one local maximum. Now calculating the signal area $\mathbb{A}$, we arrive at

$$\mathbb{A} = \frac{1}{2}\int_0^T \dot{y}(t)u(t) - \dot{u}(t)y(t)\mathrm{d}t = \int_0^T \dot{y}(t)u(t)\mathrm{d}t - \frac{1}{2}u(T)y(T) + \frac{1}{2}u(0)y(0). \quad (2.10)$$

Since the input is periodic signal with period T, $u(0) = u(T)$ and $y(0) = y(T)$, thus equation (2.10) leads to the following counterclockwise dissipation inequality

$$\int_0^T \dot{y}(t)u(t)dt \geq 0. \quad (2.11)$$

Note that in the Green's theorem, it is assumed to have a simple closed curve. For the cases when the closed curves are not simple, the enclosed area is the summation of integrals evaluated over each simple closed curve.

Based on the Green's theorem and Definition 2.3.2, the definition of the CCW dynamics for any bounded input and output can be given as follows

Definition 2.3.3 *[1], [39] A (nonlinear) operator $G : AC(\mathbb{R}_+) \to AC(\mathbb{R}_+)$ is counter-clockwise (CCW) if for every $u \in AC(\mathbb{R}_+)$ with the corresponding output map $y := Gu$, the following inequality holds*

$$\liminf_{T\to\infty} \int_0^T \dot{y}(t)u(t)dt > -\infty. \tag{2.12}$$

For an operator G, inequality (2.12) holds if there exists a function $V_G : \mathbb{R}^2 \to \mathbb{R}_+$ such that for every input signal u, the inequality $\frac{\mathrm{d}V_G(y(t),u(t))}{\mathrm{d}t} \leq \dot{y}(t)u(t)$, holds for almost every t where the output signal $y := Gu$. Note that, this definition can be interpreted by the classical passivity theory in the way that if the system is passive from the input to the derivative of the output (instead of the output as in the classical passivity theory), then the system is CCW.

Definition 2.3.4 *A (nonlinear) operator $G : AC(\mathbb{R}_+) \to AC(\mathbb{R}_+)$ is strictly counter-clockwise (S-CCW) (see also [1]), if for every input $u \in AC(\mathbb{R}_+)$, there exists a constant $\varepsilon > 0$ such that the inequality*

$$\liminf_{T\to\infty} \int_0^T \dot{y}(t)u(t) - \varepsilon|\dot{y}(t)|^2\mathrm{d}t > -\infty, \tag{2.13}$$

holds where $y := Gu$.

Note that for systems described by the state space representation as follows:

$$\Sigma : \begin{cases} \dot{x} &= f(x,u), \qquad x(0) = x_0 \\ y &= h(x), \end{cases} \tag{2.14}$$

where $x(t) \in \mathbb{R}^n$ is the state, $u(t) \in \mathbb{R}$ is the input, $y(t) \in \mathbb{R}$ is the output and f, h are sufficiently smooth functions, the following lemma provides sufficient conditions for Σ to be CCW (and S-CCW).

Lemma 2.3.5 *Consider the state space system in* (2.14)*. If there exists a differentiable function $V_G : \mathbb{R}^n \to \mathbb{R}_+$ and $\varepsilon \geq 0$, such that*

$$\frac{\partial V_G(x)}{\partial x} f(x,u) \leq \frac{\partial h(x)}{\partial x} f(x,u)u - \varepsilon \left| \frac{\partial h(x)}{\partial x} f(x,u) \right|^2, \tag{2.15}$$

holds for all $x \in \mathbb{R}^n$ and $u \in \mathbb{R}$, then (2.14) *is CCW. Moreover if $\varepsilon > 0$, it is S-CCW.*

Proof: Taking integrals of both sides of (2.15) from 0 to $T > 0$, then

$$\int_0^T \frac{\partial V_G(x)}{\partial x} f(x,u)\mathrm{d}t \leq \int_0^T \frac{\partial h(x)}{\partial x} f(x,u)u - \varepsilon \left| \frac{\partial h(x)}{\partial x} f(x,u) \right|^2 \mathrm{d}t,$$

Since $V_G(x(T)) \geq 0$, we obtain

$$\int_0^T \frac{\partial h(x)}{\partial x} f(x,u)u - \varepsilon \left| \frac{\partial h(x)}{\partial x} f(x,u) \right|^2 \mathrm{d}t \geq V_G(x(0)) \geq -\infty,$$

which leads to (2.12). □

We would like to remark that the definitions of the CCW dynamics and CW dynamics are for both the nonlinear system and the linear system. In case of linear systems the concept CCW dynamics is equivalent to the concept of negative imaginary systems as given in [40, 48]. This equivalency has been shown in [39] and [60]. The definition of the CCW dynamics can be related to the classical dissipativity theory as in [62]. In this case the system is dissipative with respect to the supply-rate function $\dot{y}(t)u(t)$, which is a particular class of general supply-rate functions as discussed in [56].

2.3.2 Clockwise Dynamics

Dual to the concept of counterclockwise I/O dynamics, the clockwise I/O dynamics can be defined by a clockwise dissipation inequality which is dual to that for counterclockwise systems. Consider an input-output pair (u, y) of a second-order linear system with a periodic input $u(t) \in \mathbb{R}$ and the corresponding output $y(t) \in \mathbb{R}$, as shown in Figure 2.2.

The arrows in the figure indicates that the output y leads the input u, i.e. the curves generated by the chosen input-output pair has CW orientation. The area $\mathbb{A}$ enclosed by the curve is given in yellow. Applying the Green's theorem 2.3.1, the clockwise traversal corresponds to the negative orientation of $\mathcal{C}$ and the signed area A is negative when the closed curve $\mathcal{C}$ has clockwise orientation. The CW I/O dynamics can then be defined as follows.

Definition 2.3.6 *[39] A (nonlinear) operator $G : AC(\mathbb{R}_+) \to AC(\mathbb{R}_+)$ is clockwise (CW) if for every input $u \in AC(\mathbb{R}_+)$ with the corresponding output map $y := Gu$, the following inequality holds:*

$$\liminf_{T\to\infty} \int_0^T y(t)\dot{u}(t)\mathrm{d}t > -\infty. \tag{2.16}$$

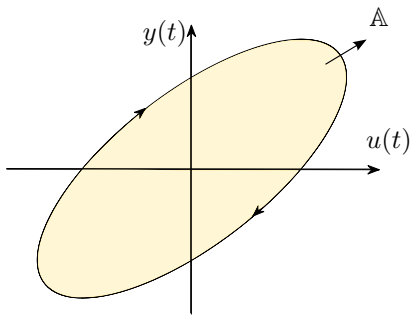

Figure 2.2: A graphical illustration of clockwise (CW) input-output behavior from a pair of (u, y).

For a nonlinear operator G, inequality (2.16) holds if there exists a C^1 function $V_G : \mathbb{R}^2 \to \mathbb{R}_+$ such that for every input signal $u \in AC(\mathbb{R}_+)$, the inequality $\frac{\mathrm{d}V_G(y(t),u(t))}{\mathrm{d}t} \leq y(t)\dot{u}(t)$, holds for a.e. t where the output signal $y := Gu$.

Lemma 2.3.7 *Consider the state space system as*

$$\begin{cases} \dot{x} &= f(x,u), \qquad x(0) = x_0 \\ y &= h(x,u), \end{cases} \tag{2.17}$$

If there exist $\theta : \mathbb{R}^{n+1} \to \mathbb{R}_+$, a differentiable function $V_G : \mathbb{R}^{n+1} \to \mathbb{R}_+$ such that V_G is positive definite and proper (radially unbounded), and

$$\begin{bmatrix} \frac{\partial V_G(u,x)}{\partial u} & \frac{\partial V_G(u,x)}{\partial x} \end{bmatrix} \begin{bmatrix} v_i \\ f(x,u) \end{bmatrix} \leq h(x,u)v_i - \theta(u,x), \tag{2.18}$$

holds for all $x \in \mathbb{R}^n$, $u \in \mathbb{R}$ and $v_i \in \mathbb{R}$, then (2.17) *is CW.*

Proof: Define the extended state space system (2.17) as follows

$$\begin{aligned} \dot{u} &= v_i, \\ \dot{x} &= f(x,u), \\ y &= h(x,u). \end{aligned} \tag{2.19}$$

It follows from (2.18) and (2.19) that $\dot{V}_G \leq h(x,u)v_i - \theta(x,u) = y\dot{u} - \theta(x,u)$. Integrating $\dot{V}_G$ from 0 to $T > 0$ and by using $v_i = \dot{u}$, we obtain (2.16). □

2.4 Hysteresis Operator

In this section, the definition of the hysteresis operator is based on the work in [4]. This definition has been used in many analysis for hysteresis systems (see for example, [31], [61]) and provide a general mathematical definition for hysteresis operator.

Definition 2.4.1 *[4] A function $\varphi : \mathbb{R}_+ \to \mathbb{R}_+$ is called a time transformation if $\varphi(t)$ is continuous, increasing and satisfies $\varphi(0) = 0$ and $\lim_{t\to\infty} \varphi(t) = \infty$.*

Definition 2.4.2 *[4] An operator $\Phi : C(\mathbb{R}_+) \to C(\mathbb{R}_+)$ is called rate independent if*

$$(\Phi(\nu \circ \varphi))(t) = \Phi(\nu) \circ \varphi(t),$$

holds for all $\nu \in C(\mathbb{R}_+)$, $t \in \mathbb{R}_+$ and all admissible time transformations.

Generally speaking, rate independent means that the hysteresis loops are determined only by the past extremum values of input, while the speed of the variations of input between the extremum points does not affect the hysteresis loops. As illustrated in Figure 2.3, two different inputs $u_1(t)$ and $u_2(t)$ which have the same extremum points but at different time scale, and the variation between the extremum points are also different. However, for a rate independent operator, these two inputs will result in the same input-output map.

Definition 2.4.3 *[4] An operator $\Phi : C(\mathbb{R}_+) \to C(\mathbb{R}_+)$ is said to be causal if for all $\tau > 0$ and all $\nu_1, \nu_2 \in C(\mathbb{R}_+)$, $\nu_1 = \nu_2$ on $[0, \tau]$ implies $\Phi(\nu_1) = \Phi(\nu_2)$ on $[0, \tau]$.*

Based on the definition of rate-independent and causality, we give the definition of the hysteresis operator which is used in the rest of this thesis.

Definition 2.4.4 *[4] An operator $\Phi : C(\mathbb{R}_+) \to C(\mathbb{R}_+)$ is called an hysteresis operator if it is causal and rate-independent.*

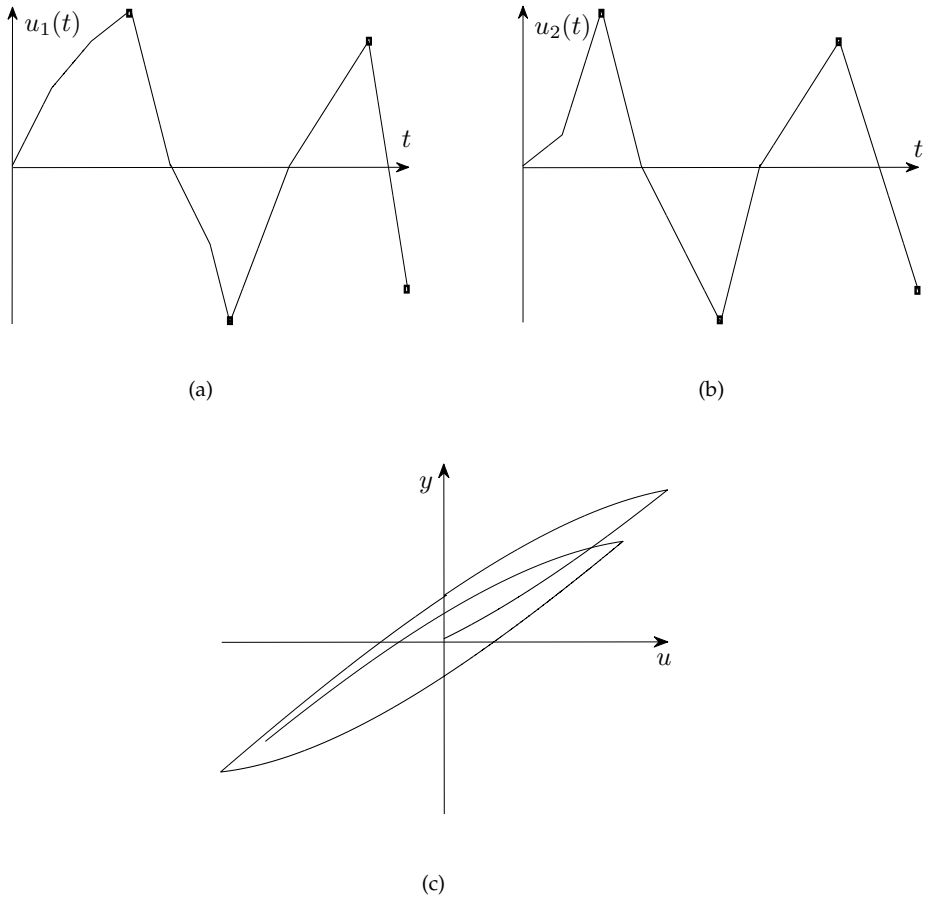

(a) (b)

(c)

Figure 2.3: Graphical illustration of rate independency.

Chapter 3

Duhem Hysteresis Operator and Its Applications

In this chapter, a comprehensive introduction of the Duhem hysteresis operator is given, in which we introduce the general representation of Duhem operator, the properties and the possible applications of the Duhem hysteresis operator. To show the possible applications of the Duhem hysteresis operator, we investigate several standard hysteresis models which are used in several applications, such as: gear train, electro-magnetic applications, elastic-plastic element and mechanical friction. These hysteresis models are studied in two categories:with saturated output (the input-output pair of the hysteresis operator exists only in a subset of $\mathbb{R}^2$) and with unsaturated output (the input-output pair of the hysteresis operator exists in the whole $\mathbb{R}^2$). We show that the hysteresis models present in both categories are all Duhem-type hysteresis, i.e. they can be recasted into the Duhem framework.

3.1 Definition of The Duhem Hysteresis Operator

The Duhem operator $\Phi : AC(\mathbb{R}_+) \times \mathbb{R} \to AC(\mathbb{R}_+), (u_\Phi, y_{\Phi_0}) \mapsto \Phi(u_\Phi, y_{\Phi_0}) =: y_\Phi$ is described by

$$\dot{y}_\Phi(t) = f_1(y_\Phi(t), u_\Phi(t))\dot{u}_{\Phi+}(t) + f_2(y_\Phi(t), u_\Phi(t))\dot{u}_{\Phi-}(t),\ y_\Phi(0) = y_{\Phi_0}, \qquad (3.1)$$

where $\dot{u}_{\Phi+}(t) := \max\{0, \dot{u}_\Phi(t)\}$, $\dot{u}_{\Phi-}(t) := \min\{0, \dot{u}_\Phi(t)\}$ and $f_1, f_2 : \mathbb{R}^2 \to \mathbb{R}$. Note that the Duhem operator defines a dynamical system and the differential equation (3.1) can also be put into a state-space form where the state consists of both variables u_Φ, y_Φ and the control input is $\dot{u}_\Phi$.

In this thesis, the signal (y_Φ, u_Φ) is often involved in scalar calculations at arbitrary time. Hence, for notational clarity, $\gamma \in \mathbb{R}$ is used to denote $y_\Phi(t_c)$ for arbitrary time $t_c \in \mathbb{R}_+$ and $\upsilon \in \mathbb{R}$ is used to denote $u_\Phi(t_c)$ for some time instance $t_c \in \mathbb{R}_+$ in the rest of this thesis.

The Duhem hysteresis operator as defined in (3.1) has the following properties:

- **Existence of solution**[32]
  The existence of solutions to (3.1) has been reviewed in [32]. In particular, if for every $\upsilon \in \mathbb{R}$, the functions f_1, f_2 are C^1 and satisfy

$$\begin{aligned}(\gamma_1 - \gamma_2)[f_1(\gamma_1, \upsilon) - f_1(\gamma_2, \upsilon)] &\leq \lambda_1(\upsilon)(\gamma_1 - \gamma_2)^2, \\ (\gamma_1 - \gamma_2)[f_2(\gamma_1, \upsilon) - f_2(\gamma_2, \upsilon)] &\geq -\lambda_2(\upsilon)(\gamma_1 - \gamma_2)^2,\end{aligned} \tag{3.2}$$

  for all γ_1, $\gamma_2 \in \mathbb{R}$, where λ_1 and λ_2 are nonnegative, then (3.1) has a unique global solution.

- **Monotonicity**[61]
  If $f_1, f_2 \geq 0$, then the Duhem operator Φ given in (3.1) is piecewise monotone, i.e. for every $u_\Phi \in AC(\mathbb{R}_+)$, the inequality $\dot{y}_\Phi \dot{u}_\Phi \geq 0$ holds a.e. $t \in \mathbb{R}_+$.

- **Rate-independent**[35, 61]
  The rate-independency property of the Duhem operator given in (3.1) can be interpreted as follows, let $\tau : [0, \infty) \to [0, \infty)$ be a continuous nondecreasing function satisfying $\tau(0) = 0$ and $\lim_{t\to\infty} \tau(t) = \infty$, i.e. τ is the time transformation, then $\Phi(u_\Phi \circ \tau, y_{\Phi_0}) = \Phi(u_\Phi, y_{\Phi_0}) \circ \tau$. In other words, for any periodic input u_Φ, the I/O relation does not depends on the input frequency.

- **Causality**[61]
  Let $T > 0$, the causality of the Duhem operator in (3.1) can be interpreted as

$$u_{\Phi_1}|_{[0,t]} = u_{\Phi_2}|_{[0,t]} \Rightarrow \Phi(u_{\Phi_1}, y_{\Phi_0})(t) = \Phi(u_{\Phi_2}, y_{\Phi_0})(t), \forall t \in [0, T]. \tag{3.3}$$

From the rate-independency and causality property given above, it can be seen that the Duhem operator is a hysteresis operator as defined in Chapter 2. Although this thesis focuses on the rate-independent Duhem hysteresis operator, we would like remark that the Duhem hysteresis operator in (3.1) can also represent rate-dependent hysteresis: i) by using the generalized form as given in [35], i.e.

$$\dot{y}_\Phi(t) = f_1(y_\Phi(t), u_\Phi(t))g(\dot{u}_{\Phi_+}(t)) + f_2(y_\Phi(t), u_\Phi(t))g(\dot{u}_{\Phi_-}(t)),\ y_\Phi(0) = y_{\Phi_0}, \tag{3.4}$$

where g is a non-positive homogeneous function; ii) let the functions $f_1, f_2 : \mathbb{R}^2 \times \mathbb{R}_+ \to \mathbb{R}$ be time varying as follows

$$\dot{y}_\Phi(t) = f_1(y_\Phi(t), u_\Phi(t), t)\dot{u}_{\Phi+}(t) + f_2(y_\Phi(t), u_\Phi(t), t)\dot{u}_{\Phi-}(t),\ y_\Phi(0) = y_{\Phi_0}. \tag{3.5}$$

3.2 Duhem Hysteresis Operator with Unsaturated Output

In this section we introduce several standard hysteresis models with unsaturated output. Here by unsaturated output we mean that the range of the hysteresis operator is equal to $\mathbb{R}$.

3.2.1 The Backlash Operator

The backlash (or play) operator is widely used for mechanical models, for example, for models of gear trains or of hydraulic servo-valves. The mathematical analysis of the backlash operator can be found in [4, 33].

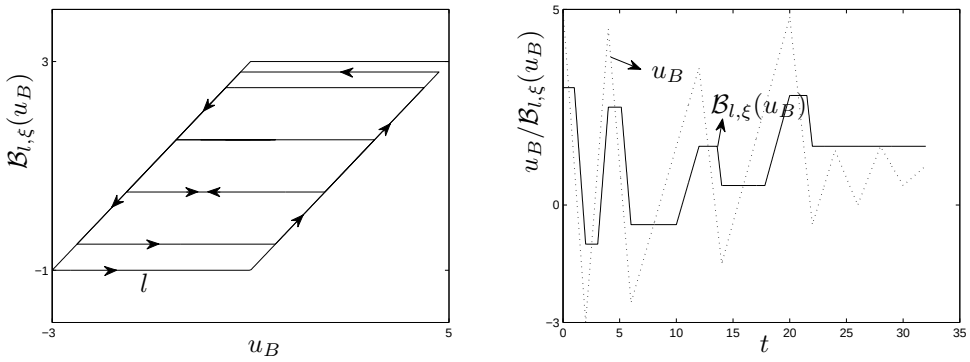

Figure 3.1: Backlash operator $\mathcal{B}_{l,\xi}$ ($l = 2$, $\xi = 3$)

For each $l \in \mathbb{R}_+$, the function $b_l : \mathbb{R}^2 \to \mathbb{R}$ is defined by

$$b_l(\gamma, \upsilon) := \max\{\upsilon - l, \min\{\upsilon + l, \gamma\}\}.$$

For all $\xi \in \mathbb{R}$, we introduce a backlash operator $\mathcal{B}_{l,\xi}$ defined on the space $C_{\mathrm{pm}}(\mathbb{R}_+)$ of piecewise monotone functions, by defining, for every $u_{\mathcal{B}} \in C_{\mathrm{pm}}(\mathbb{R}_+)$,

$$\left.\begin{aligned} &(\mathcal{B}_{l,\xi}(u_{\mathcal{B}}))(0) := b_l(u_{\mathcal{B}}(0), \xi) \\ &(\mathcal{B}_{l,\xi}(u_{\mathcal{B}}))(t) := b_l(u_{\mathcal{B}}(t), (\mathcal{B}_{l,\xi}(u_{\mathcal{B}}))(t_i)) \quad t \in (t_{i-1}, t_i],\ i \in \mathbb{N} \end{aligned}\right\} \tag{3.6}$$

where ξ is the initial condition, l is the width of the backlash operator and $0 = t_0 < t_1 < t_2 < \dots$ is a partition of $\mathbb{R}_+$, such that u is monotone on each of the intervals $[t_{i-1}, t_i]$, $i \in \mathbb{N}$. It is well known, see, for example, [4, page 42], that the operator $\mathcal{B}_{l,\xi} : C_{\text{pm}}(\mathbb{R}_+) \to C(\mathbb{R}_+)$ can be extended uniquely to an operator $\mathcal{B}_{l,\xi} : C(\mathbb{R}_+) \to C(\mathbb{R}_+)$. The action of a backlash operator is illustrated in Figure 3.1.

The backlash operator $\mathcal{B}_{l,\xi} : C^1(\mathbb{R}_+) \to C^1(\mathbb{R}_+)$ can be defined by the Duhem hysteresis operator (3.1). Let $\Phi_{l,\xi}$ denote $\mathcal{B}_{l,\xi}$ and u_Φ denote $u_\mathcal{B}$, then the f_1, f_2 functions as defined in (3.1) can be given as follows

$$f_1(\gamma, \upsilon) = \begin{cases} 1 & \text{if } \gamma = \upsilon - l \\ 0 & \text{elsewhere,} \end{cases} \tag{3.7}$$

$$f_2(\gamma, \upsilon) = \begin{cases} 1 & \text{if } \gamma = \upsilon + l \\ 0 & \text{elsewhere,} \end{cases} \tag{3.8}$$

and with $y_{\Phi_0} = \max\{u_\Phi(0) - l, \min\{u_\Phi(0) + l, \xi\}\}$.

The Duhem description of a backlash operator can be easily extended to a generalized backlash operator. For instance, the generalized backlash operator $\Phi_{\mu_1,\mu_2,l,\xi} : C^1(\mathbb{R}_+) \to C^1(\mathbb{R}_+)$ with $\mu_1 > \mu_2 \geq 0$, $l > 0$, then the backlash operator can be defined by (3.1) where

$$f_1(\gamma, \upsilon) = \begin{cases} \mu_1 & \text{if } \gamma = \mu_1(\upsilon - l) \\ \mu_2 & \text{elsewhere,} \end{cases} \tag{3.9}$$

$$f_2(\gamma, \upsilon) = \begin{cases} \mu_1 & \text{if } \gamma = \mu_1(\upsilon + l) \\ \mu_2 & \text{elsewhere,} \end{cases} \tag{3.10}$$

and y_{Φ_0} is defined properly inside the hysteresis domain, i.e. $\mu_1(u_{\Phi_0} - l) \leq y_{\Phi_0} \leq \mu_1(u_{\Phi_0} + l)$.

3.2.2 The Coleman-Hodgdon Model

The hysteresis model proposed by Coleman and Hodgdon [6, 58] is commonly used to represent hysteresis in ferromagnetic materials inside a magnetic field. It exhibits saturated hysteresis loops and nested loops. In its original form as in [6], the model is given by

$$\dot{y}_\Phi(t) = C_\alpha |\dot{u}_\Phi(t)| [f(u_\Phi(t)) - y_\Phi(t)] + \dot{u}_\Phi(t) g(u_\Phi(t)), \qquad y_\Phi(0) = y_{\Phi_0}, \tag{3.11}$$

where u_Φ denotes the magnetic field, y_Φ denotes the magnetic flux, C_α is a positive constant, $f : \mathbb{R} \to \mathbb{R}$ is a monotone increasing and locally Lipschitz function, such that $f(0) = 0$ and g is a locally Lipschitz function. The Coleman-Hodgdon model in

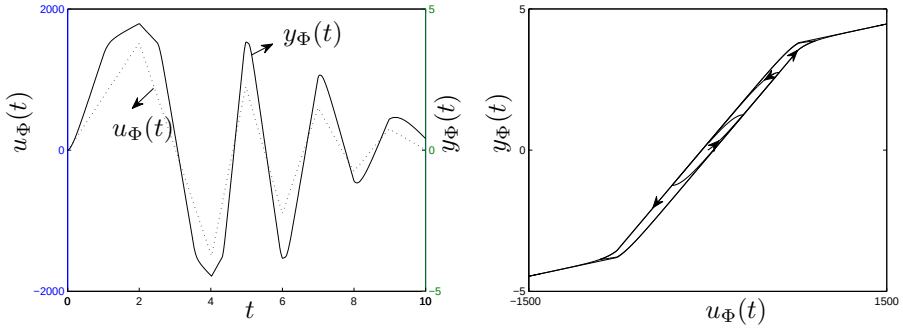

(a) (b)

Figure 3.2: Behaviour of the Coleman-Hodgdon model using f and g as in (3.11) with $C_\alpha = 0.1$, $C_b = 5 \times 10^{-3}$, $C_a = 9 \times 10^{-4}$, $u_s = 760$ and $y_{\Phi_0} = 0$.

(3.11) can be rewritten into the form of (3.1) where

$$\begin{cases} f_1(\gamma, \upsilon) &= C_\alpha[f(\upsilon) - \gamma] + g(\upsilon) \\ f_2(\gamma, \upsilon) &= -C_\alpha[f(\upsilon) - \gamma] + g(\upsilon). \end{cases} \tag{3.12}$$

Figure 3.2 shows the behaviour of the Coleman-Hodgdon model using the functions f and g proposed in [6], i.e.

$$f(\upsilon) = \begin{cases} C_a[\upsilon + u_s] - C_b u_s, & \text{if } \upsilon < -u_s, \\ C_b \upsilon, & \text{if } u_s \leq \upsilon \leq u_s, \\ C_a[\upsilon - u_s] + C_b u_s, & \text{if } \upsilon > u_s, \end{cases}$$

and

$$g(\upsilon) = C_a,$$

where u_s, C_a and C_b are positive constants.

3.2.3 The Jiles-Atherton Model

The Jiles-Atherton model also represents hysteresis behavior in ferromagnets. In contrast to the phenomenological modeling of Coleman-Hodgdon model, the Jiles-Atherton model is based on the physical modeling of the magnetization process (domain wall motion) [25]. Let u_Φ be the magnetic field and y_Φ be the magnetiza-

tion. The Jiles-Atherton model as proposed in [25] is then given by:

$$\frac{\mathrm{d}y_\Phi}{\mathrm{d}u_\Phi} = (1-c)\frac{(y_{an}-y_\Phi)}{\mathrm{sign}(\dot{u}_\Phi)K - J_\alpha(y_{an}-y_\Phi)} - c\frac{\mathrm{d}y_{an}}{\mathrm{d}u_\Phi}, \tag{3.13}$$

where sign(.) is the sign operator, c, K and J_α are positive constants, and y_{an} is the unique solution of an implicit equation:

$$y_{an} = M_s f(u_\Phi + J_\alpha y_{an}). \tag{3.14}$$

The parameter M_s defines the saturation magnetization and f is a function which

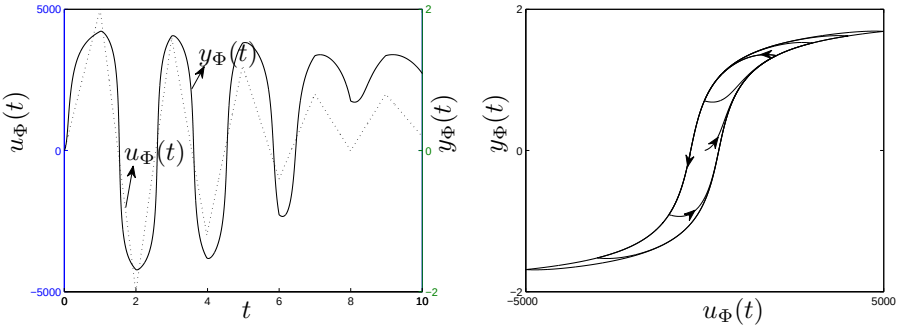

(a) (b)

Figure 3.3: Behaviour of the Jiles-Atherton model with $J_\alpha = 1.6 \times 10^{-3}$, $J_a = 11$, $c = 0.2$ and $K = 9$.

satisfies $f(0) = 0$, $\lim_{s\to\infty} f(s) = 1$ and $\lim_{s\to-\infty} f(s) = -1$. Jiles and Atherton in [25, 51] proposed to use the modified Langevin expression for f in (3.14). More precisely, y_{an} is given by:

$$y_{an} = M_s\left(\coth\left(\frac{u_\Phi + J_\alpha y_{an}}{J_a}\right) - \frac{J_a}{(u_\Phi + J_\alpha y_{an})}\right), \tag{3.15}$$

where J_a is a positive constant. We rewrite it in an explicit form as follows.

Lemma 3.2.1 *If $J_a > M_s J_\alpha/3$, then* (3.15) *has a unique solution y_{an} for every $u_\Phi \in \mathbb{R}$ and it can be represented into the following explicit form:*

$$y_{an} = f_{an}(u_\Phi). \tag{3.16}$$

Proof: Firstly, denote $b = (u_\Phi + J_\alpha y_{an})/J_a$ and rewrite (3.15) into:

$$u_\Phi = -M_s J_\alpha \coth(b) + \frac{M_s J_\alpha}{b} + J_a b. \tag{3.17}$$

Let $g(b) = -M_s J_\alpha \coth(b) + \frac{M_s J_\alpha}{b} + J_a b$. The first two components of g define the Langevin function, which is continuous for all b in $\mathbb{R}$. It is clear that $J_a b$ is a continuous function of b. This implies that g is a continuous function.

The uniqueness of the solution of (3.15) is proved by showing that $g(b)$ is invertible, so that according to the definition of b, y_{an} can be given by

$$y_{an} = \frac{a g^{-1}(u_\Phi) - u_\Phi}{J_\alpha} \tag{3.18}$$

The function g is invertible if it is strictly increasing. The gradient of g is given by:

$$\frac{\partial g(b)}{\partial b} = M_s J_\alpha \frac{4e^{2b}}{(e^{2b}-1)^2} - M_s J_\alpha \frac{1}{b^2} + J_a. \tag{3.19}$$

Now, let $N(b) = M_s J_\alpha (\frac{4e^{2b}}{(e^{2b}-1)^2} - \frac{1}{b^2})$. It can be checked that $\lim_{b\to 0} N(b) = -\frac{1}{3} M_s J_\alpha$, $\dot{N}(b) < 0$ if $b < 0$ and $\dot{N}(b) > 0$ if $b > 0$. Hence, if $J_a > M_s J_\alpha/3$, then $\frac{\partial g(b)}{\partial b} > 0$ for all $b \in \mathbb{R}$. This implies that g is strictly increasing and invertible.

Therefore, if $J_a > M_s J_\alpha/3$, y_{an} is given by (3.18). □

Using Lemma 3.2.1, we can replace y_{an} in (3.13) with $f_{an}(u_\Phi)$ as follows:

$$\frac{\mathrm{d}y_\Phi}{\mathrm{d}u_\Phi} = (1-c)\frac{(f_{an}(u_\Phi) - y_\Phi)}{\mathrm{sign}(\dot{u}_\Phi)K - J_\alpha(f_{an}(u_\Phi) - y_\Phi)} - c\frac{\mathrm{d}f_{an}(u_\Phi)}{\mathrm{d}u_\Phi} \tag{3.20}$$

and formulate the Jiles-Atherton model into Duhem model (3.1) with

$$\begin{cases} f_1(\gamma, \upsilon) = (1-c)\frac{(f_{an}(\upsilon)-\gamma)}{K - J_\alpha(f_{an}(\upsilon)-\gamma)} - c\frac{\mathrm{d}f_{an}(\upsilon)}{\mathrm{d}\upsilon} \\ f_2(\gamma, \upsilon) = (1-c)\frac{(f_{an}(\upsilon)-\gamma)}{-K - J_\alpha(f_{an}(\upsilon)-\gamma)} - c\frac{\mathrm{d}f_{an}(\upsilon)}{\mathrm{d}\upsilon} \end{cases} \tag{3.21}$$

An illustration of the Jiles-Atherton model is shown in Figure 3.3.

3.2.4 The Bouc-Wen Model

The Bouc-Wen model is commonly used to model the hysteresis phenomena in the magnetorheological damper [10], [18]. Moreover, it is also used to represent the

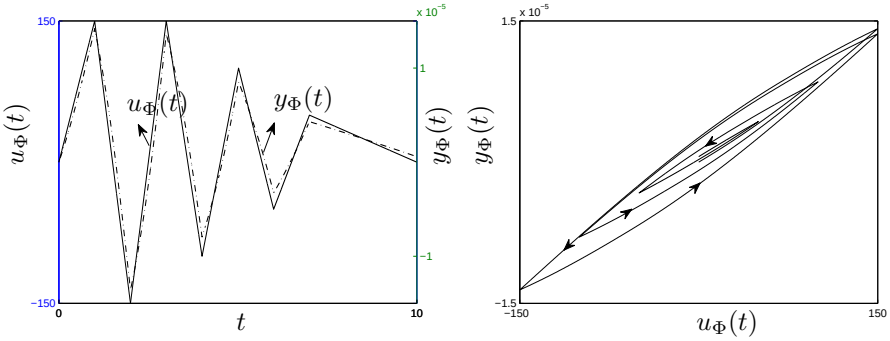

(a) (b)

Figure 3.4: The input-output dynamics of the Bouc-Wen model with $k_x = 1.2117 \times 10^{-7}$, $k_w = -5.08 \times 10^{-6}$, $n = 1.27$, $\rho = 8.93 \times 10^{-3}$ and $\sigma = 0.74$.

hysteresis phenomena in the piezo-actuators [17]. The general representation of the Bouc-Wen model is given by

$$\begin{aligned} y_\Phi(t) &= k_x u_\Phi(t) + k_w h(t) \\ \dot{h}(t) &= \rho \dot{u}_\Phi(t) - \rho\sigma|\dot{u}_\Phi(t)||h(t)|^{n-1}h(t) - \rho(1-\sigma)\dot{u}_\Phi(t)|h(t)|^n, \end{aligned}$$

where $n \geq 1$ and k_x, k_w, ρ, σ are the parameters determine the shape of the hysteresis curve. For the case of piezo-actuators, u_Φ denotes the voltage, y_Φ denotes the displacement.

The Bouc-Wen model can be described by the Duhem hysteresis operator (3.1) with

$$\begin{cases} f_1(\gamma, \upsilon) & = k_x + k_w\rho - k_w\rho\sigma|\frac{\gamma - k_x\upsilon}{k_w}|^{n-1}\frac{\gamma - k_x\upsilon}{k_w} - k_w\rho(1-\sigma)|\frac{\gamma - k_x\upsilon}{k_w}|^n \\ f_2(\gamma, \upsilon) & = k_x + k_w\rho + k_w\rho\sigma|\frac{\gamma - k_x\upsilon}{k_w}|^{n-1}\frac{\gamma - k_x\upsilon}{k_w} - k_w\rho(1-\sigma)|\frac{\gamma - k_x\upsilon}{k_w}|^n. \end{cases} \tag{3.22}$$

In Figure 3.4, we illustrate the behavior of the Bouc-Wen model with $k_x = 1.2117 \times 10^{-7}$, $k_w = -5.08 \times 10^{-6}$, $n = 1.27$, $\rho = 8.93 \times 10^{-3}$ and $\sigma = 0.74$.

3.2.5 The Chua-Stromsmoe Model

The Chua-Stromsmoe model is used to represent the hysteresis phenomena observed in ferromagnetic inductors. As introduced in [5], the Chua-Stromsmoe model can represent not only the rate-independent hysteresis behavior but also the rate-dependent hysteresis behavior, such as loop widening or narrowing for different

input frequencies. A general representation of the Chua-Stromsmoe model is given by

$$\dot{y}_\Phi(t) = q(\dot{u}_\Phi(t))h(y_\Phi(t))g(u_\Phi(t) - f(y_\Phi(t))), \tag{3.23}$$

where the functions f, g and h satisfy the following conditions: (i) f, g and h are

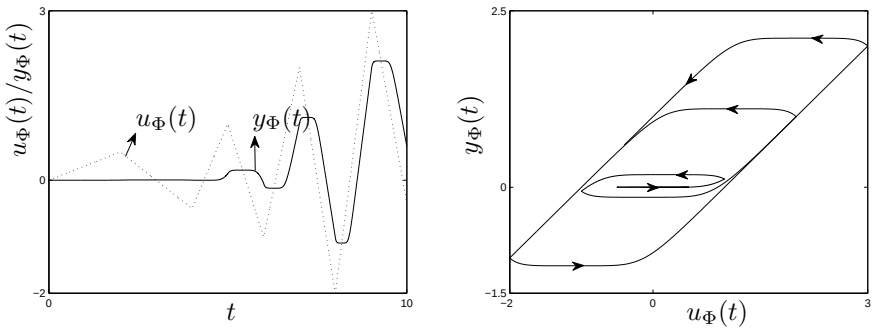

(a) (b)

Figure 3.5: Behaviour of the Chua-Stromsmoe model using $f(\gamma) = \gamma$, $h(\gamma) = 1$ and $g(\upsilon - f(\gamma)) = (\upsilon - f(\gamma))^5$.

C^1; (ii) f, g: $E^1 \to E^1$ bijectively; (iii) For all $y_\Phi \in E^1$, there exists H_{min} and H_{max}, such that $0 < H_{min} \leq h(y_\Phi) \leq H_{max} < \infty$.(iv) $q \in C^0$ and $q(\dot{u}_\Phi) \geq 0$.

Let $q(\dot{u}_\Phi) = |\dot{u}_\Phi|$, which implies that q is a positively homogeneous function, then the Chua-Stromsmoe model in (3.23) is rate-independent and can be rewritten into the form of (3.1) where

$$\begin{cases} f_1(\gamma, \upsilon) &= h(\gamma)g(\upsilon - f(\gamma)) \\ f_2(\gamma, \upsilon) &= -h(\gamma)g(\upsilon - f(\gamma)). \end{cases} \tag{3.24}$$

An illustration of the behavior of the Chua-Stromsmoe model is shown in Figure 3.5 with $f(\gamma) = \gamma$, $h(\gamma) = 1$ and $g(\upsilon - f(\gamma)) = (\upsilon - f(\gamma))^5$.

3.3 Duhem hysteresis Operator with Saturated Output

In contrast to the previous section, we illustrate some hysteresis model with saturated output, i.e., for every $u_\Phi \in \mathbb{R}$, the corresponding $y_\Phi \in \mathcal{D}$, where $\mathcal{D} \subset \mathbb{R}$.

3.3.1 The Elastic-Plastic operator

The elastic-plastic operator (which is also called the stop operator) models the stress-strain relationship in the elastic-plastic element. We use the same description of elastic-plastic operator as in [4, 33]. For all $l \in \mathbb{R}^+$ and all $\xi \in \mathbb{R}$, we introduce an elastic-plastic operator $\mathcal{E}_{l,\xi}$ defined on the space $C_{\rm pm}(\mathbb{R}_+)$ of piecewise monotone functions, by defining, for every $u_\mathcal{E} \in C_{\rm pm}(\mathbb{R}_+)$,

$$(\mathcal{E}_{l,\xi}(u_\mathcal{E}))(t) = \begin{cases} e_l(u_\mathcal{E}(0) - \xi) & \text{for } t = 0, \\ e_l(u_\mathcal{E}(t) - u_\mathcal{E}(t_i) + (a_{l,\xi}(u_\mathcal{E})(t_i))) & \text{for } t \in (t_{i-1}, t_i], \end{cases} \tag{3.25}$$

where the function $e_l : \mathbb{R}^2 \to \mathbb{R}$ is defined by $e_l(u_\mathcal{E}) = \min\{l, \max\{-l, u\}\}$, for all

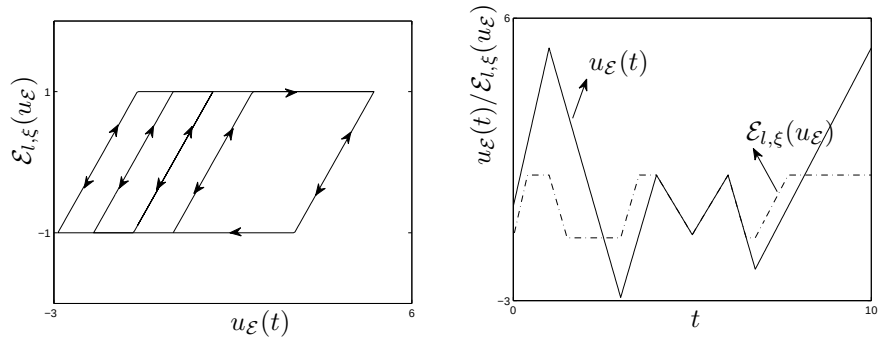

Figure 3.6: The input-output dynamics of the elastic-plastic operator with $l = 1$.

$l \in \mathbb{R}_+$, and $0 = t_0 < t_1 < t_2 < \ldots$ is a partition of $\mathbb{R}_+$, such that $u_\mathcal{E}$ is monotone on each of the intervals $[t_{i-1}, t_i]$, $i \in \mathbb{N}$. Following the results in [29], the operator $\mathcal{E}_{l,\xi}$ can be extended to the space of piecewise continuous functions. An illustration of the elastic-plastic operator is shown in Figure 3.6.

Extending $\mathcal{E}_{l,\xi}$ to the space of absolutely continuous functions, the elastic-plastic operator $\mathcal{E}_{l,\xi} : AC(\mathbb{R}_+) \to AC(\mathbb{R}_+)$ can also be described by the Duhem hysteresis operator (3.1). Let $\Phi_{l,\xi}$ denote the elastic-plastic operator and u_Φ denote the $u_\mathcal{E}$, then the f_1, f_2 functions can be given as follows

$$f_1(\gamma, \upsilon) = \begin{cases} 0 & \text{if } \gamma \geq l, \\ 1 & \text{if } -l < \gamma < l \end{cases} \tag{3.26}$$

$$f_2(\gamma, \upsilon) = \begin{cases} 0 & \text{if } \gamma \leq -l, \\ 1 & \text{if } -l < \gamma < l \end{cases} \tag{3.27}$$

and with $y_{\Phi_0} = \min\{l, \max\{-l, u_\Phi(0)\}\}$.

3.3.2 The Dahl Model

The Dahl model [7, 9, 38] is commonly used in mechanical systems, which represents the friction force with respect to the relative displacement between two surfaces in contact. The general representation of the Dahl model is given by

$$\dot{y}_\Phi(t) = \rho \left| 1 - \frac{y_\Phi(t)}{F_c} \text{sgn}(\dot{u}_\Phi(t)) \right|^n \text{sgn}\left(1 - \frac{y_\Phi(t)}{F_c} \text{sgn}(\dot{u}_\Phi(t)) \right) \dot{u}_\Phi(t), \tag{3.28}$$

where y_Φ denotes the friction force, u_Φ denotes the displacement, $F_c > 0$ denotes

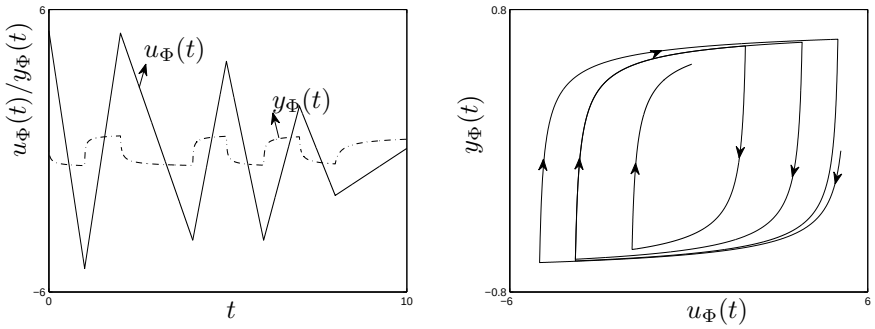

(a) (b)

Figure 3.7: The input-output dynamics of the Dahl model with $F_c = 0.75$, $\rho = 1.5$ and $r = 3$.

the Coulomb friction force, $\rho > 0$ denotes the rest stiffness and $n \geq 1$ is a parameter that determines the shape of the hysteresis loops.

The Dahl model can be described by the Duhem hysteresis operator (3.1) with

$$\begin{cases} f_1(\gamma, \upsilon) &= \rho \left| 1 - \frac{\gamma}{F_c} \right|^n \text{sgn}\left(1 - \frac{\gamma}{F_c} \right) \\ f_2(\gamma, \upsilon) &= \rho \left| 1 + \frac{\gamma}{F_c} \right|^n \text{sgn}\left(1 + \frac{\gamma}{F_c} \right). \end{cases} \tag{3.29}$$

In Figure 3.7, we illustrate the behavior of the Dahl model where $F_c = 0.75$, $\rho = 1.5$ and $n = 3$.

3.3.3 The LuGre Model

The LuGre model [38, 9] is another hysteresis model which is commonly used to describe the friction in mechanical systems. In this model, the asperities of two contact surfaces are modeled as the elastic bristles. The general representations of the LuGre model is given by

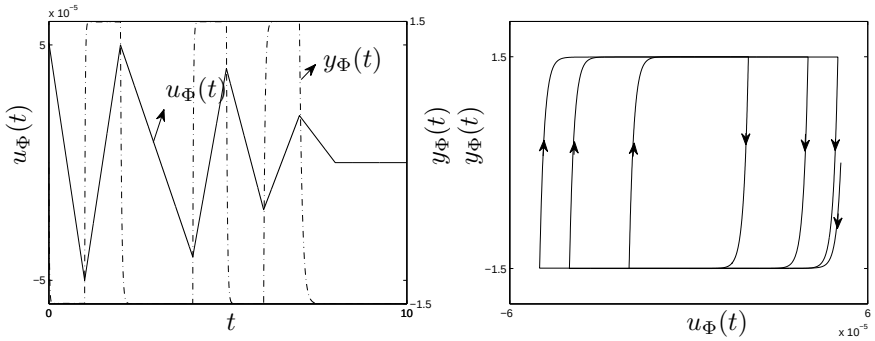

(a) (b)

Figure 3.8: The input-output dynamics of the LuGre model with $F_c = 1$, $F_S = 1.5$, $v_S = 0.001$ and $\rho_L = 10^5$.

$$\dot{y}_\Phi(t) = \rho_L(\dot{u}_\Phi(t) - \frac{|\dot{u}_\Phi(t)|}{r(\dot{u}_\Phi(t))} y_\Phi(t)), \tag{3.30}$$

where y_Φ denotes the friction force, u_Φ denotes the relative displacement, $\rho_L > 0$ is the stiffness coefficient and $r(\dot{u}_\Phi(t))$ (as in [9]) is defined by

$$r(\dot{u}_\Phi(t)) = \frac{F_C}{\rho_L} + \frac{F_S - F_C}{\rho_L} e^{-(\dot{u}_\Phi(t)/v_S)^2}, \tag{3.31}$$

where F_S is the stiction force and v_S is the Stribeck velocity.

The LuGre model can be described by the Duhem hysteresis operator (3.1) with

$$\begin{cases} f_1(\gamma, v) &= \rho_L \left(1 - \frac{\gamma}{r(\dot{v}(t))}\right) \\ f_2(\gamma, v) &= \rho_L \left(1 + \frac{\gamma}{r(\dot{v}(t))}\right). \end{cases} \tag{3.32}$$

In Figure 3.8, we illustrate the behavior of the LuGre model where $F_c = 0.75$, $F_S = 1.5$, $\rho_L = 10^5$ and $v_S = 0.001$.

3.4 Concluding Remarks

In this chapter the Duhem hysteresis operator and its properties are introduced. Furthermore, it has been shown that the Duhem-type hysteresis operator is useful to describe the hysteresis phenomena in many applications.

Chapter 4

Dissipativity of The Duhem Hysteresis Operator

In this chapter, we discuss two dissipativity properties of the Duhem hysteresis operator: the Duhem hysteresis operator with CCW I/O behavior and Duhem hysteresis operator with CW I/O behavior. Based on the definitions of the CCW and CW I/O dynamics, sufficient conditions on the Duhem operator such that it is CCW (or CW) are given in Theorem 4.2.1 and 4.2.6 (or, Theorem 4.3.1 and 4.3.6). In particular, we show the dissipativity property of the CCW (or CW) Duhem hysteresis operator by constructing explicit storage functions satisfying the CCW (or CW) dissipation inequality. The relations between these storage functions and the available storage functions used in the classical dissipation theory are also discussed.

4.1 Function Definition

In this section, we introduce four functions which play important roles in the construction of the storage function and in the characterization of dissipativity. They are : an *anhysteresis function*, a *traversing function*, a *CCW intersecting function* for the Duhem operator with CCW I/O behavior and a *CW intersecting function* for the Duhem operator with CW I/O behavior. These functions are defined based on f_1 and f_2 (c.f., the Duhem equation in (3.1)). In our main results, we use the same definition of anhysteresis and traversing functions for studying the dissipativity of both CCW and CW Duhem operators. However we use different definition of intersecting function for each case.

Generally speaking, the anhysteresis function defines the curve where $f_1 = f_2$, i.e. an idea curve which does not contain hysteresis. The anhysteresis curve is commonly used in construction the mathematical models for hysteresis, see, for example [25], [6]. The traversing function describes the trajectory of the Duhem operator Φ when a monotone increasing u_Φ or a monotone decreasing u_Φ is applied from a given initial condition. For the CCW Duhem hysteresis operator the CCW intersecting function defines the intersection of the anhysteresis function (curve) and the

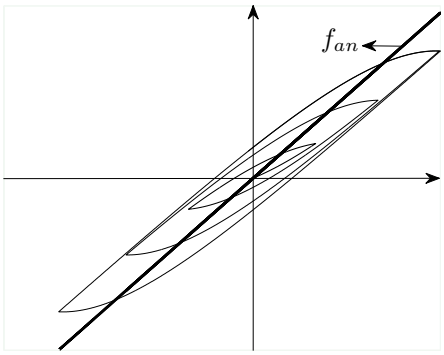

Figure 4.1: Graphical interpretation of the anhysteresis curve: f_{an} for the Duhem hysteresis operator Φ with $f_1(\gamma, \upsilon) = -0.15\gamma + 0.48\upsilon + 1.5$,$f_2(\gamma, \upsilon) = 0.15\gamma - 0.48\upsilon + 1.5$.

traversing function from a given initial condition. A similar interpretation is applicable to the CW intersecting function for the CW Duhem hysteresis operator.

4.1.1 The Anhysteresis Function

In order to define the anhysteresis function, we rewrite f_1 and f_2 as follows

$$\left.\begin{array}{ll} f_1(\gamma, \upsilon) & = F(\gamma, \upsilon) + G(\gamma, \upsilon) \\ f_2(\gamma, \upsilon) & = -F(\gamma, \upsilon) + G(\gamma, \upsilon) \end{array}\right\} \forall (\gamma, \upsilon) \in \mathbb{R}^2 \,. \tag{4.1}$$

where $F := \frac{f_1 - f_2}{2}$, $G := \frac{f_1 + f_2}{2}$. We assume that the implicit function $\upsilon \mapsto \{\gamma \in \mathbb{R}, F(\gamma, \upsilon) = 0\}$ admits a unique explicit solution $\gamma = f_{an}(\upsilon)$ (or $\upsilon = g_{an}(\gamma)$) where f_{an} (or g_{an}) is C^1. Such function f_{an} (or g_{an}) is called *an anhysteresis function* and the corresponding graph $\{(\upsilon, f_{an}(\upsilon)) | \upsilon \in \mathbb{R}\}$ (or $\{(g_{an}(\gamma), \gamma | \gamma \in \mathbb{R}\}$) is called *an anhysteresis curve*. Using f_{an}, it can be checked that $f_1(f_{an}(\upsilon), \upsilon) = f_2(f_{an}(\upsilon), \upsilon)$ holds for all $\upsilon \in \mathbb{R}$.

As an example, let us consider a Duhem hysteresis operator Φ with $f_1(\gamma, \upsilon) = -0.15\gamma + 0.48\upsilon + 1.5$ and $f_2(\gamma, \upsilon) = 0.15\gamma - 0.48\upsilon + 1.5$. It can be checked that $f_{an}(\upsilon) = 3.2\upsilon$ and it is illustrated in Figure 4.1.

4.1.2 The Traversing Function

The traversing function ω_Φ

For every pair $(y_{\Phi_0}, u_{\Phi_0}) \in \mathbb{R}^2$, let $\omega_{\Phi,1}(\cdot, y_{\Phi_0}, u_{\Phi_0}) : [u_{\Phi_0}, \infty) \to \mathbb{R}$ be the solution z of

$$z(\upsilon) - y_{\Phi_0} = \int_{u_{\Phi_0}}^{\upsilon} f_1(z(\sigma), \sigma)\, \mathrm{d}\sigma, \qquad z(u_{\Phi_0}) = y_{\Phi_0}, \quad \forall \upsilon \in [u_{\Phi_0}, \infty),$$

and let $\omega_{\Phi,2}(\cdot, y_{\Phi_0}, u_{\Phi_0}) : (-\infty, u_{\Phi_0}] \to \mathbb{R}$ be the solution z of

$$z(\upsilon) - y_{\Phi_0} = \int_{u_{\Phi_0}}^{\upsilon} f_2(z(\sigma), \sigma)\, \mathrm{d}\sigma, \qquad z(u_{\Phi_0}) = y_{\Phi_0}, \quad \forall \upsilon \in (-\infty, u_{\Phi_0}].$$

Using the above definitions, for every pair $(y_{\Phi_0}, u_{\Phi_0}) \in \mathbb{R}^2$, the function $\omega_\Phi(\cdot, y_{\Phi_0}, u_{\Phi_0}) : \mathbb{R} \to \mathbb{R}$ is defined by the concatenation of $\omega_{\Phi,2}(\cdot, y_{\Phi_0}, u_{\Phi_0})$ and $\omega_{\Phi,1}(\cdot, y_{\Phi_0}, u_{\Phi_0})$:

$$\omega_\Phi(\upsilon, y_{\Phi_0}, u_{\Phi_0}) = \begin{cases} \omega_{\Phi,2}(\upsilon, y_{\Phi_0}, u_{\Phi_0}) & \forall \upsilon \in (-\infty, u_{\Phi_0}) \\ \omega_{\Phi,1}(\upsilon, y_{\Phi_0}, u_{\Phi_0}) & \forall \upsilon \in [u_{\Phi_0}, \infty). \end{cases} \tag{4.2}$$

The traversing function ν_Φ

Similarly, we can introduce the function ν_Φ which is dual to the construction of ω_Φ. For every pair $(y_{\Phi_0}, u_{\Phi_0}) \in \mathbb{R}^2$, let $\nu_{\Phi,1}(\cdot, y_{\Phi_0}, u_{\Phi_0}) : [u_{\Phi_0}, \infty) \to \mathbb{R}$ be the solution z of

$$z(\upsilon) - y_{\Phi_0} = \int_{u_{\Phi_0}}^{\upsilon} f_2(z(\sigma), \sigma)\, \mathrm{d}\sigma, \qquad z(u_{\Phi_0}) = y_{\Phi_0}, \quad \forall \upsilon \in [u_{\Phi_0}, \infty),$$

and let $\nu_{\Phi,2}(\cdot, y_{\Phi_0}, u_{\Phi_0}) : (-\infty, u_{\Phi_0}] \to \mathbb{R}$ be the solution z of

$$z(\upsilon) - y_{\Phi_0} = \int_{u_{\Phi_0}}^{\upsilon} f_1(z(\sigma), \sigma)\, \mathrm{d}\sigma, \qquad z(u_{\Phi_0}) = y_{\Phi_0}, \quad \forall \upsilon \in (-\infty, u_{\Phi_0}].$$

Using the above definitions, for every pair $(y_{\Phi_0}, u_{\Phi_0}) \in \mathbb{R}^2$, the function $\nu_\Phi(\cdot, y_{\Phi_0}, u_{\Phi_0}) : \mathbb{R} \to \mathbb{R}$ is defined by the concatenation of $\nu_{\Phi,2}(\cdot, y_{\Phi_0}, u_{\Phi_0})$ and $\nu_{\Phi,1}(\cdot, y_{\Phi_0}, u_{\Phi_0})$:

$$\nu_\Phi(\upsilon, y_{\Phi_0}, u_{\Phi_0}) = \begin{cases} \nu_{\Phi,2}(\upsilon, y_{\Phi_0}, u_{\Phi_0}) & \forall \upsilon \in (-\infty, u_{\Phi_0}) \\ \nu_{\Phi,1}(\upsilon, y_{\Phi_0}, u_{\Phi_0}) & \forall \upsilon \in [u_{\Phi_0}, \infty). \end{cases} \tag{4.3}$$

A graphical interpretation of the traversing functions ω_Φ and ν_Φ of the Duhem hysteresis operator Φ with $f_1(\gamma, \upsilon) = -0.15\gamma + 0.48\upsilon + 1.5$, $f_2(\gamma, \upsilon) = 0.15\gamma - 0.48\upsilon + 1.5$ is shown in Figure 4.2.

4.1.3 The CCW Intersecting Function

As indicated before, the function Ω defines the intersection between $\omega_\Phi(\cdot, \gamma, \upsilon)$ and $f_{an}(\cdot)$. More precisely, the function $\Omega : \mathbb{R}^2 \to \mathbb{R}$ is an *CCW intersecting function* (corresponding to ω_Φ and f_{an}) if

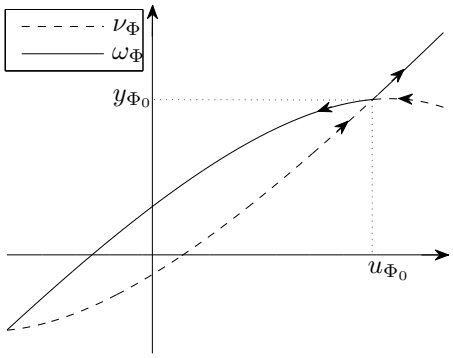

Figure 4.2: Graphical interpretation of the defined traversing curve: ω_Φ in (4.2) and ν_Φ in (4.3), where the Duhem hysteresis operator Φ is defined in (3.1) with $f_1(\gamma, \upsilon) = -0.15\gamma + 0.48\upsilon + 1.5$,$f_2(\gamma, \upsilon) = 0.15\gamma - 0.48\upsilon + 1.5$.

- $\omega_\Phi(\Omega(\gamma, \upsilon), \gamma, \upsilon) = f_{an}(\Omega(\gamma, \upsilon))$ for all $(\gamma, \upsilon) \in \mathbb{R}^2$;
- $\Omega(\gamma, \upsilon) \geq \upsilon$ whenever $\gamma \geq f_{an}(\upsilon)$ and $\Omega(\gamma, \upsilon) < \upsilon$ otherwise.

This implies that the two functions $\omega_\Phi(\cdot, \gamma, \upsilon)$ and $f_{an}(\cdot)$ intersect at a unique point larger or smaller than υ depending on the sign of $\gamma - f_{an}(\upsilon)$.

The following lemma gives sufficient conditions on f_1 and f_2 for the existence of such an intersecting function.

Lemma 4.1.1 *Assume that f_1 and f_2 in* (4.1) *be such that f_1, f_2 and f_{an} are C^1. Moreover, assume that f_{an} is strictly increasing and there exists a positive real number ϵ such that for all $(\gamma, \upsilon) \in \mathbb{R}^2$*

$$f_2(\gamma, \upsilon) < \frac{\mathrm{d}f_{an}(\upsilon)}{\mathrm{d}\upsilon} - \epsilon \quad \textit{whenever} \quad \gamma > f_{an}(\upsilon), \ \textit{and} \tag{4.4}$$

$$f_1(\gamma, \upsilon) < \frac{\mathrm{d}f_{an}(\upsilon)}{\mathrm{d}\upsilon} - \epsilon \quad \textit{whenever} \quad \gamma < f_{an}(\upsilon) \tag{4.5}$$

hold. Then there exists an intersecting function $\Omega \in C^1(\mathbb{R}^2)$ (corresponding to ω_Φ and f_{an}) such that

(1) *$\Omega(\gamma, \upsilon) \geq \upsilon$ whenever $\gamma \geq f_{an}(\upsilon)$ and $\Omega(\gamma, \upsilon) < \upsilon$ otherwise.*

(2) *$\omega_\Phi(\Omega(\gamma, \upsilon), \gamma, \upsilon) = f_{an}(\Omega(\gamma, \upsilon))$.*

(3) *Moreover, for all $u_\Phi \in C^1$, $y_\Phi := \Phi(u_\Phi)$, $\frac{\mathrm{d}}{\mathrm{d}t}\Omega(y_\Phi(t), u_\Phi(t))$ exists.*

Proof: Consider the continuous function $\varphi : \mathbb{R}^3 \to \mathbb{R}$ defined as $\varphi(\upsilon, y_{\Phi_0}, u_{\Phi_0}) = \omega_\Phi(\upsilon, y_{\Phi_0}, u_{\Phi_0}) - f_{an}(\upsilon)$. Consider also A_0 and A_1 the two subsets of $\mathbb{R}^3$ defined as,

$$A_0 = \{(\upsilon, y_{\Phi_0}, u_{\Phi_0}) \in \mathbb{R}^3 \,|\, y_{\Phi_0} > f_{an}(u_{\Phi_0}) \,,\ \upsilon > u_{\Phi_0}\} \,,$$
$$A_1 = \{(\upsilon, y_{\Phi_0}, u_{\Phi_0}) \in \mathbb{R}^3 \,|\, y_{\Phi_0} < f_{an}(u_{\Phi_0}) \,,\ \upsilon < u_{\Phi_0}\} \,.$$

Note that the function f_{an} being strictly increasing by assumption, it implies that these sets are open sets. Also, the function ω_Φ satisfies

$$\frac{\partial \omega_\Phi}{\partial \upsilon}(\upsilon, y_{\Phi_0}, u_{\Phi_0}) = f_1(\omega_\Phi(\upsilon, y_{\Phi_0}, u_{\Phi_0}), \upsilon), \quad \forall (\upsilon, y_{\Phi_0}, u_{\Phi_0}) \in A_0,$$
$$\frac{\partial \omega_\Phi}{\partial \upsilon}(\upsilon, y_{\Phi_0}, u_{\Phi_0}) = f_2(\omega_\Phi(\upsilon, y_{\Phi_0}, u_{\Phi_0}), \upsilon), \quad \forall (\upsilon, y_{\Phi_0}, u_{\Phi_0}) \in A_1.$$

Consequently, $\omega_\Phi(\upsilon, y_{\Phi_0}, u_{\Phi_0})$ is the solution of the ordinary differential equations computed from the C^1 vector field. With [15, Theorem V.3.1], it implies that ω_Φ is a C^1 function in $A_0 \cup A_1$. Moreover, the function f_{an} being C^1 implies that the function φ is C^1 in $A_0 \cup A_1$. With (4.4) and (4.5), the function φ satisfies, $\frac{\partial \varphi}{\partial \upsilon}(\upsilon, y_{\Phi_0}, u_{\Phi_0}) < -\epsilon \neq 0$ for all $(\upsilon, y_{\Phi_0}, u_{\Phi_0}) \in A_0 \cup A_1$. Consequently, φ is a strictly decreasing function in its first argument in the set $A_0 \cup A_1$. This also implies that

$$\varphi(\upsilon, y_{\Phi_0}, u_{\Phi_0}) < \varphi(u_{\Phi_0}, y_{\Phi_0}, u_{\Phi_0}) - \epsilon(\upsilon - u_{\Phi_0}), \quad \forall (\upsilon, y_{\Phi_0}, u_{\Phi_0}) \in A_0,$$
$$\varphi(\upsilon, y_{\Phi_0}, u_{\Phi_0}) > \varphi(u_{\Phi_0}, y_{\Phi_0}, u_{\Phi_0}) - \epsilon(\upsilon - u_{\Phi_0}), \quad \forall (\upsilon, y_{\Phi_0}, u_{\Phi_0}) \in A_1.$$

Note that if $y_{\Phi_0} > f_{an}(u_{\Phi_0})$, then $\varphi(u_{\Phi_0}, y_{\Phi_0}, u_{\Phi_0}) > 0$ ($y_{\Phi_0} > f_{an}(u_{\Phi_0})$ indicates that the trajectory ω_Φ is located above the anhysteresis curve, i.e., $\varphi(\upsilon, y_{\Phi_0}, u_{\Phi_0}) = \omega_\Phi(\upsilon, y_{\Phi_0}, u_{\Phi_0}) - f_{an}(\upsilon) > 0$). Consequently, due to the strictly decreasing property of φ, there exists a unique real number u^*_Φ such that $\varphi(u^*_\Phi, y_{\Phi_0}, u_{\Phi_0}) = 0$ and $(u^*_\Phi, y_{\Phi_0}, u_{\Phi_0}) \in A_0$. On the other hand, if $y_{\Phi_0} < f_{an}(u_{\Phi_0})$, then $\varphi(u_{\Phi_0}, y_{\Phi_0}, u_{\Phi_0}) < 0$ and consequently there exists a unique real number u^*_Φ such that $\varphi(u^*_\Phi, y_{\Phi_0}, u_{\Phi_0}) = 0$ and $(u^*_\Phi, y_{\Phi_0}, u_{\Phi_0}) \in A_1$.

Therefore, denoting $\Omega(y_{\Phi_0}, u_{\Phi_0}) = u^*_\Phi$, by employing the implicit function theorem and using the fact that φ is C^1, it can be shown that Ω is C^1. □

Roughly speaking the existence of function Ω satisfying **(1)–(3)** in Lemma 4.1.1 implies that for all (γ, υ), the two functions $\omega_\Phi(\cdot, \gamma, \upsilon)$ and $f_{an}(\cdot)$ intersect at a unique point larger or smaller than u_{Φ_0} depending on the sign of $\gamma - f_{an}(\upsilon)$. Moreover, along the solutions of (3.1), the time derivative of the intersecting point exists.

Similarly, we can define an intersecting function Υ describing the intersection between $\nu_\Phi(\cdot, \gamma, \upsilon)$ and $f_{an}(\cdot)$. The function $\Upsilon : \mathbb{R}^2 \to \mathbb{R}$ is an *CCW intersecting function* (which is corresponding to ν_Φ and f_{an}) if $\nu_\Phi(\Upsilon(\gamma, \upsilon), \gamma, \upsilon) = f_{an}(\Upsilon(\gamma, \upsilon))$

for all $(\gamma, \upsilon) \in \mathbb{R}^2$; and $\Upsilon(\gamma, \upsilon) \geq \upsilon$ whenever $\gamma \geq f_{an}(\upsilon)$ and $\Upsilon(\gamma, \upsilon) < \upsilon$ otherwise. The following lemma gives sufficient conditions on f_1 and f_2 for the existence of such an intersecting function Υ.

Lemma 4.1.2 *Assume that f_1 and f_2 in* (4.1) *be such that f_1, f_2 and f_{an} are C^1. Moreover, assume that f_{an} is strictly increasing and there exists a positive real number ϵ such that for all $(\gamma, \upsilon) \in \mathbb{R}^2$ the conditions* (4.4) *and* (4.5) *given in Lemma 4.1.1 hold. Then there exists an intersecting function $\Upsilon \in C^1(\mathbb{R}^2)$ (corresponding to ν_Φ and f_{an}) such that*

(1) *$\Upsilon(\gamma, \upsilon) \geq \upsilon$ whenever $\gamma \geq f_{an}(\upsilon)$ and $\Upsilon(\gamma, \upsilon) < \upsilon$ otherwise.*

(2) *$\nu_\Phi(\Upsilon(\gamma, \upsilon), \gamma, \upsilon) = f_{an}(\Upsilon(\gamma, \upsilon))$.*

(3) *Moreover, for all $u_\Phi \in C^1$, $y_\Phi := \Phi(u_\Phi)$, $\frac{\mathrm{d}}{\mathrm{d}t}\Upsilon(y_\Phi(t), u_\Phi(t))$ exists.*

The proof of the Lemma 4.1.2 is similar to the proof of Lemma 4.1.1.

4.1.4 The CW Intersecting Function

For the Duhem hysteresis operator with CW I/O behavior, we define the intersecting function Λ which has different properties than the intersecting function Ω for the CCW Duhem operator. The intersecting function Λ describes the intersection between the anhysteresis curve f_{an} and the curve ω_Φ. The function $\Lambda : \mathbb{R}^2 \to \mathbb{R}$ is a *CW intersecting function* (corresponding to ω_Φ and f_{an}) if:

- $\omega_\Phi(\Lambda(\gamma, \upsilon), \gamma, \upsilon) = f_{an}(\Lambda(\gamma, \upsilon))$ for all $(\gamma, \upsilon) \in \mathbb{R}^2$;
- $\Lambda(\gamma, \upsilon) \leq \upsilon$ whenever $\gamma \geq f_{an}(\upsilon)$ and $\Lambda(\gamma, \upsilon) > \upsilon$ otherwise.

This implies that the two functions $\omega_\Phi(\cdot, \gamma, \upsilon)$ and $f_{an}(\cdot)$ intersect at a unique point larger or smaller than υ depending on the sign of $\gamma - f_{an}(\upsilon)$.

In the following lemma we give sufficient conditions for the existence of such intersecting function Λ.

Lemma 4.1.3 *Assume that f_1 and f_2 in* (4.1) *be such that f_1, f_2 are C^1. Moreover, assume that f_{an} is strictly increasing and there exists a positive real constant $\epsilon > 0$ such that for all $(\gamma, \upsilon) \in \mathbb{R}^2$ the following inequality holds*

$$f_1(\gamma, \upsilon) > \frac{\mathrm{d}f_{an}(\upsilon)}{\mathrm{d}\upsilon} + \epsilon \quad \textit{whenever} \quad \gamma > f_{an}(\upsilon)\,, \tag{4.6}$$

$$f_2(\gamma, \upsilon) > \frac{\mathrm{d}f_{an}(\upsilon)}{\mathrm{d}\upsilon} + \epsilon \quad \textit{whenever} \quad \gamma < f_{an}(\upsilon)\,. \tag{4.7}$$

Then there exists an intersecting function $\Lambda \in C^1(\mathbb{R}^2, \mathbb{R})$ such that

(1) $\Lambda(\gamma, \upsilon) \leq \upsilon$ *whenever* $\gamma \geq f_{an}(\upsilon)$ *and* $\Lambda(\gamma, \upsilon) > \upsilon$ *otherwise.*

(2) $\omega_\Phi(\Lambda(\gamma, \upsilon), \gamma, \upsilon) = f_{an}(\Lambda(\gamma, \upsilon))$. *(4.8)*

(3) *Moreover, for all* $u_\Phi \in C^1$, $y_\Phi := \Phi(u_\Phi, y_{\Phi_0})$, *we have that* $\frac{\mathrm{d}}{\mathrm{d}t}\Lambda(y_\Phi(t), u_\Phi(t))$ *exists.*

Proof: Following the same procedure of the proof of 4.1.1, we first define the continuous function $\varphi : \mathbb{R}^3 \to \mathbb{R}$ defined as $\varphi(\upsilon, y_{\Phi_0}, u_{\Phi_0}) = \omega_\Phi(\upsilon, y_{\Phi_0}, u_{\Phi_0}) - f_{an}(\upsilon)$. Consider also A_0 and A_1 the two subsets of $\mathbb{R}^3$ defined as,

$$A_0 = \{(\upsilon, y_{\Phi_0}, u_{\Phi_0}) \in \mathbb{R}^3,\ y_{\Phi_0} > f_{an}(u_{\Phi_0})\ ,\ \upsilon < u_{\Phi_0}\}\ ,$$
$$A_1 = \{(\upsilon, y_{\Phi_0}, u_{\Phi_0}) \in \mathbb{R}^3,\ y_{\Phi_0} < f_{an}(u_{\Phi_0})\ ,\ \upsilon > u_{\Phi_0}\}\ .$$

Note that the function f_{an} being strictly increasing by assumption, implies that these sets are open sets. Also, the function ω_Φ satisfies

$$\frac{\partial \omega_\Phi}{\partial \upsilon}(\upsilon, y_{\Phi_0}, u_{\Phi_0}) = f_2(\omega_\Phi(\upsilon, y_{\Phi_0}, u_{\Phi_0}), \upsilon) \qquad \forall (\upsilon, y_{\Phi_0}, u_{\Phi_0}) \in A_0\ ,$$
$$\frac{\partial \omega_\Phi}{\partial \upsilon}(\upsilon, y_{\Phi_0}, u_{\Phi_0}) = f_1(\omega_\Phi(\upsilon, y_{\Phi_0}, u_{\Phi_0}), \upsilon) \qquad \forall (\upsilon, y_{\Phi_0}, u_{\Phi_0}) \in A_1\ .$$

Consequently, $\omega_\Phi(\upsilon, y_{\Phi_0}, u_{\Phi_0})$ is the solution of the ordinary differential equations computed from C^1 vector field. With [15, Theorem V.3.1], it implies that ω_Φ is a C^1 function in $A_0 \cup A_1$. Moreover, the function f_{an} being C^1 implies that the function φ is C^1 in $A_0 \cup A_1$. With (4.6) and (4.7), the function φ satisfies,

$$\frac{\partial \varphi}{\partial \upsilon}(\upsilon, y_{\Phi_0}, u_{\Phi_0}) \quad > \quad \epsilon \neq 0\ ,\ \forall (\upsilon, y_{\Phi_0}, u_{\Phi_0}) \in A_0 \cup A_1\ .$$

Consequently, φ is a strictly increasing function in its first argument in the set $A_0 \cup A_1$. This also implies that,

$$\varphi(\upsilon, y_{\Phi_0}, u_{\Phi_0}) < \varphi(u_{\Phi_0}, y_{\Phi_0}, u_{\Phi_0}) + \epsilon(\upsilon - u_{\Phi_0})$$
$$\forall (\upsilon, y_{\Phi_0}, u_{\Phi_0}) \in A_0\ ,$$
$$\varphi(\upsilon, y_{\Phi_0}, u_{\Phi_0}) > \varphi(u_{\Phi_0}, y_{\Phi_0}, u_{\Phi_0}) + \epsilon(\upsilon - u_{\Phi_0})$$
$$\forall (\upsilon, y_{\Phi_0}, u_{\Phi_0}) \in A_1\ .$$

Note that if $y_{\Phi_0} > f_{an}(u_{\Phi_0})$, then $\varphi(u_{\Phi_0}, y_{\Phi_0}, u_{\Phi_0}) > 0$ and consequently there exists a unique real number u^*_Φ such that $\varphi(u^*_\Phi, y_{\Phi_0}, u_{\Phi_0}) = 0$ and $(u^*_\Phi, y_{\Phi_0}, u_{\Phi_0}) \in A_0$. On the other hand, if $y_{\Phi_0} < f_{an}(u_{\Phi_0})$, then $\varphi(u_{\Phi_0}, y_{\Phi_0}, u_{\Phi_0}) < 0$ and consequently there exists a unique real number u^*_Φ such that $\varphi(u^*_\Phi, y_{\Phi_0}, u_{\Phi_0}) = 0$ and $(u^*_\Phi, y_{\Phi_0}, u_{\Phi_0}) \in A_1$.

Therefore, denoting $\Lambda(y_{\Phi_0}, u_{\Phi_0}) = u^*_\Phi$, by employing the implicit function theorem and using the fact that φ is C^1, it can be shown that Λ is C^1. □

Similarly, using the traversing function ν_Φ, we can define an intersecting function Γ, which describes the intersection between $\nu_\Phi(\cdot, \gamma, \upsilon)$ and $f_{an}(\cdot)$. The function $\Gamma : \mathbb{R}^2 \to \mathbb{R}$ is an *CW intersecting function* (corresponding to ν_Φ and f_{an}) if $\nu_\Phi(\Gamma(\gamma, \upsilon), \gamma, \upsilon) = f_{an}(\Gamma(\gamma, \upsilon))$ for all $(\gamma, \upsilon) \in \mathbb{R}^2$; and $\Gamma(\gamma, \upsilon) \geq \upsilon$ whenever $\gamma \geq f_{an}(\upsilon)$ and $\Gamma(\gamma, \upsilon) < \upsilon$ otherwise. The following lemma gives sufficient conditions on f_1 and f_2 for the existence of such an intersecting function Γ.

Lemma 4.1.4 *Assume that f_1 and f_2 in* (4.1) *be such that f_1, f_2 and f_{an} are C^1. Moreover, assume that f_{an} is strictly increasing and there exists a positive real number ϵ such that for all $(\gamma, \upsilon) \in \mathbb{R}^2$ the inequalities* (4.6) *and* (4.7) *given in Lemma 4.1.3 hold. Then there exists an intersecting function $\Gamma \in C^1(\mathbb{R}^2)$ (corresponding to ν_Φ and f_{an}) such that*

(1) *$\Gamma(\gamma, \upsilon) \leq \upsilon$ whenever $\gamma \geq f_{an}(\upsilon)$ and $\Gamma(\gamma, \upsilon) > \upsilon$ otherwise.*

(2) *$\nu_\Phi(\Gamma(\gamma, \upsilon), \gamma, \upsilon) = f_{an}(\Gamma(\gamma, \upsilon))$.*

(3) *Moreover, for all $u_\Phi \in C^1$, $y_\Phi := \Phi(u_\Phi)$, $\frac{\mathrm{d}}{\mathrm{d}t}\Gamma(y_\Phi(t), u_\Phi(t))$ exists.*

The proof of Lemma 4.1.4 is similar to the proof of Lemma 4.1.3.

4.2 Dissipativity of The Duhem Hysteresis Operator with CCW I/O Behavior

Based on the functions we defined in the previous section, the dissipativity property of the Duhem hysteresis operator is analyzed in this section and Section 4.3. Here, we focus on the Duhem hysteresis operator with CCW I/O behavior. First, two candidates of storage functions are proposed by using the traversing function ω_Φ and its dual ν_Φ. Then, we show that these storage functions satisfy the CCW dissipation inequality.

4.2.1 Storage Function Using ω_Φ

Using f_{an}, ω_Φ and Ω, we can define a candidate storage function $H_{\circlearrowleft_1} : \mathbb{R}^2 \to \mathbb{R}$ by

$$H_{\circlearrowleft_1}(\gamma, \upsilon) = \gamma\upsilon + \int_{\upsilon}^{\Omega(\gamma,\upsilon)} \omega_\Phi(\sigma, \gamma, \upsilon)\mathrm{d}\sigma - \int_{0}^{\Omega(\gamma,\upsilon)} f_{an}(\sigma)\mathrm{d}\sigma. \tag{4.9}$$

where Ω is the CCW intersecting function (corresponding to ω_Φ and f_{an}) as in Lemma 4.1.1. The graphical interpretation of $H_{\circlearrowleft_1}$ is shown in Figure 4.3 using an I/O phase plot which is obtained from a Duhem hysteresis operator Φ with

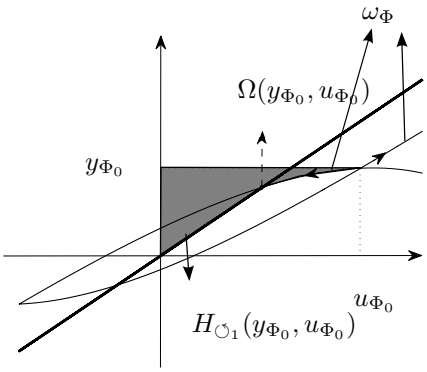

Figure 4.3: Graphical interpretation of the storage function $H_{\circlearrowleft_1}(y_{\Phi_0}, u_{\Phi_0})$ in (4.9), where the Duhem hysteresis operator Φ is defined in (3.1) with $f_1(\gamma, \upsilon) = -0.15\gamma + 0.48\upsilon + 1.5$,$f_2(\gamma, \upsilon) = 0.15\gamma - 0.48\upsilon + 1.5$. For a given (y_{Φ_0}, u_{Φ_0}), $H_{\circlearrowleft_1}$ is equal to the area in dark grey

$f_1(\gamma, \upsilon) = -0.15\gamma + 0.48\upsilon + 1.5$, $f_2(\gamma, \upsilon) = 0.15\gamma - 0.48\upsilon + 1.5$. In this figure, given a point (y_{Φ_0}, u_{Φ_0}) the value of $H_{\circlearrowleft_1}(y_{\Phi_0}, u_{\Phi_0})$ is equal to the dark grey area enclosed by the vertical axis, the curve ω_Φ and the anhysteresis curve f_{an}.

Theorem 4.2.1 *Consider the Duhem hysteresis operator Φ defined in* (3.1) *with C^1 functions $f_1, f_2 : \mathbb{R}^2 \to \mathbb{R}$ and the corresponding anhysteresis function f_{an} be C^1. Suppose that there exists an CCW intersecting function Ω and the following condition holds for all $(\gamma, \upsilon) \in \mathbb{R}^2$*

(A) *$f_1(\gamma, \upsilon) \geq f_2(\gamma, \upsilon)$ whenever $\gamma \leq f_{an}(\upsilon)$, and $f_1(\gamma, \upsilon) < f_2(\gamma, \upsilon)$ otherwise.*

Then for every $u_\Phi \in AC(\mathbb{R}_+)$ and for every $y_{\Phi_0} \in \mathbb{R}$, the function $t \mapsto H_{\circlearrowleft_1}\big((y_\Phi(t), u_\Phi(t)\big)$ with $y_\Phi := \Phi(u_\Phi, y_{\Phi_0}))$ and $H_{\circlearrowleft_1}$ as in (4.9) *is right-differentiable and satisfies*

$$\frac{\mathrm{d}H_{\circlearrowleft_1}(y_\Phi(t), u_\Phi(t))}{\mathrm{d}t} \leq \dot{y}_\Phi(t) u_\Phi(t). \tag{4.10}$$

Moreover, if $f_1 \geq 0$ and $f_2 \geq 0$ then Φ is CCW and dissipative with respect to the supply rate $\dot{y}_\Phi u_\Phi$ with the storage function $H_{\circlearrowleft_1}$, i.e., $H_{\circlearrowleft_1}$ is non-negative.

Proof:

For any real valued function z, we denote $\frac{\mathrm{d}}{\mathrm{d}t} z(t) := \lim_{h \searrow 0_+} \frac{z(t+h) - z(t)}{h}$. The proof of Theorem 4.2.1 consists of two parts. In the first part we show that for al-

most all $t \in \mathbb{R}_+$, $\dot{H}_{\circlearrowleft_1}\big((\Phi(u_\Phi, y_{\Phi_0}))(t), u_\Phi(t)\big)$ exists. In the second part we show the nonnegativity of $H_{\circlearrowleft_1}$.

1. Let $u_\Phi \in AC(\mathbb{R}_+), y_{\Phi_0} \in \mathbb{R}$ and denote $u_\Phi^* := \Omega(y_\Phi, u_\Phi)$.

First, we prove that for almost all $t \in \mathbb{R}_+$, $\dot{H}_{\circlearrowleft_1}\big((\Phi(u_\Phi, y_{\Phi_0}))(t), u_\Phi(t)\big)$ exists. Using (4.9) and denoting $y_\Phi := (\Phi(u_\Phi, y_{\Phi_0}))$, we have

$$\frac{\mathrm{d}H_{\circlearrowleft_1}\big(y_\Phi(t), u_\Phi(t)\big)}{\mathrm{d}t} = \dot{y}_\Phi(t)u_\Phi(t) + \int_{u_\Phi(t)}^{u_\Phi^*(t)} \frac{\mathrm{d}}{\mathrm{d}t}\omega_\Phi(\upsilon, y_\Phi(t), u_\Phi(t))\mathrm{d}\upsilon + \Big[\omega_\Phi(u_\Phi^*(t), y_\Phi(t), u_\Phi(t)) - f_{an}(u_\Phi^*(t))\Big]\dot{u}_\Phi^*(t), \quad (4.11)$$

where we have invoked $\omega_\Phi(u_\Phi(t), y_\Phi(t), u_\Phi(t)) = y_\Phi(t)$. Let $t \geq 0$. The first term in the RHS of (4.11) exists for almost all $t \geq 0$ since $y_\Phi(t)$ satisfies (3.1). Note that since $\omega_\Phi(u_\Phi^*(t), y_\Phi(t), u_\Phi(t)) = f_{an}(u_\Phi^*(t))$, the third term in the RHS of (4.11) is zero since $\dot{u}_\Phi^*(t)$ exists by the definition of Ω.

In order to get the dissipativity with the supply rate (4.10), it remains to check whether the second term in the RHS of (4.11) exists, is finite and satisfies

$$\int_{u_\Phi(t)}^{u_\Phi^*(t)} \frac{\mathrm{d}}{\mathrm{d}t}\omega_\Phi(\upsilon, y_\Phi(t), u_\Phi(t))\mathrm{d}\upsilon \leq 0. \quad (4.12)$$

It suffices to show that, for every $\upsilon \in [u_\Phi(t), u_\Phi^*(t)]$, the following right derivative

$$\lim_{\epsilon \searrow 0^+} \frac{1}{\epsilon}[\omega_\Phi(\upsilon, y_\Phi(t+\epsilon), u_\Phi(t+\epsilon)) - \omega_\Phi(\upsilon, y_\Phi(t), u_\Phi(t))] \quad (4.13)$$

exists and the limit is less or equal to zero when $u_\Phi^*(t) > u_\Phi(t)$ and the limit is greater or equal to zero elsewhere. For any $\epsilon \geq 0$, let us introduce the continuous function $\omega_\epsilon : \mathbb{R} \to \mathbb{R}$ by

$$\omega_\epsilon(\upsilon) = \omega_\Phi(\upsilon, y_\Phi(t+\epsilon), u_\Phi(t+\epsilon)). \quad (4.14)$$

More precisely, for every $\epsilon \geq 0$, ω_ϵ is the unique solution of

$$\omega_\epsilon(\upsilon) = \begin{cases} y_\Phi(t+\epsilon) + \displaystyle\int_{u_\Phi(t+\epsilon)}^{\upsilon} f_1(\omega_\epsilon(\sigma), \sigma)\mathrm{d}\sigma, & \forall \upsilon \geq u_\Phi(t+\epsilon), \\ y_\Phi(t+\epsilon) + \displaystyle\int_{u_\Phi(t+\epsilon)}^{\upsilon} f_2(\omega_\epsilon(\sigma), \sigma)\mathrm{d}\sigma, & \forall \upsilon \leq u_\Phi(t+\epsilon). \end{cases} \quad (4.15)$$

Note that $\omega_0(\upsilon) = \omega_\Phi(\upsilon, y_\Phi(t), u_\Phi(t))$ for all $\upsilon \in \mathbb{R}$ and

$$\omega_\epsilon(u_\Phi(t+\epsilon)) = y_\Phi(t+\epsilon), \qquad \forall\, \epsilon \in \mathbb{R}_+. \quad (4.16)$$

In order to show the existence of (4.13), we consider several cases depending on the sign of $\dot{u}_\Phi(t)$ and $y_\Phi(t) - f_{an}(u_\Phi(t))$.

First, we assume that $\dot{u}_\Phi(t) > 0$. This implies that there exists a sufficiently small $\delta > 0$ such that for every $\epsilon \in (0, \delta]$, we have $u_\Phi(t+\epsilon) > u_\Phi(t)$ and $\omega_0(u_\Phi(t+\epsilon)) = y_\Phi(t) + \int_{u_\Phi(t)}^{u_\Phi(t+\epsilon)} f_1(\omega_0(\sigma), \sigma)\, \mathrm{d}\sigma$. Moreover, with the change of integration variable $\sigma = u_\Phi(\tau)$ we obtain

$$\omega_0(u_\Phi(t+\epsilon)) = y_\Phi(t) + \int_t^{t+\epsilon} f_1(\omega_0(u_\Phi(\tau)), u_\Phi(\tau))\ \dot{u}_\Phi(\tau)\ \mathrm{d}\tau, \quad \forall \epsilon \in [0, \delta].$$

The functions $\epsilon \mapsto \omega_0(u_\Phi(t+\epsilon))$ and $\epsilon \mapsto y_\Phi(t+\epsilon)$ with $\epsilon \in (0, \delta]$ are two AC functions which are solutions of the same locally Lipschitz ODE and with the same initial value. By uniqueness of solution, we get $\omega_0(u_\Phi(t+\epsilon)) = y_\Phi(t+\epsilon)$. This fact together with (4.16) shows that

$$\omega_\epsilon(u_\Phi(t+\epsilon)) = \omega_0(u_\Phi(t+\epsilon)), \qquad \forall \epsilon \in [0, \delta].$$

Let us evaluate (4.13) when $y_\Phi(t) \geq f_{an}(u_\Phi(t))$. In this case, we have $u_\Phi(t) < u_\Phi^*(t)$ from the property of Ω. Also, since for every $\epsilon \in (0, \delta]$ the two functions $\omega_\epsilon(\upsilon)$ and $\omega_0(\upsilon)$ satisfy the same ODE for $\upsilon \in [u_\Phi(t+\epsilon), u_\Phi^*(t)]$ (we have for all $\tau \in [u_\Phi(t+\epsilon), u_\Phi^*(t)]$:$\frac{\mathrm{d}\omega_\epsilon(\tau)}{\mathrm{d}\tau} = f_1(\omega_\epsilon(\tau), \tau)$, $\frac{\mathrm{d}\omega_0(\tau)}{\mathrm{d}\tau} = f_1(\omega_0(\tau), \tau)$), we have $\omega_\epsilon(\upsilon) = \omega_0(\upsilon)$ for all $\upsilon \in [u_\Phi(t+\epsilon), u_\Phi^*(t)]$ and for all $\epsilon \in [0, \delta]$. This implies that

$$\lim_{\epsilon \searrow 0^+} \frac{1}{\epsilon}[\omega_\epsilon(\upsilon) - \omega_0(\upsilon)] \ = \ 0, \qquad \forall \upsilon \in [u_\Phi(t), u_\Phi^*(t)]. \tag{4.17}$$

Therefore, the inequality (4.12) holds for almost all $\dot{u}_\Phi(t) > 0$ and $y_\Phi(t) \geq f_{an}(u_\Phi(t))$. Now, we check (4.12) when $y_\Phi(t) < f_{an}(u_\Phi(t))$ and $\dot{u}_\Phi(t) > 0$ that is not of measure zero. Note that by the definition of Ω, $u_\Phi^*(t) < u_\Phi(t)$ which implies that the integrand in (4.12) is evaluated for all $\upsilon \in [u_\Phi^*(t), u_\Phi(t)]$. Also, since $\dot{u}_\Phi(t) > 0$, there exists $\delta > 0$ such that we have $\upsilon \leq u_\Phi(t) < u_\Phi(\tau)$ and $\dot{u}_\Phi(\tau) > 0$ for all $\tau \in (t, t+\gamma)$. It follows from (4.15) and assumption (**A**) that for every $\epsilon \in (0, \delta)$ and for all $\tau \in [t, t+\epsilon]$,

$$\begin{aligned} \frac{\mathrm{d}\omega_\epsilon(u_\Phi(\tau))}{\mathrm{d}\tau} &= f_2(\omega_\epsilon(u_\Phi(\tau)), u_\Phi(\tau))\ \dot{u}_\Phi(\tau) \\ &\leq f_1(\omega_\epsilon(u_\Phi(\tau)), u_\Phi(\tau))\ \dot{u}_\Phi(\tau). \end{aligned}$$

The function y_Φ satisfies

$$\frac{\mathrm{d}y_\Phi(\tau)}{\mathrm{d}\tau} \ = \ f_1(y_\Phi(\tau), u_\Phi(\tau))\ \dot{u}_\Phi(\tau), \qquad \forall \tau \ \in \ [t, t+\epsilon].$$

Since $\omega_\epsilon(u_\Phi(t+\epsilon)) = y_\Phi(t+\epsilon)$ and using the comparison principle (in reverse direction), we get that for every $\epsilon \in [0, \delta)$, $\omega_\epsilon(u_\Phi(\tau)) \ \geq \ y_\Phi(\tau)$ for all $\tau \in [t, t+\epsilon]$.

Since the two functions $\omega_\epsilon(\upsilon)$ and $\omega_0(\upsilon)$ for $\upsilon \in [u^*_\Phi(t), u_\Phi(t)]$ are two solutions of the same ODE, it follows that $\omega_\epsilon(\upsilon) \geq \omega_0(\upsilon)$, for all $\tau \leq u_\Phi(t)$ (Otherwise there exist $\tau_1 < \tau_2$ such that $\omega_\epsilon(\tau_1) = \omega_0(u_\Phi(\tau_1))$ and $\omega_\epsilon(\tau_2) > \omega_0(u_\Phi(\tau_2))$ which contradict the uniqueness of the solution of the locally Lipschitz ODE). The next step is to show that whether the following limit exists:

$$\lim_{\epsilon \searrow 0^+} \frac{1}{\epsilon}[\omega_\epsilon(\upsilon) - \omega_0(\upsilon)] \geq 0, \qquad \forall \upsilon \in [u^*_\Phi(t), u_\Phi(t)]. \tag{4.18}$$

To show the existence of (4.18), we compute a bound on the function $\epsilon \mapsto \frac{1}{\epsilon}[\omega_\epsilon(\upsilon) - \omega_0(\upsilon)]$. Note that for every $\epsilon \in [0, \delta]$,

$$\begin{aligned} |\omega_\epsilon(\upsilon) - \omega_0(\upsilon)| \leq |y_\Phi(t+\epsilon) - y_\Phi(t)| &+ \int_{u_\Phi(t)}^{u_\Phi(t+\epsilon)} |f_2(\omega_\epsilon(\sigma), \sigma)| \mathrm{d}\sigma \\ &+ \int_{\upsilon}^{u_\Phi(t)} |f_2(\omega_\epsilon(\sigma), \sigma) - f_2(\omega_0(\sigma), \sigma)| \mathrm{d}\sigma, \\ &\forall \upsilon \in [u^*_\Phi(t), u_\Phi(t)]. \end{aligned}$$

By the locally Lipschitz property of f_2, by the boundedness of f_2 and by the boundedness of ω_ϵ on $[\upsilon, u_\Phi(t)]$ for all $\epsilon \in [0, \delta]$, we obtain

$$\begin{aligned} |\omega_\epsilon(\upsilon) - \omega_0(\upsilon)| \leq |y_\Phi(t+\epsilon) - y_\Phi(t)| &\\ + \int_{\upsilon}^{u_\Phi(t)} L\,|\omega_\epsilon(\sigma) - \omega_0(\sigma)|\,\mathrm{d}\sigma &+ \varsigma |u_\Phi(t+\epsilon) - u_\Phi(t)|, \end{aligned}$$

where ς is a bound of f_2 on a compact set and L is the Lipschitz constant of f_2 on $[\omega_{\min}, \omega_{\max}] \times [\upsilon, u_\Phi(t)]$ with

$$\omega_{\min} := \min_{(\epsilon,\sigma) \in [0,\delta] \times [\upsilon, u_\Phi(t)]} \omega_\epsilon(\sigma), \quad \omega_{\max} := \max_{(\epsilon,\sigma) \in [0,\delta] \times [\upsilon, u_\Phi(t)]} \omega_\epsilon(\sigma).$$

With the Gronwall's lemma [27], this implies that for every $\epsilon \in [0, \delta]$,

$$\begin{aligned} |\omega_\epsilon(\upsilon) - \omega_0(\upsilon)| \leq \exp((u_\Phi(t) - \upsilon)L) \Big[|y_\Phi(t+\epsilon) - y_\Phi(t)| + \varsigma |u_\Phi(t+\epsilon) - u_\Phi(t)| \Big], \\ \forall \upsilon \in [u^*_\Phi(t), u_\Phi(t)]. \end{aligned}$$

Hence

$$\begin{aligned} \lim_{\epsilon \searrow 0^+} \frac{1}{\epsilon} |\omega_\epsilon(\upsilon) - \omega_0(\upsilon)| \leq \exp((u_\Phi(t) - \upsilon)L) \Big[|f_1(y_\Phi(t), u_\Phi(t))| + \varsigma \Big] \dot{u}(t), \\ \forall \upsilon \in [u^*_\Phi(t), u_\Phi(t)]. \end{aligned}$$

Consequently the limit given in (4.33) exists. It implies that the inequality (4.12) holds for almost all $\dot{u}_\Phi(t) > 0$ and $y_\Phi(t) < f_{an}(u_\Phi(t))$. We can use similar arguments to prove that (4.12) is satisfied for almost all $\dot{u}_\Phi(t) < 0$. Finally, when $\dot{u}_\Phi(t) = 0$, we simply get $\lim_{\epsilon \searrow 0^+} \frac{1}{\epsilon}|\omega_\epsilon(\upsilon) - \omega_0(\upsilon)| = 0$, by the continuity of the above bound.

2. To prove the last claim, we need to show that $H_{\circlearrowleft_1}$ is non-negative.

$$H_{\circlearrowleft_1}(y_\Phi(t), u_\Phi(t)) = \int_0^{u_\Phi(t)} y_\Phi(t) - f_{an}(\upsilon)\,\mathrm{d}\upsilon + \int_{u_\Phi(t)}^{\Omega(y_\Phi(t),u_\Phi(t))} \omega_\Phi(\upsilon, y_\Phi(t), u_\Phi(t)) - f_{an}(\upsilon)\,\mathrm{d}\upsilon \geq 0.$$

It is assumed in the hypotheses that f_1 is positive. If $u_\Phi(t) \geq 0$ and $y_\Phi(t) \geq f_{an}(u_\Phi(t))$, we have that $f_{an}(\upsilon) \leq y_\Phi(t)$ for all $\upsilon \in [0, u_\Phi(t)]$ and $f_{an}(\upsilon) \leq \omega_\Phi(\upsilon, y_\Phi(t), u_\Phi(t))$ for all $\upsilon \in [u_\Phi(t), \Omega(y_\Phi(t), u_\Phi(t))]$ by the definition of Ω.

On the other hand, if $u_\Phi(t) < 0$ and $y_\Phi(t) \geq f_{an}(u_\Phi(t))$, we have that $y_\Phi(t) \leq \omega_\Phi(\upsilon, y_\Phi(t), u_\Phi(t))$ for all $\upsilon \in [u_\Phi(t), 0]$ (due to the positivity of f_1). Also, by the definition of Ω, $\Omega(y_\Phi(t), u_\Phi(t)) \geq 0$ implies that $f_{an}(\upsilon) \leq \omega_\Phi(\upsilon, y_\Phi(t), u_\Phi(t))$ for all $\upsilon \in [0, \Omega(y_\Phi(t), u_\Phi(t))]$. Similarly, $\Omega(y_\Phi(t), u_\Phi(t)) < 0$ implies that $f_{an}(\upsilon) > \omega_\Phi(\upsilon, y_\Phi(t), u_\Phi(t))$ for all $\upsilon \in [\Omega(y_\Phi(t), u_\Phi(t)), 0]$. Hence

$$H_{\circlearrowleft_1}(y_\Phi(t), u_\Phi(t)) = -\int_{u_\Phi(t)}^{0} y_\Phi(t) - \omega_\Phi(\upsilon, y_\Phi(t), u_\Phi(t))\,\mathrm{d}\upsilon + \int_0^{\Omega(y_\Phi(t),u_\Phi(t))} \omega_\Phi(\upsilon, y_\Phi(t), u_\Phi(t)) - f_{an}(\upsilon)\,\mathrm{d}\upsilon \geq 0.$$

For the case $y_\Phi(t) < f_{an}(u_\Phi(t))$, the non-negativity of $H_{\circlearrowleft_1}$ can be checked using the same routine and using the positivity of f_2.

The CCW property can be easily checked by integrating (4.9) from 0 to T we have

$$H_{\circlearrowleft_1}\big(y_\Phi(T), u_\Phi(T)\big) - H_{\circlearrowleft_1}\big(y_\Phi(0), u_\Phi(0)\big) = \int_0^T \dot{y}_\Phi(\tau) u_\Phi(\tau)\mathrm{d}\tau.$$

Since $H_{\circlearrowleft_1}$ is nonnegative then

$$\int_0^T \dot{y}_\Phi(\tau) u_\Phi(\tau)\mathrm{d}\tau \geq -H_{\circlearrowleft_1}(y_\Phi(0), u_\Phi(0)) > -\infty.$$

□

Remark 4.2.2 *In addition to the result in Theorem 4.2.1, if f_1 and f_2 satisfy the hypotheses given in Theorem 4.2.1, then for every $u_\Phi \in AC(\mathbb{R}_+)$ and $y_{\Phi_0} \in \mathbb{R}$, the function $t \to H_{\circlearrowleft_1}(y_\Phi(t), u_\Phi(t))$ with $H_{\circlearrowleft_1}$ as in* (4.9) *is left-differentiable and satisfies*

$$\lim_{h \nearrow 0^-} \frac{H_{\circlearrowleft_1}(y_\Phi(t+h), u_\Phi(t+h)) - H_{\circlearrowleft_1}(y_\Phi(t), u_\Phi(t))}{h} \leq y_\Phi(t)\dot{u}_\Phi(t).$$

The proof of this claim follows a similar line as that of Theorem 4.2.1.

The results given in Theorem 4.2.1 can be slightly generalized in order to incorporate the case when the Duhem hysteresis operator Φ has saturated output. Consider the set $\mathcal{D} \subset \mathbb{R}^2$ which contains all relations of Φ, i.e., $\mathbf{R}_{y_{\Phi_0}, u_\Phi} := \{(y_\Phi(t), u_\Phi(t)) \in \mathbb{R}^2 | y_\Phi = \Phi(u_\Phi, y_{\Phi_0}), t \in \mathbb{R}_+\} \subset \mathcal{D}$ holds for all $u_\Phi \in AC(\mathbb{R}_+)$ and $(y_{\Phi_0}, u_\Phi(0)) \in \mathcal{D}$.

Proposition 4.2.3 *Consider the Duhem hysteresis operator Φ defined in* (3.1) *with C^1 functions $f_1, f_2 : \mathcal{D} \to \mathbb{R}$ and with the traversing function ω_Φ and the anhysteresis function f_{an}. Assume that the anhysteresis curve is in $\mathcal{D}$ and there exists an CCW intersecting function Ω (e.g., the hypotheses in Lemma 4.1.1 hold). Assume further that the Assumption* **(A)** *holds for all (γ, υ) in $\mathcal{D}$. Then for every $u_\Phi \in AC(\mathbb{R}_+)$ and $(y_{\Phi_0}, u_\Phi(0)) \in \mathcal{D}$, the function $t \to H_{\circlearrowleft_1}(y_\Phi(t), u_\Phi(t))$ with $H_{\circlearrowleft_1}$ as in* (4.9) *and $y_\Phi := \Phi(u_\Phi, y_{\Phi_0})$ is right differentiable and satisfies* (4.10)*, i.e. the Duhem operator is CCW.*

The proof of Proposition 4.2.3 follows the same arguments as that of Theorem 4.2.1. In the following proposition, we show the radially unboundedness of $H_{\circlearrowleft_1}$ with respect to its first argument.

Proposition 4.2.4 *Consider the Duhem operator Φ with $f_1, f_2 \geq 0$ satisfying the hypotheses in Theorem 4.2.1. Suppose that $f_{an}(0) = 0$. Then the function $H_{\circlearrowleft_1}(\cdot, \upsilon)$ (where $H_{\circlearrowleft_1}$ is as in* (4.9)*) is radially unbounded for every υ.*

Proof: Let us consider $\upsilon > 0$. To show the properness of $H_{\circlearrowleft_1}(\cdot, \upsilon)$, let us first consider the case where $\gamma \geq f_{an}(\upsilon)$. In this case, we rewrite the function $H_{\circlearrowleft_1}$, as follows

$$H_{\circlearrowleft_1}(\gamma, \upsilon) = \int_0^\upsilon \gamma - f_{an}(\sigma)\mathrm{d}\sigma + \int_\upsilon^{\Omega(\gamma,\upsilon)} \omega_\Phi(\sigma, \gamma, \upsilon) - f_{an}(\sigma)\mathrm{d}\sigma$$

Due to the property of the CCW intersecting function Ω, $\gamma \geq f_{an}(\upsilon)$ implies that $\Omega(\gamma, \upsilon) \geq \upsilon$. Hence the last term on the RHS of the above equation is non-negative,

i.e., $\int_{\upsilon}^{\Omega(\gamma,\upsilon)} \omega_\Phi(\sigma,\gamma,\upsilon) - f_{an}(\sigma)\mathrm{d}\sigma \geq 0$. Then,

$$\begin{aligned} H_{\circlearrowleft_1}(\gamma,\upsilon) &\geq \int_0^{\upsilon} \gamma - f_{an}(\sigma)\mathrm{d}\sigma \\ &\geq \int_0^{\upsilon} \gamma - f_{an}(\upsilon)\mathrm{d}\sigma \qquad (4.19) \\ &= (\gamma - c)\upsilon, \qquad (4.20) \end{aligned}$$

where $c := f_{an}(\upsilon)$. Equation (4.19) indicates that for every $\upsilon > 0$, $H_{\circlearrowleft_1}(\gamma,\upsilon) \to \infty$ as $\gamma \to \infty$.

To evaluate the other limit when $\gamma \to -\infty$, let us consider the case when $\gamma < 0$. Note that in this case $\gamma < f_{an}(\upsilon)$ due to the monotonicity assumption on f_{an} and $f_{an}(0) = 0$. Rewriting $H_{\circlearrowleft_1}$, we have

$$\begin{aligned} H_{\circlearrowleft_1}(\gamma,\upsilon) &= \int_0^{\Omega(\gamma,\upsilon)} \gamma - f_{an}(\sigma)\mathrm{d}\sigma + \int_{\Omega(\gamma,\upsilon)}^{\upsilon} \gamma - \omega_\Phi(\sigma,\gamma,\upsilon)\mathrm{d}\sigma \\ &\geq \int_0^{\Omega(\gamma,\upsilon)} \gamma - f_{an}(\sigma)\mathrm{d}\sigma \\ &= \int_{\Omega(\gamma,\upsilon)}^{0} f_{an}(\sigma) - \gamma\mathrm{d}\sigma. \end{aligned}$$

The last inequality is obtained due to the property of the CCW intersecting function Ω, where $\Omega(\gamma,\upsilon) < \upsilon$ whenever $\gamma < f_{an}(\upsilon)$. Since ω_Φ is monotone and non-decreasing (due to the positivity of f_1 and f_2) and using the fact that f_{an} is monotone increasing and $f_{an}(0) = 0$, it can be checked that $\gamma < 0$ implies that $\Omega(\gamma,\upsilon) < 0$.

Now let us fix $\bar{\gamma}$ such that $0 > \bar{\gamma} > \gamma$. Using the fact that $\omega_\Phi(\sigma,\bar{\gamma},\upsilon) \geq \omega_\Phi(\sigma,\gamma,\upsilon)$ for all $\sigma < \upsilon$ and using monotonicity of f_{an}, it follows that $0 > \bar{\Omega} > \Omega(\gamma,\upsilon)$ where the constant $\bar{\Omega} := \Omega(\bar{\gamma},\upsilon)$. Thus

$$\begin{aligned} H_{\circlearrowleft_1}(\gamma,\upsilon) &\geq \int_{\Omega(\gamma,\upsilon)}^{0} f_{an}(\sigma) - \gamma\mathrm{d}\sigma \\ &= \int_{\Omega(\gamma,\upsilon)}^{\bar{\Omega}} f_{an}(\sigma) - \gamma\mathrm{d}\sigma + \int_{\bar{\Omega}}^{0} f_{an}(\sigma) - \gamma\mathrm{d}\sigma \\ &\geq \int_{\bar{\Omega}}^{0} f_{an}(\sigma) - \gamma\mathrm{d}\sigma \\ &\geq \int_{\bar{\Omega}}^{0} f_{an}(\bar{\Omega}) - \gamma\mathrm{d}\sigma \\ &= (\gamma - f_{an}(\bar{\Omega}))\bar{\Omega}. \end{aligned}$$

The last equality shows that as $\gamma \to -\infty$, $H_{\circlearrowleft_1} \to \infty$ since $\bar{\Omega} < 0$. Therefore, we can conclude that for the case $\upsilon > 0$, the function $H_{\circlearrowleft_1}(\cdot, \upsilon)$ is radially unbounded.

Using similar arguments we can get the same conclusion for the case when $\upsilon \leq 0$. □

Example 4.2.5 *Consider a semi-linear Duhem model [35] with* $A_+ = -\alpha_1, B_+ = \alpha_2, E_+ = \alpha_3, A_- = \alpha_1, B_- = -\alpha_2, E_- = \alpha_3, C = 1$ *and* $D = 0$. *In this case,*

$$f_1(\gamma, \upsilon) = -\alpha_1\gamma + \alpha_2\upsilon + \alpha_3, \qquad f_2(\gamma, \upsilon) = \alpha_1\gamma - \alpha_2\upsilon + \alpha_3,$$

and it can be computed that $f_{an}(\upsilon) = \frac{\alpha_2}{\alpha_1}\upsilon$ *for all* $\upsilon \in \mathbb{R}$. *Moreover, the hypotheses of Lemma 4.1.1 holds if* $\alpha_3 < \frac{\alpha_2}{\alpha_1}$.

A routine calculation of the curve ω_Φ (4.2) *gives us*

$$\begin{aligned}\omega_\Phi(\upsilon, y_\Phi(t), u_\Phi(t)) &= \upsilon\frac{\alpha_2}{\alpha_1} - \frac{\alpha_2}{\alpha_1^2} + \frac{\alpha_3}{\alpha_1} \\ &\quad + \left[y_\Phi(t) - u_\Phi(t)\frac{\alpha_2}{\alpha_1} + \frac{\alpha_2}{\alpha_1^2} - \frac{\alpha_3}{\alpha_1}\right] e^{(-\alpha_1(\upsilon - u_\Phi(t)))}, \quad \forall \upsilon \in [u_\Phi(t), \infty)\end{aligned}$$

and

$$\begin{aligned}\omega_\Phi(\upsilon, y_\Phi(t), u_\Phi(t)) &= \upsilon\frac{\alpha_2}{\alpha_1} + \frac{\alpha_2}{\alpha_1^2} - \frac{\alpha_3}{\alpha_1} \\ &\quad + \left[y_\Phi(t) - u_\Phi(t)\frac{\alpha_2}{\alpha_1} - \frac{\alpha_2}{\alpha_1^2} + \frac{\alpha_3}{\alpha_1}\right] e^{(\alpha_1(\upsilon - u_\Phi(t)))}, \quad \forall \upsilon \in (-\infty, u_\Phi(t)].\end{aligned}$$

The intersecting function $\Omega(y_\Phi(t), u_\Phi(t))$ *which is determined by* $f_{an}(u_\Phi^*(t))$ $= \omega_\Phi(u_\Phi^*(t), y_\Phi(t), u_\Phi(t))$. *The intersecting function* $\Omega(y_\Phi(t), u_\Phi(t))$ *for the case when* $y_\Phi(t) > f_{an}(u_\Phi(t))$ *is given by*

$$\Omega(y_\Phi(t), u_\Phi(t)) = u_\Phi(t) - \frac{1}{\alpha_1} ln\left[\frac{\frac{\alpha_2}{\alpha_1^2} - \frac{\alpha_3}{\alpha_1}}{y_\Phi(t) - u_\Phi(t)\frac{\alpha_2}{\alpha_1} + \frac{\alpha_2}{\alpha_1^2} - \frac{\alpha_3}{\alpha_1}}\right]$$

Note that by the assumption on α_3 *and since we consider* $y_\Phi(t) > \frac{\alpha_2}{\alpha_1}u_\Phi(t)$, *we have that* $\Omega(y_\Phi(t), u_\Phi(t)) > u_\Phi(t)$, *i.e., the intersection point is located to the right of* $u_\Phi(t)$. *On the other hand, when* $y_\Phi(t) \leq \frac{\alpha_2}{\alpha_1}u_\Phi(t)$, *the function* $\Omega(y_\Phi(t), u_\Phi(t))$ *is given by*

$$\Omega(y_\Phi(t), u_\Phi(t)) = u_\Phi(t) + \frac{1}{\alpha_1} ln\left[\frac{\frac{\alpha_3}{\alpha_1} - \frac{\alpha_2}{\alpha_1^2}}{y_\Phi(t) - u_\Phi(t)\frac{\alpha_2}{\alpha_1} - \frac{\alpha_2}{\alpha_1^2} + \frac{\alpha_3}{\alpha_1}}\right].$$

By the assumption on α_3 *and since we consider* $y_\Phi(t) \leq \frac{\alpha_2}{\alpha_1}u_\Phi(t)$, *we have that* $\Omega(y_\Phi(t), u_\Phi(t)) \leq u_\Phi(t)$.

It follows from the above computation that $\frac{\mathrm{d}}{\mathrm{d}t}\Omega(y_\Phi(t), u_\Phi(t))$ *exists and it is continuously differentiable.*

As an example on the construction of storage function, let us denote $k_1 = \frac{\alpha_2}{\alpha_1}$, $k_2 = \frac{\alpha_2}{\alpha_1^2} - \frac{\alpha_3}{\alpha_1}$ *and* $u_\Phi^*(t) = \Omega(y_\Phi(t), u_\Phi(t))$. *Using the construction of storage function as in Theorem 4.2.1 and using* ω_Φ *and* Ω *as above, the storage function* $H_{\circlearrowleft_1}$ *(when* $y_\Phi(t) > f_{an}(u_\Phi(t))$ *and* $u_\Phi(t) \leq 0$*) can be explicitly given by*

$$H_{\circlearrowleft_1}(y_\Phi(t), u_\Phi(t)) = y_\Phi(t)u_\Phi(t) - \frac{1}{2}k_1(u_\Phi(t))^2 - k_2\big(u_\Phi^*(t) - u_\Phi(t)\big) + \frac{1}{\alpha_1}\left[y_\Phi(t) - u_\Phi(t)k_1 + k_2\right]\left[1 - e^{(-\alpha_1(u_\Phi^*(t) - u_\Phi(t)))}\right].$$

In this subsection, we have shown the dissipativity property of the CCW Duhem hysteresis operator by constructing the storage function $H_{\circlearrowleft_1}$ (4.9) based on the traversing function ω_Φ. Furthermore, the radially unboundedness of $H_{\circlearrowleft_1}$ has also been studied.

4.2.2 Storage Function Using ν_Φ

Dual to the results from the previous subsection, using f_{an}, ν_Φ and Υ as given before, we can also define another candidate storage function $H_{\circlearrowleft_2} : \mathbb{R}^2 \to \mathbb{R}$ by

$$H_{\circlearrowleft_2}(\gamma, \upsilon) = \gamma\upsilon + \int_\upsilon^{\Upsilon(\gamma,\upsilon)} \nu_\Phi(\sigma, \gamma, \upsilon)\mathrm{d}\sigma - \int_0^{\Upsilon(\gamma,\upsilon)} f_{an}(\sigma)\mathrm{d}\sigma. \tag{4.21}$$

where Υ is the intersecting function (corresponding to ν_Φ and f_{an}) as in Lemma 4.1.2. The graphic interpretation of $H_{\circlearrowleft_2}$ is illustrated by the I/O phase plot of a Duhem hysteresis operator Φ with $f_1(\gamma, \upsilon) = -0.15\gamma + 0.48\upsilon + 1.5$, $f_2(\gamma, \upsilon) = 0.15\gamma - 0.48\upsilon + 1.5$ as in Figure 4.4. In the figure, given a point (y_{Φ_0}, u_{Φ_0}), the value of $H_{\circlearrowleft_2}(y_{\Phi_0}, u_{\Phi_0})$ is equal to the difference between light grey area and the dark grey area.

Theorem 4.2.6 *Consider the Duhem hysteresis operator* Φ *defined in* (3.1)-(4.1) *with* C^1 *functions* $f_1, f_2 : \mathbb{R}^2 \to \mathbb{R}$ *and the corresponding anhysteresis function* f_{an} *be* C^1. *Suppose that there exists an CCW intersecting function* Υ *and Assumption* **(A)** *in Theorem 4.2.1 hold. Then for every* $u_\Phi \in AC(\mathbb{R}_+)$ *and for every* $y_{\Phi_0} \in \mathbb{R}$, *the function* $t \mapsto H_{\circlearrowleft_2}\big((y_\Phi(t), u_\Phi(t)\big)$ *with* $y_\Phi := \Phi(u_\Phi, y_{\Phi_0}))$ *and* $H_{\circlearrowleft_2}$ *as in* (4.21) *is right-differentiable and satisfies* (4.10). *Moreover, if* $f_1 \geq 0$ *and* $f_2 \geq 0$ *then* Φ *is CCW and dissipative with respect to the supply rate* $\dot{y}_\Phi u_\Phi$ *with the storage function* $H_{\circlearrowleft_2}$, *i.e.,* $H_{\circlearrowleft_2}$ *is non-negative.*

The proof is similar to the proof of Theorem 4.2.1.

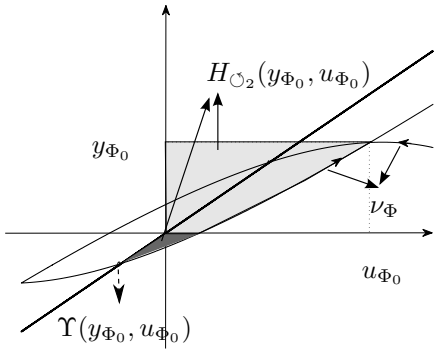

Figure 4.4: Graphical interpretation of the storage function $H_{\circlearrowleft_2}(y_{\Phi_0}, u_{\Phi_0})$ in (4.21), where the Duhem hysteresis operator Φ is defined as in (3.1) with $f_1(\gamma, \upsilon) = -0.15\gamma + 0.48\upsilon + 1.5$,$f_2(\gamma, \upsilon) = 0.15\gamma - 0.48\upsilon + 1.5$. For a given (y_{Φ_0}, u_{Φ_0}), $H_{\circlearrowleft_2}$ is equal to the difference between the area in light grey and the area in dark grey

Remark 4.2.7 *In addition to the result in Theorem 4.2.6, if f_1 and f_2 satisfy the hypotheses given in Theorem 4.2.6, then for every $u_\Phi \in AC(\mathbb{R}_+)$ and $y_{\Phi_0} \in \mathbb{R}$, the function $t \to H_{\circlearrowleft_2}(y_\Phi(t), u_\Phi(t))$ with $H_{\circlearrowleft_2}$ as in* (4.9) *is left-differentiable and satisfies*

$$\lim_{h \nearrow 0^-} \frac{H_{\circlearrowleft_2}(y_\Phi(t+h), u_\Phi(t+h)) - H_{\circlearrowleft_1}(y_\Phi(t), u_\Phi(t))}{h} \leq y_\Phi(t)\dot{u}_\Phi(t).$$

Remark 4.2.8 *If f_1 and f_2 satisfy the assumptions in both Theorem 4.2.1 and Theorem 4.2.6, the convex combination of $H_{\circlearrowleft_1}$ and $H_{\circlearrowleft_2}$ is also a storage function which satisfies* (4.10)*. Moreover, if additionally, it is assumed that f_1 and f_2 are positive then the convex combination of $H_{\circlearrowleft_1}$ and $H_{\circlearrowleft_2}$ is also a non-negative storage function.* △

Similar to Proposition 4.2.3, generalization for the Duhem operator with saturated output can also be done for this case, which is given in the following proposition.

Proposition 4.2.9 *Consider the Duhem hysteresis operator Φ defined in* (3.1) *with C^1 functions $F, G : \mathcal{D} \to \mathbb{R}$ and with the traversing function ν_Φ and the anhysteresis function f_{an}. Assume that the anhysteresis curve is in $\mathcal{D}$ and there exists an CCW intersecting function Υ (e.g., the hypotheses in Lemma 4.1.2 hold). Assume further that the Assumption* **(A)** *holds for all (γ, υ) in $\mathcal{D}$. Then for every $u_\Phi \in AC(\mathbb{R}_+)$ and $(y_{\Phi_0}, u_\Phi(0)) \in \mathcal{D}$, the function*

$t \to H_{\circlearrowleft_2}(y_\Phi(t), u_\Phi(t))$ with $H_{\circlearrowleft_2}$ as in (4.21) *and $y_\Phi := \Phi(u_\Phi, y_{\Phi_0})$ is right differentiable and satisfies* (4.10)*, i.e. the Duhem operator is CCW.*

In this subsection, we have shown the dissipativity property of the CCW Duhem hysteresis operator by constructing the storage function $H_{\circlearrowleft_2}$ (4.21) based on the traversing function ν_Φ. Furthermore, the radially unboundedness of $H_{\circlearrowleft_2}$ has also been studied.

4.2.3 Relations to the Available Storage Functions

In the previous sections we have discussed a storage function for the Duhem hysteresis operator using ω_Φ. It is natural to investigate the relation between this storage function and the available storage function as given in Willems [62]. This is summarized in the following proposition.

Proposition 4.2.10 *Consider the Duhem operator Φ satisfying the hypotheses in Theorem 4.2.1. Furthermore, we assume that the anhysteresis function $f_{an}(\upsilon)$ is the vertical line where $\upsilon = 0$, i.e. for every $u_\Phi \in AC(\mathbb{R}_+)$, $\Omega(y_\Phi(t), u_\Phi(t)) = 0$. Then for every $y_{\Phi_0}, u_{\Phi_0} \in \mathbb{R}$, the function $H_{\circlearrowleft_1}$ as in* (4.9) *satisfies*

$$H_{\circlearrowleft_1}(y_{\Phi_0}, u_{\Phi_0}) = \sup_{\substack{u_\Phi \in AC(\mathbb{R}_+) \\ u_\Phi(0) = u_{\Phi_0}}} -\int_0^T \dot{y}_\Phi(\tau) u_\Phi(\tau) \mathrm{d}\tau,$$

where $y_\Phi := \Phi(u_\Phi, y_{\Phi_0})$. In other words, $H_{\circlearrowleft_1}$ defines the available storage function (as discussed in [62]) where the supply rate is given by $\dot{y}_\Phi u_\Phi$ (instead of $y_\Phi u_\Phi$ as in [62]).

Proof: From the proof of the Theorem 4.2.1, we have

$$\frac{\mathrm{d}H_{\circlearrowleft_1}\big(y_\Phi(t), u_\Phi(t)\big)}{\mathrm{d}t} = \dot{y}_\Phi(t) u_\Phi(t) + \int_{u_\Phi(t)}^{u_\Phi^*(t)} \frac{\mathrm{d}}{\mathrm{d}t} \omega_\Phi(\upsilon, y_\Phi(t), u_\Phi(t)) \mathrm{d}\upsilon. \quad (4.22)$$

Let $H_{\circlearrowleft_1}(t) = H_{\circlearrowleft_1}(y_\Phi(t), u_\Phi(t))$ and integrating (4.22) from $t = 0$ to $T > 0$, we have

$$H_{\circlearrowleft_1}(T) - H_{\circlearrowleft_1}(0) = \int_0^T \dot{y}_\Phi(\tau) u_\Phi(\tau) \mathrm{d}\tau + \int_0^T \int_{u_\Phi(\tau)}^{u_\Phi^*} \frac{\mathrm{d}}{\mathrm{d}\tau} \omega_\Phi(\upsilon, y_\Phi(\tau), u_\Phi(\tau)) \mathrm{d}\upsilon \mathrm{d}\tau,$$

where $u_\Phi^* = \Omega(y_\Phi(t), u_\Phi(t)) = 0$.

By rearranging the terms in this equation, we obtain

$$-\int_0^T \dot{y}_\Phi(\tau) u_\Phi(\tau) \mathrm{d}\tau = H_{\circlearrowleft_1}(0) - H_{\circlearrowleft_1}(T) + \int_0^T \int_{u_\Phi(\tau)}^{0} \frac{\mathrm{d}}{\mathrm{d}\tau} \omega_\Phi(\upsilon, y_\Phi(\tau), u_\Phi(\tau)) \mathrm{d}\upsilon \mathrm{d}\tau,$$

(4.23)

The supremum of the LHS of (4.23) over all possible u_Φ and T defines the available storage function where the supply rate is $\dot{y}_\Phi u_\Phi$. Note that this supply rate is a particular class of the general supply rate given by [62]. Since the $H_{\circlearrowleft_1}(T) \geq 0$ based on Theorem 4.2.1 and the last term is non-positive, we show that we can define u_Φ and T such that these two terms are equal to zero, thus the supremum of the LHS of (4.23) is equal to $H_{\circlearrowleft_1}(0)$, i.e. $H_{\circlearrowleft_1}$ is the available storage function.

From a given initial condition (y_{Φ_0}, u_{Φ_0}), let us give an input signal $u_\Phi(t) = u_{\Phi_0}(T-t)$ for all $t \in [0, T]$. Since $u_\Phi(T) = 0$, the last term of (4.23) is equal to zero. Based on the assumption on the anhysteresis function f_{an}, we also have $H_{\circlearrowleft_1}(T) = 0$. This completes our proof. □

4.3 Dissipativity of The Duhem Hysteresis Operator with CW I/O Behavior

In this section, we study the dissipativity property of the Duhem operator with CW I/O behavior. The analysis follows the same procedure as we did for the CCW Duhem operator, where we first propose a candidate of the storage function based on the traversing function ω_Φ (ν_Φ), and then show that these storage functions satisfy the CW inequality.

4.3.1 Storage Function Using ω_Φ

Based on the three functions ω_Φ, f_{an} and Λ, we define $H_{\circlearrowleft_1} : \mathbb{R}^2 \to \mathbb{R}_+$ as follows

$$H_{\circlearrowleft_1}(\gamma, \upsilon) = \int_0^{\Lambda(\gamma,\upsilon)} f_{an}(\tau)\mathrm{d}\tau - \int_\upsilon^{\Lambda(\gamma,\upsilon)} \omega_\Phi(\sigma, \gamma, \upsilon)\mathrm{d}\sigma, \tag{4.24}$$

where Λ is the CW intersecting function (corresponding to ω_ϕ and f_{an}) as in Lemma 4.1.3. The graphical interpretation of $H_{\circlearrowleft_1}$ is shown in Figure 4.5, where we use a Duhem hysteresis operator Φ with $f_1(\gamma, \upsilon) = 1 - 2\gamma$, $f_2(\gamma, \upsilon) = 1 + 2\gamma$ and the value of $H_{\circlearrowleft_1}(y_{\Phi_0}, u_{\Phi_0})$ is equal to the area in light grey. In the following theorem, we give the sufficient conditions on the Duhem hysteresis operator such that it has CW I/O dynamics.

Theorem 4.3.1 *Consider the Duhem hysteresis operator Φ defined in* (3.1) *and* (4.1) *with C^1 functions $f_1, f_2 : \mathbb{R}^2 \to \mathbb{R}$ and with the traversing function ω_Φ and the anhysteresis*

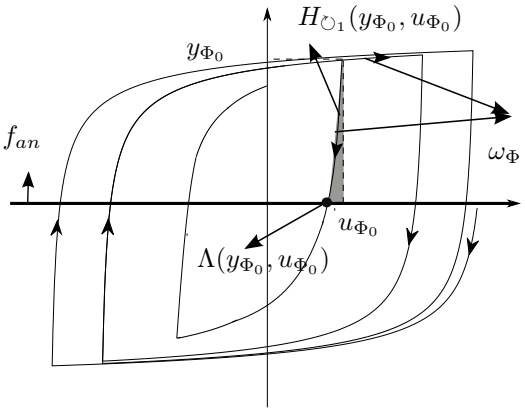

Figure 4.5: Graphical interpretation of the function $H_{\circlearrowleft_1}$ in (4.24) where the Duhem hysteresis operator Φ is defined in (3.1) with $f_1(\gamma, \upsilon) = 1 - 2\gamma$, $f_2(\gamma, \upsilon) = 1 + 2\gamma$. for any given (y_{Φ_0}, u_{Φ_0}), $H_{\circlearrowleft_1}(y_{\Phi_0}, u_{\Phi_0})$ is equal to the area in light grey.

function f_{an}. Suppose that there exists an CW intersecting function Λ (e.g. the hypotheses in Lemma 4.1.3 hold). Let the following condition holds for all (γ, υ) in $\mathbb{R}^2$

(B) *$f_1(\gamma, \upsilon) \geq f_2(\gamma, \upsilon)$ whenever $\gamma \leq f_{an}(\upsilon)$, and $f_1(\gamma, \upsilon) < f_2(\gamma, \upsilon)$ otherwise.*

Then for every $u_\Phi \in AC(\mathbb{R}_+)$ and for every $y_{\Phi_0} \in \mathbb{R}$, the function $t \to H_{\circlearrowleft_1}(y_\Phi(t), u_\Phi(t))$ with $H_{\circlearrowleft_1}$ as in (4.24) *and $y_\Phi := \Phi(u_\Phi, y_{\Phi_0})$, is right differentiable and satisfies*

$$\frac{\mathrm{d}H_{\circlearrowleft_1}(y_\Phi(t), u_\Phi(t))}{\mathrm{d}t} \leq \dot{u}_\Phi(t) y_\Phi(t) \tag{4.25}$$

Moreover, if the anhysteresis function f_{an} satisfies $f_{an}(0) = 0$, then $H_{\circlearrowleft_1} \geq 0$ and the Duhem operator is clockwise (CW).

Proof: The proof of Theorem 4.3.1 follows the same line as the proof of Theorem 4.2.1. For any real valued function z, we denote $\frac{\mathrm{d}}{\mathrm{d}t} z(t) := \lim_{h \searrow 0_+} \frac{z(t+h) - z(t)}{h}$. In the first part we prove that for all $t \in \mathbb{R}_+$, $\dot{H}_{\circlearrowleft_1}\big(y_\Phi(t), u_\Phi(t)\big)$ exists and satisfies (4.25). In the second part we show the non-negativeness of $H_{\circlearrowleft_1}\big(y_\Phi(t), u_\Phi(t)\big)$.

1. To show that $\dot{H}_{\circlearrowleft_1}\big((\Phi(u_\Phi, y_{\Phi_0}))(t), u_\Phi(t)\big)$ exists, let us denote $u_\Phi^* := \Lambda(y_\Phi, u_\Phi)$. Then we have

$$\frac{\mathrm{d}}{\mathrm{d}t} H_{\circlearrowleft_1}(y_\Phi(t), u_\Phi(t)) = \dot{u}_\Phi(t) y_\Phi(t) - \int_{u_\Phi(t)}^{u_\Phi^*(t)} \frac{\mathrm{d}}{\mathrm{d}t} \omega_\Phi(\upsilon, y_\Phi(t), u_\Phi(t)) \mathrm{d}\upsilon, \tag{4.26}$$

where $u_\Phi^*(t) = \Lambda(y_\Phi(t), u_\Phi(t))$ The first term in the RHS of (4.26) exists for all $t \geq 0$ since $u_\Phi(t)$ satisfies (3.1). In order to get (4.25), it remains to check whether the last term of (4.26) exists, is finite and satisfies

$$\int_{u_\Phi(t)}^{u_\Phi^*(t)} \frac{\mathrm{d}}{\mathrm{d}t}\omega_\Phi(\upsilon, y_\Phi(t), u_\Phi(t))\mathrm{d}\upsilon \geq 0. \tag{4.27}$$

It suffices to show that, for every $\upsilon \in [u_\Phi(t), u_\Phi^*(t)]$, the following limit

$$\lim_{\epsilon \searrow 0^+} \frac{1}{\epsilon}[\omega_\Phi(\upsilon, y_\Phi(t+\epsilon), u_\Phi(t+\epsilon)) - \omega_\Phi(\upsilon, y_\Phi(t), u_\Phi(t))] \tag{4.28}$$

exist and the limit of (4.28) is greater or equal to zero when $u_\Phi^*(t) > u_\Phi(t)$ and the limit is less or equal to zero elsewhere.

For any $\epsilon \geq 0$, let us introduce the continuous function $\omega_\epsilon : \mathbb{R} \to \mathbb{R}$ by

$$\omega_\epsilon(\upsilon) = \omega_\Phi(\upsilon, y_\Phi(t+\epsilon), u_\Phi(t+\epsilon)). \tag{4.29}$$

More precisely, using (4.2), ω_ϵ is the unique solution of

$$\omega_\epsilon(\upsilon) = \begin{cases} y_\Phi(t+\epsilon) + \displaystyle\int_{u_\Phi(t+\epsilon)}^{\tau} f_1(\omega_\epsilon(\sigma), \sigma)\mathrm{d}\sigma \quad \forall \sigma \geq u_\Phi(t+\epsilon) \\ \\ y_\Phi(t+\epsilon) + \displaystyle\int_{u_\Phi(t+\epsilon)}^{\tau} f_2(\omega_\epsilon(\sigma), \sigma)\mathrm{d}\sigma \quad \forall \sigma \leq u_\Phi(t+\epsilon). \end{cases} \tag{4.30}$$

Note that $\omega_0(\upsilon) = \omega_\Phi(\upsilon, y_\Phi(t), u_\Phi(t))$ as in (4.2) for all $\upsilon \in \mathbb{R}$ and

$$\omega_\epsilon(u_\Phi(t+\epsilon)) = y_\Phi(t+\epsilon) \qquad \forall\, \epsilon \,\in\, \mathbb{R}_+ \,. \tag{4.31}$$

In order to show the existence of (4.28) and the validity of (4.27), we consider several cases depending on the sign of $\dot{u}_\Phi(t)$ and $F(y_\Phi(t), u_\Phi(t))$. It can be checked that the hypothesis **(B)** on F implies that $f_1(y_\Phi(t), u_\Phi(t)) \geq f_2(y_\Phi(t), u_\Phi(t))$ whenever $y_\Phi(t) \leq f_{an}(u_\Phi)$, and $f_1(y_\Phi(t), u_\Phi(t)) < f_2(y_\Phi(t), u_\Phi(t))$ otherwise.

First, we assume that $\dot{u}_\Phi(t) > 0$ and $y_\Phi(t) \geq f_{an}(u_\Phi(t))$. In this case, according to Lemma 4.1.3, we have $u_\Phi^*(t) < u_\Phi(t)$. Since $\dot{u}_\Phi(t) > 0$, there exists $\delta > 0$ such that $\upsilon \leq u_\Phi(t) < u_\Phi(\tau)$ for all τ in $(t, t+\delta)$. It follows from (4.30) and assumption (**B**) that for every $\epsilon \in (0, \delta)$:

$$\begin{aligned} \frac{\mathrm{d}\omega_\epsilon(u_\Phi(\tau))}{\mathrm{d}\tau} &= f_2(\omega_\epsilon(u_\Phi(\tau)), u_\Phi(\tau))\ \dot{u}_\Phi(\tau) \\ &\geq f_1(\omega_\epsilon(u_\Phi(\tau)), u_\Phi(\tau))\ \dot{u}_\Phi(\tau) \quad \forall \tau \in [t, t+\epsilon], \end{aligned}$$

and the function ω_0 satisfies

$$\frac{\mathrm{d}\omega_0(u_\Phi(\tau))}{\mathrm{d}\tau} \;=\; f_1(y_\Phi(\tau),u_\Phi(\tau))\;\dot{u}_\Phi(\tau) \qquad \forall \tau \;\in\; [t,t+\epsilon].$$

Since the functions $\epsilon \mapsto w_0(u_\Phi(t+\epsilon))$ and $\epsilon \mapsto y_\Phi(t+\epsilon)$ with $\epsilon \in (0,\delta]$ are two C^1 functions which are solutions of the same locally Lipschitz ODE and with the same initial value. By uniqueness of solution, we get $\omega_0(u_\Phi(t+\epsilon)) = y_\Phi(t+\epsilon)$.

This together with the fact that $\omega_\epsilon(u_\Phi(t+\epsilon)) = y_\Phi(t+\epsilon)$ and using the comparison principle (in reverse direction), we get that for every $\epsilon \in [0,\delta)$:

$$\omega_\epsilon(u_\Phi(\tau)) \;\leq\; \omega_0(u_\Phi(\tau)) \qquad \forall\, \tau \;\in\; [t,t+\epsilon].$$

Since the two functions $\omega_\epsilon(\upsilon)$ and $\omega_0(\upsilon)$ for $\upsilon \in [u_\Phi^*(t),u_\Phi(t)]$ are two solutions of the same ODE, it follows that $\omega_\epsilon(\upsilon) \;\geq\; \omega_0(\upsilon)$ and we get that if it exists:

$$\lim_{\epsilon \searrow 0^+} \frac{1}{\epsilon}[\omega_\epsilon(\upsilon)-\omega_0(\upsilon)] \;\leq\; 0 \qquad \forall \upsilon \in [u_\Phi^*(t),u_\Phi(t)]. \tag{4.32}$$

Then it is clear that

$$\lim_{\epsilon \searrow 0^+} \frac{1}{\epsilon}[\omega_\epsilon(\upsilon)-\omega_0(\upsilon)] \;\geq\; 0 \qquad \forall \upsilon \in [u_\Phi(t),u_\Phi^*(t)]. \tag{4.33}$$

In the following, we show the existence of the limit given in (4.32) by computing a bound on the function $\epsilon \mapsto \frac{1}{\epsilon}[\omega_\epsilon(\upsilon)-\omega_0(\upsilon)]$. Note that for every $\epsilon \in [0,\delta]$,

$$\begin{aligned}
|\omega_\epsilon(\upsilon)-\omega_0(\upsilon)| &\leq |y_\Phi(t+\epsilon)-y_\Phi(t)| + \left|\int_{u_\Phi(t+\epsilon)}^{u_\Phi(t)} f_2(\omega_\epsilon(\sigma),\sigma)\,\mathrm{d}\sigma\right| \\
&\quad + \left|\int_{u_\Phi(t)}^{\upsilon} f_2(\omega_\epsilon(\sigma),\sigma) - f_2(\omega_0(\sigma),\sigma)\,\mathrm{d}\sigma\right| \\
&\leq |y_\Phi(t+\epsilon)-y_\Phi(t)| + \int_{u_\Phi(t)}^{u_\Phi(t+\epsilon)} |f_2(\omega_\epsilon(\sigma),\sigma)|\,\mathrm{d}\sigma \\
&\quad + \int_{\upsilon}^{u_\Phi(t)} |f_2(\omega_\epsilon(\sigma),\sigma) - f_2(\omega_0(\sigma),\sigma)|\,\mathrm{d}\sigma,
\end{aligned}$$

for all $\upsilon \in [u_\Phi^*(t),u_\Phi(t)]$. By the locally Lipschitz property of f_2 and by the boundedness of ω_ϵ on $[\upsilon,u_\Phi(t)]$ for all $\epsilon \in [0,\delta]$, it can be shown that there exists α, such that α is a bound of f_2 on a compact set. Then

$$\begin{aligned}
|\omega_\epsilon(\upsilon)-\omega_0(\upsilon)| &\leq |y_\Phi(t+\epsilon)-y_\Phi(t)| \\
&\quad + \int_{\upsilon}^{u_\Phi(t)} L\,|\omega_\epsilon(\sigma)-\omega_0(\sigma)|\,\mathrm{d}\sigma + \alpha|u_\Phi(t+\epsilon)-u_\Phi(t)|\,,
\end{aligned}$$

where L is the Lipschitz constant of f_2 on $[\omega_{\min}, \omega_{\max}] \times [\upsilon, u_\Phi(t)]$ with

$$\begin{aligned}\omega_{\min} &= \min_{(\epsilon,\sigma)\in[0,\delta]\times[\upsilon,u_\Phi(t)]} \omega_\epsilon(\sigma),\\ \omega_{\max} &= \max_{(\epsilon,\sigma)\in[0,\delta]\times[\upsilon,u_\Phi(t)]} \omega_\epsilon(\sigma)\ .\end{aligned}$$

With Gronwall's lemma, this implies that for every $\epsilon \in [0, \delta]$

$$|\omega_\epsilon(\upsilon)-\omega_0(\upsilon)| \le \exp((u_\Phi(t)-\upsilon)L)\Big[|y_\Phi(t+\epsilon)-y_\Phi(t)|+\alpha|u_\Phi(t+\epsilon)-u_\Phi(t)|\Big],$$

for all $\upsilon \in [u^*_\Phi(t), u_\Phi(t)]$. Hence

$$\lim_{\epsilon\searrow 0^+}\frac{1}{\epsilon}|\omega_\epsilon(\upsilon)-\omega_0(\upsilon)| \le \exp((u_\Phi(t)-\upsilon)L)\Big[|f_1(y_\Phi(t),u_\Phi(t))|+\alpha\Big]\,\dot{u}_\Phi(t),$$

for all $\upsilon \in [u^*_\Phi(t), u_\Phi(t)]$. Consequently the limit given in (4.32) exists. It implies that the inequality (4.27) holds when $\dot{u}_\Phi(t) > 0$ and $y_\Phi(t) \ge f_{an}(u_\Phi(t))$.

For the next case, we assume that $\dot{u}_\Phi(t) > 0$ and $y_\Phi(t) < f_{an}(u(t))$. Again, according to Lemma 4.1.3, we have $u^*_\Phi(t) > u_\Phi(t)$. Since for every $\epsilon \in (0, \delta]$ the two functions $\omega_\epsilon(\upsilon)$ and $\omega_0(\upsilon)$ satisfy the same ODE for $\upsilon \in [u_\Phi(t+\epsilon), u^*_\Phi(t)]$, we have

$$\omega_\epsilon(\upsilon) = \omega_0(\upsilon) \qquad \forall \upsilon \in [u_\Phi(t+\epsilon), u^*_\Phi(t)],$$

for all $\epsilon \in [0, \delta]$. This implies that

$$\lim_{\epsilon\searrow 0^+}\frac{1}{\epsilon}[\omega_\epsilon(\upsilon)-\omega_0(\upsilon)] \;=\; 0. \tag{4.34}$$

We can use similar arguments to prove that (4.27) is satisfied when $\dot{u}_\Phi(t) < 0$.

Finally, when $\dot{u}_\Phi(t) = 0$, we simply get

$$\lim_{\epsilon\searrow 0^+}\frac{1}{\epsilon}|\omega_\epsilon(\upsilon)-\omega_0(\upsilon)| = 0,$$

by continuity of the above bound.

2. For the second step, we need to show that $H_{\circlearrowleft_1}$ is non-negative. Consider the case when $y_\Phi(t) \ge f_{an}(u_\Phi(t))$, we have $u^*_\Phi(t) < u_\Phi(t)$ and $\omega_\Phi(\upsilon) \ge f_{an}(\upsilon)$ for all $\upsilon \in [u^*_\Phi(t), u_\Phi(t)]$ by Lemma 4.1.3. Since $f_{an}(\upsilon)$ belongs to the sector $[0,\ \infty)$ for all $\upsilon \in \mathbb{R}$, we have

$$H_{\circlearrowleft_1}(y_\Phi(t),u_\Phi(t)) = \int_0^{u_\Phi(t)} f_{an}(\upsilon)\mathrm{d}\upsilon + \int_{u_\Phi(t)}^{u^*_\Phi(t)} f_{an}(\upsilon) - \omega_\Phi(\upsilon, y_\Phi(t), u_\Phi(t))\mathrm{d}\upsilon \ge 0.$$

In case when $y_\Phi(t) < f_{an}(u_\Phi(t))$, we can show the non-negativeness of $H_{\circlearrowleft_1}$ by using similar arguments. □

Remark 4.3.2 *In addition to the result in Theorem 4.3.1, if f_1 and f_2 satisfy the hypotheses given in Theorem 4.3.1, then for every $u_\Phi \in AC(\mathbb{R}_+)$ and $y_{\Phi_0} \in \mathbb{R}$, the function $t \to H_{\circlearrowleft_1}(y_\Phi(t), u_\Phi(t))$ with $H_{\circlearrowleft_1}$ as in* (4.24) *is left-differentiable and satisfies*

$$\lim_{h \nearrow 0^-} \frac{H_{\circlearrowleft_1}(y_\Phi(t+h), u_\Phi(t+h)) - H_{\circlearrowleft_1}(y_\Phi(t), u_\Phi(t))}{h} \leq y_\Phi(t)\dot{u}_\Phi(t).$$

The proof of this claim follows a similar line as that of Theorem 4.3.1.

Example 4.3.3 *Consider the Dahl model [7, 38] given in 3.3.2 with $r = 1$, then the model can be given by* (3.1) *with*

$$f_1(y_\Phi, u_\Phi) = \rho\left(1 - \frac{y_\Phi}{F_c}\right),\ f_2(y_\Phi, u_\Phi) = \rho\left(1 + \frac{y_\Phi}{F_c}\right). \tag{4.35}$$

It is immediate to check that the anhysteresis function is $f_{an}(u_\Phi(t)) = 0$.

Calculating the curve ω_Φ, we have

$$\omega_\Phi(\upsilon, y_\Phi(t), u_\Phi(t)) = \begin{cases} F_c + (y_\Phi(t) - F_c)\, e^{\frac{\rho}{F_c}(u_\Phi(t) - \upsilon)} & \upsilon \in [u_\Phi(t),\ \infty), \\ -F_c + (y_\Phi(t) + F_c)\, e^{\frac{\rho}{F_c}(\upsilon - u_\Phi(t))} & \upsilon \in (-\infty,\ u_\Phi(t)]. \end{cases} \tag{4.36}$$

The CW intersecting function $\Lambda(y_\Phi(t), u_\Phi(t))$ is given by

$$\Lambda(y_\Phi(t), u_\Phi(t)) = \begin{cases} u_\Phi(t) + \frac{F_c}{\rho}\ln\frac{F_c}{y_\Phi(t)+F_c} & y_\Phi(t) \geq 0, \\ u_\Phi(t) - \frac{F_c}{\rho}\ln\frac{-F_c}{y_\Phi(t)-F_c} & y_\Phi(t) < 0, \end{cases} \tag{4.37}$$

Denoting $u^*_\Phi(t) = \Lambda(y_\Phi(t), u_\Phi(t))$, we can compute explicitly the function $H_{\circlearrowleft_1}$ in (4.24) *as follows*

$$H_{\circlearrowleft_1}(y_\Phi(t), u_\Phi(t)) = \begin{cases} -F_c(u_\Phi(t) - u^*_\Phi(t)) + \frac{F_c}{\rho}(y_\Phi(t) + F_c)(1 - e^{\frac{\rho}{F_c}(u^*_\Phi(t) - u_\Phi(t))}) \\ \qquad\qquad y_\Phi(t) \geq 0, \\ F_c(u_\Phi(t) - u^*_\Phi(t)) + \frac{F_c}{\rho}(y_\Phi(t) - F_c)(e^{\frac{\rho}{F_c}(u_\Phi(t) - u^*_\Phi(t))} - 1) \\ \qquad\qquad y_\Phi(t) < 0. \end{cases}$$

The results given in Theorem 4.3.1 can also be generalized in order to incorporate the case when the Duhem hysteresis operator Φ has saturated output, i.e. the input-output pair exists in a subset $\mathcal{D} \subset \mathbb{R}^2$. For example, the set $\mathcal{D}$ for the Dahl model in Example 4.3.3 is given by $\mathcal{D} = (-F_C, F_C) \times \mathbb{R}$. Using $\mathcal{D}$, we can generalize Theorem 4.3.1 as follows.

Proposition 4.3.4 *Consider the Duhem hysteresis operator Φ defined in* (3.1) *and* (4.1) *with C^1 functions $F, G : \mathcal{D} \to \mathbb{R}$ and with the traversing function ω_Φ and the anhysteresis*

function f_{an}. Assume that the anhysteresis curve is in $\mathcal{D}$ and there exists an CW intersecting function Λ (e.g., the hypotheses in Lemma 4.1.3 hold). Assume further that the Assumption **(B)** *holds for all (γ, υ) in $\mathcal{D}$. Then for every $u_\Phi \in AC(\mathbb{R}_+)$ and $(y_{\Phi_0}, u_\Phi(0)) \in \mathcal{D}$, the function $t \to H_{\circlearrowleft_1}(y_\Phi(t), u_\Phi(t))$ with $H_{\circlearrowleft_1}$ as in* (4.24) *and $y_\Phi := \Phi(u_\Phi, y_{\Phi_0})$ is right differentiable and satisfies* (4.25)*. Moreover, if the anhysteresis function f_{an} satisfies $f_{an}(0) = 0$, then $H_{\circlearrowleft_1} \geq 0$ and the Duhem operator is CW.*

The proof of Proposition 4.3.4 is similar to the proof of Theorem 4.3.1. In the following proposition, we show the radially unboundedness of $H_{\circlearrowleft_1}$ which will be used for stability analysis in the next chapter.

Proposition 4.3.5 *Consider a Duhem operator Φ satisfying the hypotheses in Theorem 4.3.1. Suppose that f_{an} is monotone increasing and $f_{an}(0) = 0$. Then the function $H_{\circlearrowleft_1}(\cdot, \upsilon)$ (where $H_{\circlearrowleft_1}$ is as in* (4.24)*) is radially unbounded for every υ.*

Proof: To show the properness of $H_{\circlearrowleft_1}(\cdot, \upsilon)$ for any given υ, we first consider the case $\gamma \geq f_{an}(\upsilon)$. Since the Duhem operator Φ satisfies the hypotheses in Theorem 4.3.1, the function $H_{\circlearrowleft_1}$ is nonnegative. Thus, using (4.24) and since $\Lambda(f_{an}(\upsilon), \upsilon) = \upsilon$ we have

$$\begin{aligned} H_{\circlearrowleft_1}(\gamma, \upsilon) &\geq H_{\circlearrowleft_1}(\gamma, \upsilon) - H_{\circlearrowleft_1}(f_{an}(\upsilon), \upsilon) \\ &= \int_{\Lambda(f_{an}(\upsilon),\upsilon)}^{\Lambda(\gamma,\upsilon)} f_{an}(\sigma)\mathrm{d}\sigma - \int_{\upsilon}^{\Lambda(\gamma,\upsilon)} \omega_\Phi(\sigma, \gamma, \upsilon)\mathrm{d}\sigma + \int_{\upsilon}^{\Lambda(f_{an}(\upsilon),\upsilon)} \omega_\Phi(\sigma, \gamma, \upsilon)\mathrm{d}\sigma \\ &= \int_{\upsilon}^{\Lambda(\gamma,\upsilon)} f_{an}(\sigma) - \omega_\Phi(\sigma, \gamma, \upsilon)\mathrm{d}\sigma. \end{aligned}$$

By the definition of the CW intersecting function Λ, $\gamma \geq f_{an}(\upsilon)$ implies that $\Lambda(\gamma, \upsilon) < \upsilon$. Using the monotonicity of ω_Φ, $\omega_\Phi(\sigma, \gamma, \upsilon) \leq \gamma$ for all $\sigma < \upsilon$, and thus, it follows from the above inequality that

$$\begin{aligned} H_{\circlearrowleft_1}(\gamma, \upsilon) &\geq \int_{\upsilon}^{\Lambda(\gamma,\upsilon)} f_{an}(\sigma) - \omega_\Phi(\sigma, \gamma, \upsilon)\mathrm{d}\sigma \\ &\geq \int_{\upsilon}^{\Lambda(\gamma,\upsilon)} f_{an}(\sigma) - \gamma\mathrm{d}\sigma, \end{aligned}$$

Now let us fix $\bar{\gamma}$ s.t. $f_{an}(\upsilon) < \bar{\gamma} < \gamma$. Since $\omega_\Phi(\sigma, \bar{\gamma}, \upsilon) < \omega_\Phi(\sigma, \gamma, \upsilon)$ for all $\sigma < \upsilon$ and using the monotonicity of f_{an}, we have that $\Lambda(\gamma, \upsilon) < \bar{\Lambda}$, where $\bar{\Lambda} = \Lambda(\bar{\gamma}, \upsilon)$.

Therefore,

$$H_{\circlearrowleft_1}(\gamma,\upsilon) \geq \int_{\upsilon}^{\Lambda(\gamma,\upsilon)} f_{an}(\sigma) - \gamma \mathrm{d}\sigma \geq \int_{\upsilon}^{\bar{\Lambda}} f_{an}(\sigma) - \gamma \mathrm{d}\sigma$$
$$\geq \int_{\upsilon}^{\bar{\Lambda}} f_{an}(\upsilon) - \gamma \mathrm{d}\sigma = (\gamma - c)(\upsilon - \bar{\Lambda}) > 0$$

where $c := f_{an}(\upsilon)$ and $\bar{\Lambda} = \Lambda(\bar{\gamma}, \upsilon)$ for any given υ. Hence, it implies that for every υ, $H_{\circlearrowleft_1}(\gamma,\upsilon) \to \infty$ as $\gamma \to \infty$.

We can apply similar arguments to show that for every υ, $H_{\circlearrowleft_1}(\gamma,\upsilon) \to \infty$ as $\gamma \to -\infty$ by evaluating the case when $\gamma < f_{an}(\upsilon)$. □

In this subsection, we have shown the dissipativity property of the Duhem hysteresis operator by constructing the storage function $H_{\circlearrowleft_1}$ (4.24) based on the traversing function ω_Φ. Furthermore, the radially unboundedness of $H_{\circlearrowleft_1}$ has also been studied.

4.3.2 Storage Function Using ν_Φ

Similarly, based on the three functions ν_Φ, f_{an} and Γ, we define $H_{\circlearrowleft_2} : \mathbb{R}^2 \to \mathbb{R}_+$ as follows

$$H_{\circlearrowleft_2}(\gamma,\upsilon) = \int_0^{\Gamma(\gamma,\upsilon)} f_{an}(\tau)\mathrm{d}\tau - \int_{\upsilon}^{\Gamma(\gamma,\upsilon)} \nu_\Phi(\sigma,\gamma,\upsilon)\mathrm{d}\sigma. \tag{4.38}$$

where Γ is the intersecting function (corresponding to ν_ϕ and f_{an}) as in Lemma 4.1.4. The graphical interpretation of $H_{\circlearrowleft_2}$ is shown in Figure 4.6 using a Duhem hysteresis operator Φ with $f_1(\gamma,\upsilon) = 1-2\gamma$, $f_2(\gamma,\upsilon) = 1+2\gamma$. For a given point (y_{Φ_0}, u_{Φ_0}), the value of $H_{\circlearrowleft_2}(y_{\Phi_0}, u_{\Phi_0})$ is equal to the area in light grey.

Theorem 4.3.6 *Consider the Duhem hysteresis operator Φ defined in* (3.1) *and* (4.1) *with C^1 functions $f_1, f_2 : \mathbb{R}^2 \to \mathbb{R}$ and with the traversing function ν_Φ and the anhysteresis function f_{an}. Suppose that there exists an intersecting function Γ and Assumption* **B** *in Theorem 4.3.1 hold. Then for every $u_\Phi \in AC(\mathbb{R}_+)$ and for every $y_{\Phi_0} \in \mathbb{R}$, the function $t \to H_{\circlearrowleft_2}(y_\Phi(t), u_\Phi(t))$ with $H_{\circlearrowleft_2}$ as in* (4.24) *and $y_\Phi := \Phi(u_\Phi, y_{\Phi_0})$, is right differentiable and satisfies* (4.25)*. Moreover, if the anhysteresis function f_{an} satisfies $f_{an}(0) = 0$, then $H_{\circlearrowleft_2} \geq 0$ and the Duhem operator is CW.*

The proof of Theorem 4.3.6 is omitted here, since it is similar to the proof of Theorem 4.3.1.

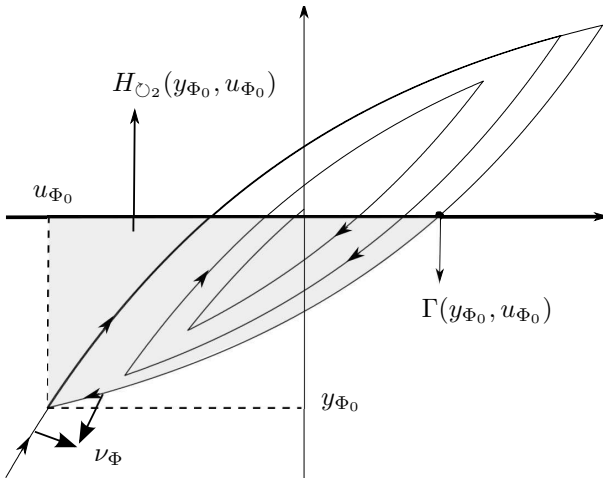

Figure 4.6: Graphical interpretation of the function $H_{\circlearrowleft_2}$ in (4.24) where the Duhem hysteresis operator Φ is defined in (3.1) with $f_1(\gamma, \upsilon) = 1 - 2\gamma$, $f_2(\gamma, \upsilon) = 1 + 2\gamma$. for any given (y_{Φ_0}, u_{Φ_0}), the value of $H_{\circlearrowleft_2}(y_{\Phi_0}, u_{\Phi_0})$ is equal to the area in light grey.

Remark 4.3.7 *In addition to the result in Theorem 4.3.6, if f_1 and f_2 satisfy the hypotheses given in Theorem 4.3.6, then for every $u_\Phi \in AC(\mathbb{R}_+)$ and $y_{\Phi_0} \in \mathbb{R}$, the function $t \to H_{\circlearrowleft_2}(y_\Phi(t), u_\Phi(t))$ with $H_{\circlearrowleft_2}$ as in* (4.38) *is left-differentiable and satisfies*

$$\lim_{h \nearrow 0^-} \frac{H_{\circlearrowleft_2}(y_\Phi(t+h), u_\Phi(t+h)) - H_{\circlearrowleft_2}(y_\Phi(t), u_\Phi(t))}{h} \leq y_\Phi(t)\dot{u}_\Phi(t).$$

To generalize Theorem 4.3.6 to the hysteresis operator with saturated output, we have the next proposition.

Proposition 4.3.8 *Consider the Duhem hysteresis operator Φ defined in* (3.1) *and* (4.1) *with C^1 functions $F, G : \mathcal{D} \to \mathbb{R}$ and with the traversing function ν_Φ and the anhysteresis function f_{an}. Assume that the anhysteresis curve is in $\mathcal{D}$ and there exists an intersecting function Γ (e.g., the hypotheses in Lemma 4.1.4 hold). Assume further that the Assumption* **(B)** *holds for all (γ, υ) in $\mathcal{D}$. Then for every $u_\Phi \in AC(\mathbb{R}_+)$ and $(y_{\Phi_0}, u_\Phi(0)) \in \mathcal{D}$, the function $t \to H_{\circlearrowleft_2}(y_\Phi(t), u_\Phi(t))$ with $H_{\circlearrowleft_2}$ as in* (4.24) *and $y_\Phi := \Phi(u_\Phi, y_{\Phi_0})$ is right differentiable and satisfies* (4.25)*. Moreover, if the anhysteresis function f_{an} satisfies $f_{an}(0) = 0$, then $H_{\circlearrowleft_2} \geq 0$ and the Duhem operator is CW.*

The proof of Proposition 4.3.8 follows the same line as the proof of Theorem 4.3.1, hence it is omitted here.

In this subsection, we have shown the dissipativity property of the Duhem hysteresis operator by constructing the storage function $H_{\circlearrowleft_2}$ (4.38) based on the traversing function ν_Φ which is dual to ω_Φ. Furthermore, the radially unboundedness of $H_{\circlearrowleft_2}$ has also been studied.

4.3.3 Relations to The Available Storage Functions

In this section, we study the relations between the proposed storage functions $H_{\circlearrowleft_1}$ to the available storage function given in [62].

Proposition 4.3.9 *Consider the Duhem operator Φ satisfying the hypotheses in Theorem 4.3.1. Moreover, we assume that the anhysteresis function f_{an} satisfies $f_{an}(\upsilon) = 0$ for all $\upsilon \in \mathbb{R}$. Then for every $y_{\Phi_0}, u_{\Phi_0} \in \mathbb{R}$, the function $H_{\circlearrowleft_1}$ as in* (4.24) *satisfies*

$$H_{\circlearrowleft_1}(y_{\Phi_0}, u_{\Phi_0}) = \sup_{\substack{u_\Phi \in AC(\mathbb{R}_+) \\ u_\Phi(0)=u_{\Phi_0}}} -\int_0^T y(\tau)\dot{u}(\tau)\mathrm{d}\tau,$$

where $y_\Phi := \Phi(u_\Phi, y_{\Phi_0})$. In other words, $H_{\circlearrowleft_1}$ defines the available storage function (as discussed in [62]) where the supply rate is given by $y_\Phi \dot{u}_\Phi$ (instead of $y_\Phi u_\Phi$ as in [62]).

Proof: As given in the first part of the proof of Theorem 4.3.1, we have

$$\frac{\mathrm{d}}{\mathrm{d}t}H_{\circlearrowleft_1}(y_\Phi(t), u_\Phi(t)) = \dot{u}_\Phi(t)y_\Phi(t) - \int_{u_\Phi(t)}^{u_\Phi^*(t)} \frac{\mathrm{d}}{\mathrm{d}t}\omega_\Phi(\upsilon, y(t), u(t))\mathrm{d}\upsilon. \tag{4.39}$$

Integrating (4.39) from $t = 0$ to T, we obtain

$$H_{\circlearrowleft_1}(T) - H_{\circlearrowleft_1}(0) = \int_0^T y_\Phi(\tau)\dot{u}_\Phi(\tau)\mathrm{d}\tau - \int_0^T \int_{u_\Phi(t)}^{u_\Phi^*} \frac{\mathrm{d}}{\mathrm{d}\tau}\omega_\Phi(\upsilon, y(\tau), u(\tau)\mathrm{d}\upsilon\mathrm{d}\tau,$$

where $u_\Phi^* = \Lambda(y_\Phi(t), u_\Phi(t))$ and we have used the shorthand notation of $H_{\circlearrowleft_1}(t) := H_{\circlearrowleft_1}(y_\Phi(t), u_\Phi(t))$.

By rearranging the terms in this equation, we arrive at

$$-\int_0^T y_\Phi(\tau)\dot{u}_\Phi(\tau)\mathrm{d}\tau = H_{\circlearrowleft_1}(0) - H_{\circlearrowleft_1}(T) - \int_0^T \int_{u_\Phi(t)}^{u_\Phi^*} \frac{\mathrm{d}}{\mathrm{d}\tau}\omega_\Phi(\upsilon, y_\Phi(\tau), u_\Phi(\tau)\mathrm{d}\upsilon\mathrm{d}\tau. \tag{4.40}$$

The supremum of the LHS of (4.40) over all possible u_Φ and T defines the available storage function where the supply rate is $y_\Phi \dot{u}_\Phi$. Note that this supply rate is a particular class of the general supply rate as studied in [62]. Since the last two terms on the RHS of (4.40) is non-positive, we show that we can define u_Φ and T such that these two terms are equal to zero, and thus the supremum of the LHS of (4.40) is equal to $H_{\circlearrowleft_1}(y_\Phi(0), u_\Phi(0))$, which is equivalent to $H_{\circlearrowleft_1}(y_{\Phi_0}, u_{\Phi_0})$, i.e., $H_{\circlearrowleft_1}$ is the available storage function.

From a given initial condition (y_{Φ_0}, u_{Φ_0}), let us introduce an input signal $u_\Phi(t) = u_{\Phi_0}(T-t) + t\Lambda(y_{\Phi_0}, u_{\Phi_0})$ for all $t \in [0, T]$ and $u_\Phi(t) = \Lambda(y_{\Phi_0}, u_{\Phi_0})$ otherwise. This means that we have an input signal u_Φ which starts from u_{Φ_0}, ends at $\Lambda(y_{\Phi_0}, u_{\Phi_0})$ at $t = T$ and remains there for all $t > T$. Together with the corresponding signal $y_\Phi = \Phi(u_\Phi, y_{\Phi_0})$, we have $\Lambda(y_\Phi(t), u_\Phi(t)) = \Lambda(y_{\Phi_0}, u_{\Phi_0})$ for all t, i.e. the intersecting point is always the same. Indeed, this follows the fact that $\Lambda(y_\Phi(t), u_\Phi(t))$ remains the same along the trajectories that converge to the intersection point $(\omega_\Phi(u^*_\Phi, y_{\Phi_0}, u_{\Phi_0}), u^*_\Phi)$ where $u^*_\Phi = \Lambda(y_{\Phi_0}, u_{\Phi_0})$.

Following the same arguments as in the proof of Theorem 4.2.1 (c.f., the arguments that lead to Eq. (4.34)), this input signal ensures that the last term on the RHS of (4.40) is equal to zero. Since $u_\Phi(T) = \Lambda(y_{\Phi_0}, u_{\Phi_0})$ for all $t > T$, we also have that $H_{\circlearrowleft_1}(y_\Phi(t), u_\Phi(t)) = 0$ for all $t > T$, i.e. the second term on the RHS of (4.40) is zero using such an input signal. Hence $H_{\circlearrowleft_1}$ as in (4.24) is the available storage function. □

As shown in Proposition 4.3.9, the storage function $H_{\circlearrowleft_1}$ defines the available storage function as shown in the classical dissipativity theory given by Willems [62] where the supply rate is given by $y_\Phi \dot{u}_\Phi$.

4.4 Concluding Remarks

In this chapter, we have discussed two dissipativity property of the Duhem operator Φ: the Duhem hysteresis operator with CCW I/O behavior and the Duhem hysteresis operator with CW I/O behavior. In both cases, explicit storage functions are proposed based on four functions: the traversing function ω_Φ (ν_Φ), the anhysteresis function f_{an}, the CCW intersecting function Ω (Υ) and the CW intersecting function Λ (Γ). It is shown that under some mild conditions on f_1 and f_2, the proposed storage functions satisfy either CCW dissipation inequalities or CW dissipation inequalities, i.e. the Duhem hysteresis operator is either CCW or CW. Furthermore, we have explored the relations between the storage functions we proposed to the available storage function given in dissipativity concept by Willems [62].

Chapter 5

Absolute stability Analysis of Systems with Duhem Hysteresis Nonlinearity

In this chapter, we investigate the absolute stability of a feedback interconnection between a linear system and a Duhem hysteresis operator. For solving this absolute stability problem, sufficient conditions are given based on the counterclockwise (CCW) and clockwise (CW) input-output property of the linear system and the Duhem operator. Furthermore, we extend the results to the case where the Duhem operator is feedback interconnected to a nonlinear system.

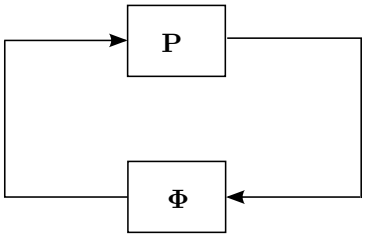

Figure 5.1: Feedback interconnection between a linear plant $\mathbf{P}$ and a Duhem operator $\mathbf{\Phi}$.

In Chapter 4, we have discussed the dissipativity property of the Duhem hysteresis operator with CCW and CW I/O dynamics. In particular, we proposed a candidate of the storage function for the Duhem operator in both cases. By exploiting the knowledge of the explicit storage functions $H_{\circlearrowleft_1}$ and $H_{\circlearrowright_1}$, we can solve the absolute stability problem of an interconnected system as shown in Figure 5.1, where $\mathbf{P}$ is a linear system and $\mathbf{\Phi}$ is a hysteresis operator. We consider four cases of interconnection where the plant $\mathbf{P}$ and hysteresis operator $\mathbf{\Phi}$ can be assumed to satisfy either CCW or CW I/O dynamics. These four cases are summarized in Table 5.1 and the stability analysis of these four cases are given in the following sections.

$\mathbf{\Phi}$ \ $\mathbf{P}$	CCW	CW
CCW	ⓐ	ⓑ
CW	ⓒ	ⓓ

Table 5.1: Four Possible cases of interconnection

5.1 CCW Linear System Interconnected with CCW Duhem Hysteresis

5.1.1 Motivating Application

In the first case, we consider the feedback interconnection ⓐ in Table 5.1, where the Duhem hysteresis operator $\mathbf{\Phi}$ has CCW I/O dynamics and the linear system $\mathbf{P}$ also has CCW I/O dynamics. This is motivated by recent results on the positive-feedback interconnection of negative imaginary system in [40] and of CCW systems [60]. Note that in Chapter 2, we have shown that for linear systems the concept *negative imaginary* is equivalent to *CCW*.

A possible application for this case is the piezo-actuated stage which is commonly used in the high-precision positioning mechanisms, see, for example [16, 28]. The piezo-actuated stage contains two parts: a piezo-actuator and a positioning mechanism, which can be described by

$$\left.\begin{array}{ll} \mathbf{P}: & \begin{array}{rl} m\ddot{q}+b\dot{q}+kq & = F_{\text{piezo}}, \\ V & = cq, \end{array} \\ \mathbf{\Phi}: & F_{\text{piezo}} = \Phi(V), \end{array}\right\} \tag{5.1}$$

where m is the mass, b is the damping constant, k is the spring constant, c is the proportional gain, V is the input voltage of the piezo-actuator, F_{piezo} denotes the force generated by the piezo-actuator, q denotes the displacement of the stage and $\mathbf{\Phi}$ denotes the hysteresis operator. It is well known that the piezoelectric actuator have CCW hysteresis loops from the input voltage to the output generated force (see, for example [8]). It can be checked that the linear mass-damper-spring system $\mathbf{P}$ is also CCW from F_{piezo} to q or, equivalently, $\mathbf{P}$ is a negative-imaginary system [40].

5.1.2 Stability Analysis

In the following theorem we show the absolute stability result of the interconnection case ⓐ.

Theorem 5.1.1 *Consider a* positive *feedback interconnection of a linear system and a Duhem operator Φ satisfying the hypotheses in Theorem 4.2.1 as follows*

$$\begin{array}{ll} \mathbf{P}: & \begin{array}{ll} \dot{x} & = Ax + Bu, \\ y & = Cx, \end{array} \\ \mathbf{\Phi}: & \dot{y}_\Phi = f_1(y_\Phi(t), u_\Phi(t))\dot{u}_{\Phi+}(t) + f_2(y_\Phi(t), u_\Phi(t))\dot{u}_{\Phi-}(t), \\ & u = y_\Phi,\ u_\Phi = y, \end{array} \tag{5.2}$$

where $A \in \mathbb{R}^{n\times n}$, $B \in \mathbb{R}^{n\times 1}$ and $C \in \mathbb{R}^{1\times n}$. Suppose that there exist matrices $L \in \mathbb{R}^{1\times n}$, $Q = Q^T > 0$ and constants $w \in \mathbb{R}$, $\xi > 0$ such that

$$A^TQ + QA + L^TL \le 0, \tag{5.3}$$
$$QB - A^TC^T = L^Tw, \tag{5.4}$$
$$2CB = w^2, \tag{5.5}$$
$$Q - \xi C^TC > 0, \tag{5.6}$$

hold and the anhysteresis function f_{an} satisfies $(f_{an}(\upsilon) - \xi\upsilon)\upsilon \le 0$ for all $\upsilon \in \mathbb{R}$ (i.e. f_{an} belongs to the sector $[0, \xi]$). Then for every initial condition $(x(0), y_\Phi(0))$, the state trajectory of the closed-loop system (5.2) *is bounded and converges to the largest invariant set in $\{(x, y_\Phi)|Lx - wy_\Phi = 0\}$.*

Proof: Using $V_G(x) = \frac{1}{2}x^TQx$ and (5.3) and (5.10), it can be checked that

$$\begin{aligned} \dot{V}_G &= \frac{1}{2}x^T(A^TQ + QA)x + x^TQBu \\ &\le -\frac{1}{2}x^TL^TLx + x^TQBu + \dot{y}u - x^T(A^TC^T)u - uCBu \\ &= \dot{y}u - \frac{1}{2}(Lx - wu)^2. \end{aligned}$$

This implies that the linear system is CCW. By the assumptions of the theorem, the Duhem operator Φ is also CCW with the storage function $H_{\circlearrowleft_1} : \mathbb{R}^2 \to \mathbb{R}_+$ as given in (4.9).

Now let $H_{cl}(x, y_\Phi) = V_G(x) + H_{\circlearrowleft_1}(y_\Phi, Cx) - Cxy_\Phi$ be a Lyapunov function candidate of the interconnected system (5.2). We show first that H_{cl} is lower bounded.

Substituting the representation of V_G and $H_{\circlearrowleft_1}$, we have

$$\begin{aligned}
H_{cl} &= \frac{1}{2}x^TQx + y_\Phi Cx - \int_0^{Cx} \omega_\Phi(\sigma, y_\Phi, Cx)\,\mathrm{d}\sigma - Cxy_\Phi \\
&\qquad + \int_0^{\Omega(y_\Phi,Cx)} \omega_\Phi(\sigma, y_\Phi, Cx)\mathrm{d}\sigma - \int_0^{\Omega(y_\Phi,Cx)} f_{an}(\sigma)\mathrm{d}\sigma \\
&= \frac{1}{2}x^TQx - \int_0^{Cx} f_{an}(\sigma)\mathrm{d}\sigma + \int_{Cx}^{\Omega(y_\Phi,Cx)} \omega_\Phi(\sigma, y_\Phi, Cx) - f_{an}(\sigma)\mathrm{d}\sigma \\
&\geq \frac{1}{2}x^TQx - \int_0^{Cx} (f_{an}(\sigma) - \xi\sigma)\mathrm{d}\sigma - \int_0^{Cx} \xi\sigma\mathrm{d}\sigma + \int_{Cx}^{\Omega(y_\Phi,Cx)} \omega_\Phi(\sigma, y_\Phi, Cx) - f_{an}(\sigma)\mathrm{d}\sigma \\
&\geq \frac{1}{2}x^T(Q - \xi C^TC)x + \int_{Cx}^{\Omega(y_\Phi,Cx)} \omega_\Phi(\sigma, y_\Phi, Cx) - f_{an}(\sigma)\mathrm{d}\sigma. \qquad (5.7)
\end{aligned}$$

where the last inequality is due to the sector condition on f_{an}. In the following, we prove that the last term on the RHS of (5.7) is lower bounded. Notice that since $f_1 \geq 0$, $f_2 \geq 0$, (4.4) and (4.5) imply that $\frac{\mathrm{d}f_{an}(v)}{\mathrm{d}v} > \epsilon$ for some $\epsilon > 0$. Hence f_{an} is strictly increasing and invertible.

Consider the case when $y_\Phi \geq f_{an}(Cx)$ which implies also that $\Omega(y_\Phi, Cx) \geq f_{an}^{-1}(y_\Phi) \geq Cx$ by the definition of Ω. Using the monotonicity of ω_Φ we have

$$\begin{aligned}
&\int_{Cx}^{\Omega(y_\Phi,Cx)} \omega_\Phi(\sigma, y_\Phi, Cx) - f_{an}(\sigma)\mathrm{d}\sigma \\
&\geq \int_{Cx}^{\Omega(y_\Phi,Cx)} y_\Phi - f_{an}(\sigma)\mathrm{d}\sigma \geq \int_{Cx}^{f_{an}^{-1}(y_\Phi)} y_\Phi - f_{an}(\sigma)\mathrm{d}\sigma.
\end{aligned}$$

Define $W(y_\Phi, Cx) := \int_{Cx}^{f_{an}^{-1}(y_\Phi)} y_\Phi - f_{an}(\sigma)\mathrm{d}\sigma$ and let $c := \frac{y_\Phi - f_{an}(Cx)}{2} + f_{an}(Cx)$. It follows that $f_{an}^{-1}(y_\Phi) \geq f_{an}^{-1}(c)$ and $f_{an}(\sigma) \leq c$ for all $\sigma \in [Cx, f_{an}^{-1}(c)]$. Therefore

$$\begin{aligned}
W(y_\Phi, Cx) &\geq \int_{Cx}^{f_{an}^{-1}(c)} y_\Phi - f_{an}(\sigma)\mathrm{d}\sigma \geq \int_{Cx}^{f_{an}^{-1}(c)} y_\Phi - c\,\mathrm{d}\sigma \\
&= \frac{1}{2}(y_\Phi - f_{an}(Cx))(f_{an}^{-1}(c) - Cx) \geq 0.
\end{aligned}$$

Thus, $\int_{Cx}^{\Omega(y_\Phi,Cx)} y_\Phi - f_{an}(\sigma)\mathrm{d}\sigma$ is lower bounded by $W(y_\Phi, Cx)$ which is positive definite (it is equal to zero only if $y_\Phi = f_{an}(Cx)$) and $W(y_\Phi, Cx) \to \infty$ as $y_\Phi \to \infty$.

When $y_\Phi < f_{an}(Cx)$, we obtain the same result where $\int_{Cx}^{\Omega(y_\Phi,Cx)} y_\Phi - f_{an}(\sigma)\mathrm{d}\sigma$ is lower bounded by $W(y_\Phi, Cx)$ which is positive definite and $W(y_\Phi, Cx) \to \infty$ as $y_\Phi \to -\infty$.

Therefore, using (5.7), we have $H_{cl} \geq \frac{1}{2}x^T(Q - \xi C^TC)x + V_G(y_\Phi, Cx)$, which is radially unbounded.

Now computing the time derivative of H_{cl}, we obtain $\dot{H}_{cl} = \dot{V}_G + \dot{H}_{\circlearrowleft_1} - C\dot{x}y_\Phi - Cx\dot{y}_\Phi \leq -\frac{1}{2}(Lx - wy_\Phi)^2$.

This inequality together with the radially unboundedness of H_{cl} implies that the trajectory (x, y_Φ) is bounded. Using LaSalle's invariance principle, we conclude that the trajectory (x, y_Φ) of (5.2) converges to the largest invariant set contained in $M := \{(x, y_\Phi) \in \mathbb{R}^n \times \mathbb{R} | Lx - wy_\Phi = 0\}$. □

We illustrate Theorem 5.1.1 in the following simple example.

Example 5.1.2 *Consider*

$$\begin{array}{rll} \mathbf{P}: & \dot{x} & = \left[\begin{smallmatrix} 0 & 1 \\ -\frac{k}{m} & -\frac{b}{m} \end{smallmatrix}\right] x + \left[\begin{smallmatrix} 0 \\ \frac{1}{m} \end{smallmatrix}\right] u, \\ & y & = \left[\begin{smallmatrix} c_1 & c_2 \end{smallmatrix}\right] x, \\ \mathbf{\Phi}: & \dot{y}_\Phi = f_1(y_\Phi(t), u_\Phi(t))\dot{u}_{\Phi+}(t) + f_2(y_\Phi(t), u_\Phi(t))\dot{u}_{\Phi-}(t), & \\ & u = y_\Phi,\ u_\Phi = y, & \end{array}$$

where $x(t) \in \mathbb{R}$, $c_1, c_2 \in \mathbb{R}_+$, $m, b, k > 0$ and the functions f_1, f_2 satisfy the hypotheses in Theorem 4.2.1. Note that this example represents the piezo-actuated stage as described in (5.1) *where $c_1 = c$ and $c_2 = 0$.*

Using $Q = \left[\begin{smallmatrix} c_1 k & c_2 k \\ c_2 k & c_2 b + c_1 m \end{smallmatrix}\right]$, it can be checked that if $c_2 k - c_1 b \leq 0$, then (5.3) − (5.5) *hold with*

$$w = \sqrt{\frac{2c_2}{m}}, \quad L = \left[\frac{k\sqrt{2c_2 m}}{m} \quad \frac{b\sqrt{2c_2 m}}{m}\right].$$

Using H_{cl} as in the proof of Theorem 5.1.1, let us define $H_{cl}(x, y_\Phi) = \frac{1}{2}x^T Q x + H_{\circlearrowleft_1}(y_\Phi, y) - yy_\Phi$ and a routine computation shows that

$$\begin{aligned} \dot{H}_{cl} &\leq \dot{y}y_\Phi + \frac{\mathrm{d}\,\widehat{\Phi(y)}}{\mathrm{d}t}y - \dot{y}y_\Phi - y\dot{y}_\Phi - \frac{1}{2}(Lx - wy_\Phi)^2 \\ &= -\frac{1}{2}(Lx - wy_\Phi)^2. \end{aligned}$$

Note that (5.6) *holds if there exists $\xi \in \mathbb{R}_+$ such that $k - \xi c_1 > 0$. This means that the result in Theorem 5.1.1 holds if the anhysteresis function f_{an} satisfies $(f_{an}(v) - \xi v)v \leq 0$, for all $v \in \mathbb{R}$ and $\xi < k/c_1$. In other words, f_{an} should belong to the sector $[0, k/c_1)$ for the stability of the closed-loop system using a positive feedback interconnection.* △

5.2 CW Linear System Interconnected with CCW Duhem Hysteresis

5.2.1 Motivating Application

In this subsection, we consider the interconnection case ⓑ in Table 5.1. A possible application for this case is the active vibration mechanism using piezo-actuator, which has been used for vibration control in mechanical structures [26, 12]. The mechanism can be described by

$$\left.\begin{array}{ll} \mathbf{P}: & \begin{array}{rl} m\ddot{q}+b\dot{q}+kq & = F_{\text{piezo}}, \\ V & = -c\ddot{q}, \end{array} \\ \mathbf{\Phi}: & F_{\text{piezo}} = \Phi(V). \end{array}\right\} \tag{5.8}$$

It is well know that the piezoelectric actuator has CCW I/O dynamics [14] and it can be checked that the mass-damper-spring system $\mathbf{P}$ is CW from F_{piezo} to $\ddot{q}$.

5.2.2 Stability Analysis

In the following theorem we show the absolute stability result of the interconnection case ⓑ.

Theorem 5.2.1 *Consider a* negative *feedback interconnection of a linear system and a Duhem operator Φ satisfying the hypotheses in Theorem 4.2.1 as follows*

$$\begin{array}{ll} \mathbf{P}: & \begin{array}{rl} \dot{x} & = Ax+Bu, \\ y & = Cx+Du, \end{array} \\ \mathbf{\Phi}: & \dot{y}_\Phi = f_1(y_\Phi(t),u_\Phi(t))\dot{u}_{\Phi+}(t) + f_2(y_\Phi(t),u_\Phi(t))\dot{u}_{\Phi-}(t), \\ & u=-y_\Phi,\ u_\Phi = y, \end{array} \tag{5.9}$$

where $A\in\mathbb{R}^{n\times n}$, $B\in\mathbb{R}^{n\times 1}$, $C\in\mathbb{R}^{1\times n}$ and $D\in\mathbb{R}$. Assume that $CB<0$ and there exist w, L and $P=P^T>0$, such that the following linear matrix inequalities (LMI)

$$\begin{bmatrix} P & C^T \\ C & D \end{bmatrix} > 0 \tag{5.10}$$

$$A^TP+PA+L^TL\le 0 \tag{5.11}$$

$$PB+A^TC^T = -L^Tw \tag{5.12}$$

$$2CB = -w^2 \tag{5.13}$$

hold. Then for every initial condition $(x(0),y_\Phi(0))$, the state trajectory of the closed-loop system (5.9) *is bounded and converges to the largest invariant set in $\{(x,y_\Phi)|Lx-wy_\Phi=0\}$.*

Proof: By the assumptions of the theorem, the Duhem operator Φ is CCW with the function $H_{\circlearrowleft_1} : \mathbb{R}^2 \to \mathbb{R}_+$ as given in (4.9).

Using $V_G = \frac{1}{2}x^T P x + (y - Du)u + \frac{D}{2}u^2$, a routine computation shows that

$$\begin{aligned}\dot{V}_G &= \frac{1}{2}x^T(A^T P + PA)x + x^T PBu + \dot{\overbrace{(y - Du)}}u + (y - Du)\dot{u} + D\dot{u}u \\ &= \frac{1}{2}x^T(A^T P + PA)x + x^T(PB + A^T C^T)u + uCBu + y\dot{u}.\end{aligned}$$

Using (5.11), (5.12) and (5.13), $\dot{V}_G \leq y\dot{u} - \frac{1}{2}(Lx - wy_\Phi)^2$. This inequality implies that the linear system defined in (5.9) is CW.

Now take $H_{cl}(x, y_\Phi) = H_{\circlearrowleft_1}(y_\Phi, Cx - Dy_\Phi) + V_G(x, -y_\Phi)$ as the Lyapunov function of the interconnected system (5.9), where H_{cl} is radially unbounded by (5.10) and the non-negativity of $H_{\circlearrowleft_1}$. It is straightforward to see that

$$\begin{aligned}\dot{H}_{cl} &= \dot{H}_{\circlearrowleft_1} + \dot{V}_G + D\dot{y}_\Phi y_\Phi \\ &\leq \dot{y}_\Phi u_\Phi + (y - Du)\dot{u} - \frac{1}{2}(Lx - wy_\Phi)^2 + D\dot{y}_\Phi y_\Phi \\ &= -\frac{1}{2}(Lx - wy_\Phi)^2 \qquad (5.14)\end{aligned}$$

where the last equation is due to the interconnection conditions $u = -y_\Phi$ and $y = u_\Phi$. It follows from (5.14) and from the radial unboundedness (or properness) of H_{cl}, the signals x and y_Φ are bounded.

Based on LaSalle's invariance principle [30], the semiflow (x, y_Φ) of (5.9) converges to the largest invariant set contained in $M := \{(x, y_\Phi) \in \mathbb{R}^n \times \mathbb{R} | Lx - wy_\Phi = 0\}$. □

To illustrate Theorem 5.2.1, let us consider the following simple example.

Example 5.2.2 *Let*

$$\begin{aligned}\mathbf{P}: \quad \dot{x} &= \begin{bmatrix} 0 & 1 \\ -\frac{k}{m} & -\frac{b}{m} \end{bmatrix} x + \begin{bmatrix} 0 \\ \frac{1}{m} \end{bmatrix} u, \\ y &= \begin{bmatrix} -c_1 & -c_2 \end{bmatrix} x + u, \\ \mathbf{\Phi}: \quad \dot{y}_\Phi &= f_1(y_\Phi(t), u_\Phi(t))\dot{u}_{\Phi+}(t) + f_2(y_\Phi(t), u_\Phi(t))\dot{u}_{\Phi-}(t), \\ u &= -y_\Phi, \ u_\Phi = y,\end{aligned}$$

where $x(t) \in \mathbb{R}$, $c_1, c_2 \in \mathbb{R}_+$, $m, b, k > 0$ and the functions f_1, f_2 satisfy the hypotheses in Theorem 4.2.1. This example represents the active vibration mechanism using piezo-actuator as described in (5.8).

By using $P = \left[\begin{smallmatrix} c_1 k & c_2 k \\ c_2 k & c_1 m + c_2 b \end{smallmatrix}\right]$, it can be checked that, if $c_2 k - c_1 b \leq 0$ and $c_1 k(c_1 m + c_2 b) - c_2^2 k^2 > c_1^3 m + c_1^2 c_2 b - c_1 c_2^2 k$, then (5.10) − (5.13) *hold with*

$$w = \sqrt{\frac{2c_2}{m}}, \quad L = \begin{bmatrix} -\frac{k\sqrt{2c_2 m}}{m} & -\frac{b\sqrt{2c_2 m}}{m} \end{bmatrix}.$$

Following the same construction as in the proof of Theorem 5.2.1, we define

$$H_{cl}(x, y_\Phi) = \frac{1}{2}x^T P x - [\,-c_1 \;\; -c_2\,]\, x y_\Phi + \frac{1}{2}y_\Phi^2 + H_{\circlearrowleft_1}(y_\Phi, [\,-c_1 \;\; -c_2\,]\, x - y_\Phi).$$

A routine computation shows that

$$\begin{aligned}\dot{H}_{cl} &\leq -\frac{1}{2}(Lx - w y_\Phi)^2 + y\dot{y}_\Phi - \dot{\overbrace{\Phi(y)}}y \\ &= -\frac{1}{2}(Lx - w y_\Phi)^2.\end{aligned}$$

Thus, we can conclude that (x, y_Φ) *converges to the invariant set contained in* $M := \{(x, y_\Phi) \in \mathbb{R}^n \times \mathbb{R} | Lx - w y_\Phi = 0\}$. △

5.3 CCW Linear System Interconnected with CW Duhem Hysteresis

5.3.1 Motivating Application

The interconnection case © specifies that $\mathbf{P}$ has CCW I/O dynamics and $\mathbf{\Phi}$ has CW I/O dynamics.

A motivating example for this case is the mechanical systems with friction [38], which is given by

$$\left.\begin{aligned}\mathbf{P}: \quad m\ddot{q} + kq &= -F_{\text{friction}}, \\ \mathbf{\Phi}: \quad F_{\text{friction}} &= \Phi(q),\end{aligned}\right\} \tag{5.15}$$

where F_{friction} is the friction force. As discussed in [38], the friction force has CW I/O dynamics where the input is the displacement. On the other hand, the mechanical system is CCW from the friction force F_{friction} to the displacement q.

5.3.2 Stability Analysis

In the following theorem we give the sufficient conditions on the linear system and the Duhem hysteresis operator which guarantee the stability of the closed-loop system of the interconnection case ©.

Theorem 5.3.1 *Consider a* negative *feedback interconnection of a linear system and a Duhem operator Φ satisfying the hypotheses in Proposition 4.3.5 as follows*

$$\begin{array}{ll} \mathbf{P}: & \begin{array}{l} \dot{x} = Ax + Bu, \\ y = Cx, \end{array} \\ \mathbf{\Phi}: & \dot{y}_\Phi = f_1(y_\Phi(t), u_\Phi(t))\dot{u}_{\Phi+}(t) + f_2(y_\Phi(t), u_\Phi(t))\dot{u}_{\Phi-}(t), \\ & u = -y_\Phi,\ u_\Phi = y, \end{array} \tag{5.16}$$

where $A \in \mathbb{R}^{n\times n}$, $B \in \mathbb{R}^{n\times 1}$ and $C \in \mathbb{R}^{1\times n}$. Suppose that there exist L, w and $Q = Q^T > 0$ such that

$$A^TQ + QA + L^TL \leq 0, \tag{5.17}$$

$$QB - A^TC^T = L^Tw, \tag{5.18}$$

$$2CB = w^2, \tag{5.19}$$

hold. Then for every initial condition $(x(0), y_\Phi(0))$, the state trajectory of the closed-loop system (5.16) *is bounded and converges to the largest invariant set in $\{(x, y_\Phi)|Lx + wy_\Phi = 0\}$.*

Proof: Let $V_G(x) = \frac{1}{2}x^TQx$, and using (5.17)−(5.19), it can be checked that $\dot{V}_G = \frac{1}{2}x^T(A^TQ + QA)x + x^TQBu \leq \dot{y}u - \frac{1}{2}(Lx + wy_\Phi)^2$. This indicates that the linear system is CCW.

By the assumptions of the theorem, the Duhem operator Φ is CW with the function $H_{\circlearrowleft_1} : \mathbb{R}^2 \to \mathbb{R}_+$ as given in (4.24).

Now let $H_{cl}(x, y_\Phi) = V_G(x) + H_{\circlearrowleft_1}(y_\Phi, Cx)$ as the Lyapunov function of the system (5.16). According to Proposition 4.3.5, $H_{\circlearrowleft_1}(y_\Phi, Cx)$ is radially unbounded for every x, which implies that $H_{cl}(x, y_\Phi)$ is radially unbounded.

Computing the time derivative of H_{cl}, we obtain

$$\dot{H}_{cl} = \dot{V}_G + \dot{H}_{\circlearrowleft_1} \leq \frac{1}{2}(Lx + wy_\Phi)^2.$$

This inequality together with the radially unboundedness of H_{cl} implies that the trajectory (x, y_Φ) is bounded. Using the LaSalle's invariance principle, we conclude that the trajectory (x, y_Φ) of (5.16) converges to the largest invariant set contained in $M := \{(x, y_\Phi) \in \mathbb{R}^n \times \mathbb{R}|Lx + wy_\Phi = 0\}$. □

To illustrate Theorem 5.3.1 we can use the following example.

Example 5.3.2

$$\begin{array}{rll} \mathbf{P}: & \dot{x} & = \left[\begin{smallmatrix} 0 & 1 \\ -\frac{k}{m} & -\frac{b}{m} \end{smallmatrix}\right] x + \left[\begin{smallmatrix} 0 \\ \frac{1}{m} \end{smallmatrix}\right] u, \\ & y & = \left[\begin{smallmatrix} c_1 & c_2 \end{smallmatrix}\right] x, \\ \mathbf{\Phi}: & \dot{y}_\Phi = f_1(y_\Phi(t), u_\Phi(t))\dot{u}_{\Phi+}(t) + f_2(y_\Phi(t), u_\Phi(t))\dot{u}_{\Phi-}(t), & \\ & u = -y_\Phi,\ u_\Phi = y, & \end{array}$$

where $x(t) \in \mathbb{R}$, $c_1, c_2 \in \mathbb{R}_+$, $m, b, k > 0$ *and the functions* f_1, f_2 *satisfy the hypotheses in Theorem 4.3.1. As given in Example 5.1.2, using* $Q = \left[\begin{smallmatrix} c_1 k & c_2 k \\ c_2 k & c_2 b + c_1 m \end{smallmatrix}\right]$, *we have that if* $c_2 k - c_1 b \leq 0$, *then* (5.17) − (5.19) *hold with*

$$w = \sqrt{\frac{2c_2}{m}}, \quad L = \left[\begin{smallmatrix} \frac{k\sqrt{2c_2 m}}{m} & \frac{b\sqrt{2c_2 m}}{m} \end{smallmatrix}\right].$$

Define $H_{cl}(x, y_\Phi) = \frac{1}{2}x^T Q x + H_{\circlearrowleft_1}(y_\Phi, \left[\begin{smallmatrix} c_1 & c_2 \end{smallmatrix}\right] x)$, *a routine computation shows that*

$$\begin{aligned} \dot{H}_{cl} &\leq \dot{y}y_\Phi - \dot{y}y_\Phi - \frac{1}{2}(Lx + wy_\Phi)^2 \\ &= -\frac{1}{2}(Lx + wy_\Phi)^2. \end{aligned}$$

This inequality implies that (x, y_Φ) *converges to the invariant set contained in* $M := \{(x, y_\Phi) \in \mathbb{R}^n \times \mathbb{R} | Lx + wy_\Phi = 0\}$. △

5.4 CW Linear System Interconnected with CW Duhem Hysteresis

To complete the Table 5.1, in this section we consider the interconnection case ⓓ where a CW linear system is positive feedback interconnected with a CW Duhem hysteresis operator.

5.4.1 Stability Analysis

Theorem 5.4.1 *Consider a* positive *feedback interconnection of a linear system and a Duhem operator* Φ *satisfying the hypotheses in Theorem 4.3.1 as follows*

$$\begin{array}{rll} \mathbf{P}: & \dot{x} & = Ax + Bu, \\ & y & = Cx + Du, \\ \mathbf{\Phi}: & \dot{y}_\Phi = f_1(y_\Phi(t), u_\Phi(t))\dot{u}_{\Phi+}(t) + f_2(y_\Phi(t), u_\Phi(t))\dot{u}_{\Phi-}(t), & \\ & u = y_\Phi,\ u_\Phi = y, & \end{array} \tag{5.20}$$

where $A \in \mathbb{R}^{n\times n}$, $B \in \mathbb{R}^{n\times 1}$, $C \in \mathbb{R}^{1\times n}$ and $D \in \mathbb{R}$. Assume that $f_1(\gamma, v) \leq \eta$ and $f_2(\gamma, v) \leq \eta$ for all $(\gamma, v) \in \mathbb{R}^2$. Suppose that there exist w, L and $P = P^T > 0$, such that

$$\begin{bmatrix} P - 2\eta C^T C & C^T(1-2\eta D) \\ C(1-2\eta D) & D(1-2\eta D^2) \end{bmatrix} > 0 \tag{5.21}$$

$$A^T P + PA + L^T L \leq 0 \tag{5.22}$$

$$PB + A^T C^T = -L^T w \tag{5.23}$$

$$2CB = -w^2 \tag{5.24}$$

hold. Then for every initial condition $(x(0), y_\Phi(0))$, the state trajectory of the closed-loop system (5.20) *is bounded and converges to the largest invariant set in $M := \{(x, y_\Phi) \in \mathbb{R}^n \times \mathbb{R} | Lx + wy_\Phi = 0\}$.*

Proof: Define $V_G(y_\Phi, x) = \frac{1}{2}x^T Px + (y - Du)u + \frac{D}{2}u^2$. Using (5.22), (5.23) and (5.24), we have $\dot{V}_G \leq y\dot{u} - \frac{1}{2}(Lx + wu)^2$, i.e., the linear system is CW.

Next we take $H_{cl}(x, y_\Phi) = H_{\circlearrowleft_1}(y_\Phi, y) + V_G(y_\Phi, x) - yy_\Phi$ as the Lyapunov function of the interconnected system. We show first that H_{cl} is lower bounded. Using the definition of V as above and $H_{\circlearrowleft_1}$ as in (4.24), we have

$$H_{cl} = \frac{1}{2}\begin{bmatrix} u & x^T \end{bmatrix}\begin{bmatrix} D & C^T \\ C & P \end{bmatrix}\begin{bmatrix} u \\ x \end{bmatrix} + \int_0^{u_\Phi} \omega_\Phi(\sigma, y_\Phi, u_\Phi)\mathrm{d}\sigma - u_\Phi y_\Phi + \int_0^{\Lambda(y_\Phi, u_\Phi)} f_{an}(\sigma) - \omega_\Phi(\sigma, y_\Phi, u_\Phi)\mathrm{d}\sigma.$$

Since $u_\Phi = y$, $u_\Phi^2 = \begin{bmatrix} u & x^T \end{bmatrix}\begin{bmatrix} D^2 & DC \\ C^T D & C^T C \end{bmatrix}\begin{bmatrix} u \\ x \end{bmatrix}$. By the assumption on P, there exists $\eta, \varepsilon > 0$ such that $\begin{bmatrix} P-2\eta C^T C & C^T(1-2\eta D) \\ C(1-2\eta D) & D(1-2\eta D^2) \end{bmatrix} > \varepsilon I$. Then

$$\begin{aligned} H_{cl} &= \frac{1}{2}\begin{bmatrix} u & x^T \end{bmatrix}\begin{bmatrix} P-2\eta C^T C & C^T(1-2\eta D) \\ C(1-2\eta D) & D(1-2\eta D^2) \end{bmatrix}\begin{bmatrix} u \\ x \end{bmatrix} + \int_0^{\Lambda(y_\Phi, u_\Phi)} f_{an}(\sigma) - \omega_\Phi(\sigma, y_\Phi, u_\Phi)\mathrm{d}\sigma \\ &\quad + \eta u_\Phi^2 + \int_0^{u_\Phi} \omega_\Phi(\sigma, y_\Phi, u_\Phi)\mathrm{d}\sigma - u_\Phi y_\Phi \\ &\geq \frac{\varepsilon}{2}\left\|\begin{bmatrix} u \\ x \end{bmatrix}\right\|^2 + \int_0^{\Lambda(y_\Phi, u_\Phi)} f_{an}(\sigma) - \omega_\Phi(\sigma, y_\Phi, u_\Phi)\mathrm{d}\sigma \\ &\quad + \int_0^{u_\Phi} (\omega_\Phi(\sigma, y_\Phi, u_\Phi) - y_\Phi + \eta u_\Phi)\,\mathrm{d}\sigma \end{aligned} \tag{5.25}$$

It can be checked that the second term of (5.25) is nonnegative. Indeed, it follows from the property of the CW intersecting function Λ that if $\Lambda(y_\Phi, u_\Phi) \geq 0$ we have that $f_{an}(\sigma) \geq \omega_\Phi(\sigma, y_\Phi, u_\Phi)$ for all $\sigma \in [0, \Lambda(y_\Phi, u_\Phi)]$ and if $\Lambda(y_\Phi, u_\Phi) < 0$ then

$f_{an}(\sigma) \leq \omega_\Phi(\sigma, y_\Phi, u_\Phi)$ for all $\sigma \in [\Lambda(y_\Phi, u_\Phi), 0]$.
To check whether the last term of (5.25) is lower bounded, we use the definition of ω_Φ given in the Section 4.1.2. Consider the case $u_\Phi \geq 0$. Using the definition of ω_Φ in (4.2), the last term of (5.25) can be written by

$$\begin{aligned}
&\int_0^{u_\Phi} (\omega_\Phi(\sigma, y_\Phi, u_\Phi) - y_\Phi + \eta u_\Phi)\,\mathrm{d}\sigma \\
&= \int_0^{u_\Phi} \left(y_\Phi + \int_{u_\Phi}^{\sigma} f_2(\omega_\Phi(s, y_\Phi, u_\Phi), s)\mathrm{d}s \right) \mathrm{d}\sigma + \int_0^{u_\Phi} \eta u_\Phi - y_\Phi \mathrm{d}\sigma \\
&= \int_0^{u_\Phi} \int_\sigma^{u_\Phi} \eta - f_2(\omega_\Phi(s, y_\Phi, u_\Phi), s)\mathrm{d}s\mathrm{d}\sigma + \frac{\eta}{2} u_\Phi^2 \geq 0,
\end{aligned}$$

where the last inequality is due to fact that $f_2(\gamma, v) \leq \eta$ for all $(\gamma, v) \in \mathbb{R}^2$. In a similar way, we can obtain the non-negativity of $\int_0^{u_\Phi} (\omega_\Phi(\sigma, y_\Phi, u_\Phi) - y_\Phi + \eta u_\Phi)\mathrm{d}\sigma$ for the case $u_\Phi < 0$. Therefore, (5.25) implies that H_{cl} is lower bounded and radially unbounded.
It can be computed that $\dot{H}_{cl} = \dot{V}_G + \dot{H}_{\circlearrowleft_1} - \dot{y} y_\Phi - y \dot{y}_\Phi \leq -\frac{1}{2}(Lx + w y_\Phi)^2$. Hence, by the radially unboundedness of H_{cl}, it implies that (x, y_Φ) is bounded. Using the LaSalle's invariance principle, we can conclude that the trajectory (x, y_Φ) of (5.20) converges to the largest invariant set contained in $M := \{(x, y_\Phi) \in \mathbb{R}^n \times \mathbb{R} | Lx + w y_\Phi = 0\}$. □

To illustrate Theorem 5.4.1, let us consider the Example 5.2.2, where we replace the negative feedback interconnection by a positive one.

Example 5.4.2

$$\begin{aligned}
\mathbf{P}: \quad & \dot{x} = \begin{bmatrix} 0 & 1 \\ -\frac{k}{m} & -\frac{b}{m} \end{bmatrix} x + \begin{bmatrix} 0 \\ \frac{1}{m} \end{bmatrix} u, \\
& y = \begin{bmatrix} -c_1 & -c_2 \end{bmatrix} x + u, \\
\mathbf{\Phi}: \quad & \dot{y}_\Phi = f_1(y_\Phi(t), u_\Phi(t)) \dot{u}_{\Phi+}(t) + f_2(y_\Phi(t), u_\Phi(t)) \dot{u}_{\Phi-}(t) \\
& u = y_\Phi,\ u_\Phi = y,
\end{aligned}$$

where $x(t) \in \mathbb{R}$, $c_1, c_2 \in \mathbb{R}_+$, $m, b, k > 0$ and the functions f_1, f_2 satisfy the hypotheses in Theorem 4.3.1. As given in Example 5.2.2, by using $P = \begin{bmatrix} c_1 k & c_2 k \\ c_2 k & c_1 m + c_2 b \end{bmatrix}$, we have that, if $c_2 k - c_1 b \leq 0$ and $c_1 k(c_1 m + c_2 b) - c_2^2 k^2 > c_1^3 m + c_1^2 c_2 b - c_1 c_2^2 k$, the conditions in (5.22), (5.23) *and* (5.24) *hold with*

$$w = \sqrt{\frac{2c_2}{m}}, \quad L = \begin{bmatrix} -\frac{k\sqrt{2c_2 m}}{m} & -\frac{b\sqrt{2c_2 m}}{m} \end{bmatrix}.$$

Additional, if there exists $\eta > 0$ such that $1 - \eta D > 0$ and $k - \frac{D^2 + 1 - \eta D}{D} c_1 > 0$, then (5.21) *holds.*

Using $H_{cl}(x, y_\Phi) = \frac{1}{2}x^T Px + \left[\begin{smallmatrix} -c_1 & -c_2 \end{smallmatrix}\right] xy_\Phi + \frac{1}{2}y_\Phi^2 + H_{\circlearrowleft_1}(y_\Phi, \left[\begin{smallmatrix} -c_1 & -c_2 \end{smallmatrix}\right] x + y_\Phi) - yy_\Phi$, *routine computation shows that* $\dot{H}_{cl} \leq -\frac{1}{2}(Lx + wy_\Phi)^2$. *Hence, if* $f_1(\gamma, v) \leq \eta$ *and* $f_2(\gamma, v) \leq \eta$ *for all* $(\gamma, v) \in \mathbb{R}^2$, *then* (x, y_Φ) *converges to the invariant set contained in* $M := \{(x, y_\Phi) \in \mathbb{R}^n \times \mathbb{R} | Lx + wy_\Phi = 0\}$ *following Theorem 5.4.1.* △

5.5 Extension to Nonlinear Plants

In the previous sections, we have discussed the absolute stability of a feedback interconnection between a Duhem hysteresis operator and a linear system. Here, we extend the previous results to the case where a Duhem hysteresis operator is feedback interconnected to a nonlinear system. Similar to the linear case, we proceed the stability analysis based on the CCW or CW properties of the nonlinear system. This study is motivated by [1] and [60], where a positive feedback interconnection between two CCW nonlinear systems has been studied.

Consider a nonlinear system of the following form

$$\dot{x} = f(x, u),\ y = h(x), \tag{5.26}$$

where $x \in \mathbb{R}^n$, $u \in \mathbb{R}$, $y \in \mathbb{R}$ and $f : \mathbb{R}^n \times \mathbb{R} \to \mathbb{R}^n$ is locally Lipschitz.

Then the feedback interconnection between the system (5.26) and a Duhem hysteresis operator can be given as follows

$$\begin{aligned} \dot{x} &= f(x, u), \\ y &= h(x), \\ \dot{y}_\Phi &= f_1(y_\Phi(t), u_\Phi(t))\dot{u}_{\Phi+}(t) + f_2(y_\Phi(t), u_\Phi(t))\dot{u}_{\Phi-}(t), \end{aligned} \tag{5.27}$$

Proposition 5.5.1 *Consider a* negative *feedback interconnection of a nonlinear system and a Duhem operator* Φ *satisfying the hypotheses in Proposition 4.3.5 as follows*

$$\begin{aligned} \dot{x} &= f(x, u), \\ y &= h(x), \\ \dot{y}_\Phi &= f_1(y_\Phi(t), u_\Phi(t))\dot{u}_{\Phi+}(t) + f_2(y_\Phi(t), u_\Phi(t))\dot{u}_{\Phi-}(t), \\ u &= -y_\Phi, y = u_\Phi \end{aligned} \tag{5.28}$$

If there exists a Lyapunov function $V_G : \mathbb{R}^n \to \mathbb{R}_+$ *and* $\varepsilon > 0$ *such that*

$$\frac{\partial V_G(x)}{\partial x} f(x, u) \leq \left\langle \frac{\partial h(x)}{\partial x} f(x, u), u \right\rangle - \varepsilon \left\| \frac{\partial h(x)}{\partial x} f(x, u) \right\|^2, \tag{5.29}$$

hold. Assume further that V_G *is radially unbounded.Then for every initial condition* $(x(0), y_\Phi(0))$, *the state trajectory of the closed-loop system* (5.27) *is bounded and converges to the largest invariant set in* $\{(x, y_\Phi) | \frac{\partial h(x)}{\partial x} f(x, y_\Phi) = 0\}$.

Proof: Since the Duhem operator satisfies the Proposition 4.3.5, then there exists a storage function $H_{\circlearrowleft_1} : \mathbb{R}^2 \to \mathbb{R}_+$ such that for every $u_\Phi \in AC(\mathbb{R}_+)$ and for every admissible y_{Φ_0}, the CW dissipation inequality (4.25) holds and $H_{\circlearrowleft_1}$ is radially unbounded w.r.t its first argument.

Let $H_{cl} = V_G(x) + H_{\circlearrowleft_1}(y_\Phi, h(x))$ be the total Lyapunov function for the closed-loop system. Then compute the time derivative of H_{cl} we have

$$\dot{H}_{cl} = \dot{V}_G + \dot{H}_{\circlearrowleft_1} \leq -\varepsilon \left\| \frac{\partial h(x)}{\partial x} f(x,u) \right\|^2,$$

where the last inequality is obtained by applying the interconnection properties $u = -y_\Phi$ and $y = u_\Phi$. Since V_G is radially unbounded, we have that H_{cl} is radially unbounded. Based on LaSalle's invariance principle, we can conclude that the trajectory (x, y_Φ) of (5.27) converges to the largest invariant set contained in $M := \{(x, y_\Phi) \in \mathbb{R}^n \times \mathbb{R} | \left\| \frac{\partial h(x)}{\partial x} f(x,u) \right\|^2 = 0\}$. □

Proposition 5.5.2 *Consider a* positive *feedback interconnection of a nonlinear system and a Duhem operator Φ satisfying the hypotheses in Theorem 4.2.1 as follows*

$$\begin{aligned} \dot{x} &= f(x,u), \\ y &= h(x), \\ \dot{y}_\Phi &= f_1(y_\Phi(t), u_\Phi(t))\dot{u}_{\Phi+}(t) + f_2(y_\Phi(t), u_\Phi(t))\dot{u}_{\Phi-}(t), \\ u &= y_\Phi, y = u_\Phi \end{aligned} \tag{5.30}$$

If there exists a Lyapunov function $V_G : \mathbb{R}^n \to \mathbb{R}_+$ and $\varepsilon > 0$ such that

$$\frac{\partial V_G(x)}{\partial x} f(x,u) \leq \left\langle \frac{\partial h(x)}{\partial x} f(x,u), u \right\rangle - \varepsilon \left\| \frac{\partial h(x)}{\partial x} f(x,u) \right\|^2, \tag{5.31}$$

hold. Assume further that $H_{cl}(x, y_\Phi) = H_{\circlearrowleft_1}(y_\Phi, h(x)) + V_G(x) - y_\Phi h(x)$ is radially unbounded. Then for every initial condition $(x(0), y_\Phi(0))$, the state trajectory of the closed-loop system (5.27) *is bounded and converges to the largest invariant set in $\{(x, y_\Phi) | \frac{\partial h(x)}{\partial x} f(x, -y_\Phi) = 0\}$.*

The Proof of Proposition 5.5.2 is omitted here, since it is similar to the proof of Proposition 5.5.1.

Now let us consider the interconnection cases: a CW nonlinear system is feedback interconnected to a CCW Duhem hysteresis operator and a CW nonlinear system is feedback interconnected to a CW Duhem hysteresis operator. The absolute stability results can be summarized in the following two propositions.

Proposition 5.5.3 *Consider a* negative *feedback interconnection of a nonlinear system and a Duhem operator Φ satisfying the hypotheses in Theorem 4.2.1 as follows*

$$\begin{aligned} \dot{x} &= f(x,u), \\ y &= h(x,u), \\ \dot{y}_\Phi &= f_1(y_\Phi(t),u_\Phi(t))\dot{u}_{\Phi+}(t) + f_2(y_\Phi(t),u_\Phi(t))\dot{u}_{\Phi-}(t), \\ u &= -y_\Phi, y = u_\Phi \end{aligned} \tag{5.32}$$

If there exists $\theta, V_G : \mathbb{R}^{n+1} \to \mathbb{R}_+$ such that

$$\begin{bmatrix} \frac{\partial V_G(u,x)}{\partial u} & \frac{\partial V_G(u,x)}{\partial x} \end{bmatrix} \begin{bmatrix} v_d \\ f(x,u) \end{bmatrix} \leq h(x,u)v_d - \theta(u,x), \tag{5.33}$$

for all $u \in \mathbb{R}$ and $v_d \in \mathbb{R}$ hold. Assume further that V_G is radially unbounded. Then for every initial condition $(x(0), y_\Phi(0))$, the state trajectory of the closed-loop system (5.27) *is bounded and converges to the largest invariant set in $\{(x, y_\Phi)|\theta(-y_\Phi, x) = 0\}$.*

The Proof of Proposition 5.5.3 is omitted here, since it follows the same line as the proof of Proposition 5.5.1.

Proposition 5.5.4 *Consider a* positive *feedback interconnection of a nonlinear system and a Duhem operator Φ satisfying the hypotheses in Theorem 4.3.1 as follows*

$$\begin{aligned} \dot{x} &= f(x,u), \\ y &= h(x,u), \\ \dot{y}_\Phi &= f_1(y_\Phi(t),u_\Phi(t))\dot{u}_{\Phi+}(t) + f_2(y_\Phi(t),u_\Phi(t))\dot{u}_{\Phi-}(t), \\ u &= y_\Phi, y = u_\Phi \end{aligned} \tag{5.34}$$

If there exists $\theta, V_G : \mathbb{R}^{n+1} \to \mathbb{R}_+$ such that

$$\begin{bmatrix} \frac{\partial V_G(u,x)}{\partial u} & \frac{\partial V_G(u,x)}{\partial x} \end{bmatrix} \begin{bmatrix} v_d \\ f(x,u) \end{bmatrix} \leq h(x,u)v_d - \theta(u,x), \tag{5.35}$$

for all $u \in \mathbb{R}$ and $v_d \in \mathbb{R}$ hold. Assume further that $H_{cl}(x, y_\Phi) = H_{\circlearrowleft_1}(y_\Phi, h(x, y_\Phi)) + V_G(y_\Phi, x) - y_\Phi h(x, y_\Phi)$ is radially unbounded. Then for every initial condition $(x(0), y_\Phi(0))$, the state trajectory of the closed-loop system (5.27) *is bounded and converges to the largest invariant set in $\{(x, y_\Phi)|\theta(y_\Phi, x) = 0\}$.*

The Proof of Proposition 5.5.4 is omitted, since it is similar to the proof of Proposition 5.5.1.

In this section, the stability analysis for a feedback interconnection of a Duhem hysteresis operator and a nonlinear plant is presented. Here, the absolute stability problem can also be solved based on the CCW or CW properties of the nonlinear system, which is an extension to the case of the linear plant.

5.6 Concluding Remarks

In this chapter, we present the stability analysis of a linear system with a Duhem hysteresis nonlinearity. The absolute stability is based on the I/O property of the corresponding hysteresis operator and the linear system. Four possible interconnection cases are discussed, which are motivated by real applications. Extension to the nonlinear case is also given. The absolute stability analysis results can be applied to design controller for hysteretic systems which are presented in Chapter 6.

Chapter 6

Controller Design for a System with Duhem Hysteresis Nonlinearity

In this chapter, we focus on the controller design for a linear system interconnected with a hysteretic actuator (sensor). Based on the stability results given in the previous chapter, a general linear controller design algorithm is proposed here. The proposed controller guarantees the stability of the closed-loop system, so that the state trajectories are converging to an invariant manifold. Furthermore, two study cases are given for a second-order linear system with a hysteretic actuator. The hysteretic actuator is modeled by a Duhem model which exhibits: (i) clockwise (CW) input-output (I/O) dynamics (such as the Dahl model, LuGre model and Maxwell-Slip model, which describe hysteresis phenomena in mechanical friction); (ii) counter-clockwise(CCW) input-output (I/O) dynamics (such as the Jiles-Atherton model, the Coleman model, which describes the hysteresis phenomena in piezo-actuator). For the case where the hysteretic actuator has CW I/O dynamics, a proportional, integral and derivative (PID) controller is applied. In particular, sufficient conditions on the controller gains are given such that the origin of the plant and the state of the hysteresis is globally attractive. For the case where the hysteretic actuator has CCW I/O dynamics, a proportional and derivative (PD) controller is applied. Similarly, sufficient conditions on the control parameters are given such that the closed-loop system is globally asymptotic stable with respect to an invariant set where the velocity is equal to zero. The robustness of the closed-loop system is also presented by using the *integral* input-to-state stability (*i*ISS) concept.

6.1 General Case

The stability analysis given in the Chapter 5 can be used to design a controller for a linear plant with hysteretic sensor/actuator. In this section, we present controller design algorithm for the general case, where we give sufficient conditions on the control parameters such that the controlled system is stable.

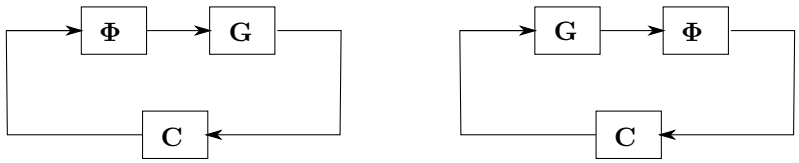

Figure 6.1: Feedback interconnection of a linear plant $\mathbf{G}$, controller $\mathbf{C}$ and hysteresis operator $\mathbf{\Phi}$. (a) An interconnection example where the plant $\mathbf{G}$ is driven by a hysteretic actuator $\mathbf{\Phi}$; (b) An interconnection example where the dynamics of $\mathbf{G}$ is measured by a hysteretic sensor $\mathbf{\Phi}$.

6.1.1 Controller Design Algorithm

Consider the closed-loop system as shown in Figure 6.1, where $\mathbf{G}$ and $\mathbf{C}$ are the linear plant and controller, respectively, and they are given by

$$\begin{aligned} \mathbf{G}: \begin{cases} \dot{x}_G &= A_G x_G + B_G u_G, \\ y_G &= C_G x_G + D_G u_G, \end{cases} \\ \mathbf{C}: \begin{cases} \dot{x}_C &= A_C x_C + B_C u_C, \\ y_C &= C_C x_C + D_C u_C. \end{cases} \end{aligned} \tag{6.1}$$

Thus depending on the location of the hysteretic element, the cascaded linear systems can be compactly written into

$$\begin{aligned} \dot{x} &= Ax + Bu \\ y &= Cx + Du, \end{aligned} \tag{6.2}$$

where $x = \left[\begin{smallmatrix} x_G \\ x_C \end{smallmatrix}\right]$ and for the case of hysteretic actuator as shown in Figure 6.1(a), $A = \left[\begin{smallmatrix} A_G & 0 \\ B_C C_G & A_C \end{smallmatrix}\right]$, $B = \left[\begin{smallmatrix} B_G \\ B_C D_G \end{smallmatrix}\right]$, $C = \left[\begin{smallmatrix} D_C C_G & C_C \end{smallmatrix}\right]$, $D = D_C D_G$, or for the case of hysteretic sensor as shown in Figure 6.1(b), $A = \left[\begin{smallmatrix} A_G & B_G C_C \\ 0 & A_C \end{smallmatrix}\right]$, $B = \left[\begin{smallmatrix} B_G D_C \\ B_C \end{smallmatrix}\right]$, $C = \left[\begin{smallmatrix} C_G & D_G C_C \end{smallmatrix}\right]$, $D = D_G D_C$.

The controller design can then be carried out as follows.

- *Control design algorithm for the case of CCW Φ:*

  1. Determine, if possible, the anhysteresis function f_{an} of the Duhem operator Φ and the desired L and w.
  2. Find $\mathbf{C}$ such that either (5.3)-(5.6) or (5.10)-(5.13) holds.

3. If (5.3)-(5.6) is solvable, then **C** stabilizes the closed-loop system with a negative feedback interconnection; otherwise
4. If (5.10)-(5.13) is solvable, then **C** stabilizes the closed-loop system with a positive feedback interconnection.

- *Control design algorithm for the case of CW* Φ*:*

1. Determine, if possible, the functions f_1 and f_2 of the Duhem operator Φ and the desired L and w.
2. Find **C** such that either (5.17)-(5.19) or (5.21)-(5.24) holds.
3. If (5.17)-(5.19) is solvable, then **C** stabilizes the closed-loop system with a negative feedback interconnection; otherwise
4. If (5.21)-(5.24) is solvable, then **C** stabilizes the closed-loop system with a positive feedback interconnection.

Based on the control design algorithm stated above, we present some numerical examples in the following subsection.

6.1.2 Mass-damper-spring System with Hysteretic Actuator

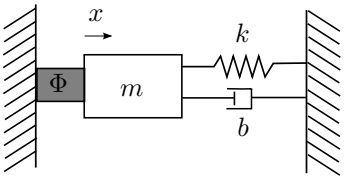

Figure 6.2: Mass-damper-spring system connected with a hysteretic actuator

As an example, let us consider a mass-damper-spring plant **G** with a hysteretic actuator **Φ**, as shown in Figure 6.2, where the input to the controller **C** is the displacement x and the control output v is the driving signal of the actuator. By considering numerical values of the mass $m = 1$, the damping constant $b = 2$ and the spring constant $k = 1$, the dynamics of the plant **G** is given by

$$\dot{x}_G = \begin{bmatrix} 0 & 1 \\ -1 & -2 \end{bmatrix} x_G + \begin{bmatrix} 0 \\ 1 \end{bmatrix} u_G,\ y_G = \begin{bmatrix} 1 & 0 \end{bmatrix} x_G. \tag{6.3}$$

CCW Hysteretic Actuator

Let us first consider the case when the hysteretic actuator has CCW I/O dynamics, such as piezo-actuators [28]. Assume that the actuator is represented by the Duhem operator (3.1) where

$$f_1(\gamma, \upsilon) = -\gamma + 0.475\upsilon + 0.3,\ f_2(\gamma, \upsilon) = \gamma - 0.475\upsilon + 0.3,\ \forall(\gamma, \upsilon) \in \mathbb{R}^2. \quad (6.4)$$

It can be verified that $f_{an}(\upsilon) = 0.475\upsilon$ and the functions f_1 and f_2 satisfy the hypotheses given in Theorem 4.2.1.

Since we have $f_{an}(\upsilon) = 0.475\upsilon$, then by taking $A_c = \left[\begin{smallmatrix} 0 & 1 \\ -2 & -4 \end{smallmatrix}\right]$, $B_c = \left[\begin{smallmatrix} 0 \\ 1 \end{smallmatrix}\right]$, $C_c = \left[\begin{smallmatrix} 1 & 1 \end{smallmatrix}\right]$ and $D_c = 0$ to the controller $\mathbf{C}$ as in (6.1), it can be checked that the cascaded system (of $\mathbf{G}$ and $\mathbf{C}$) in (6.2) satisfies (5.3)-(5.6) with $\xi = 0.5$ and

$$Q = \begin{bmatrix} 6 & 1 & -6 & -2 \\ 1 & 4 & -1 & -4 \\ -6 & -1 & 7 & 3 \\ -2 & -4 & 3 & 7 \end{bmatrix}.$$

In this case $L = \left[\begin{smallmatrix} 1 & 0 & -2 & -3 \end{smallmatrix}\right]$ and $w = 0$. Moreover, f_{an} belongs to the sector $[0, 0.5]$. It follows from Theorem 5.1.1 that the closed-loop system converges to the largest invariant set contained in $\{(x, y_\Phi) | Lx - wy_\Phi = 0\} = \{(x, y_\Phi) | \left[\begin{smallmatrix} 1 & 0 & -2 & -3 \end{smallmatrix}\right] x = 0\}$. This implies that the velocity of the mass-damper-spring system converges to zero and the position of the mass-damper-spring system converges to a constant. The simulation results is shown in Figure 6.3(a).

CW Hysteretic Actuator

For the case of a CW hysteretic actuator, see for example the magnetorheological (MR) damper used in the structure control [45], the mass-damper-spring system is given by (6.3). Assume that the actuator is represented by the Duhem operator (3.1) where

$$f_1(\gamma, \upsilon) = 0.25(1 - \gamma),\ f_2(\gamma, \upsilon) = 0.25(1 + \gamma),\ \forall(\gamma, \upsilon) \in \mathbb{R}^2. \quad (6.5)$$

The anhysteresis function for this Duhem operator is $f_{an} = 0$. In addition f_1 and f_2 satisfy the hypotheses in Theorem 4.3.1, hence the Duhem operator with (6.5) is CW by using $A_c = \left[\begin{smallmatrix} 0 & 1 \\ -2 & -4 \end{smallmatrix}\right]$, $B_c = \left[\begin{smallmatrix} 0 \\ 1 \end{smallmatrix}\right]$, $C_c = \left[\begin{smallmatrix} 1 & 1 \end{smallmatrix}\right]$ and $D_c = 0$ in the controller $\mathbf{C}$ as in (6.1). The conditions (5.17)-(5.19) are solvable for the cascaded system in (6.2) with

$$P = \begin{bmatrix} 5 & 1 & -5 & -2 \\ 1 & 3 & -1 & -3 \\ -5 & -1 & 6 & 3 \\ -2 & -3 & 3 & 6 \end{bmatrix},$$

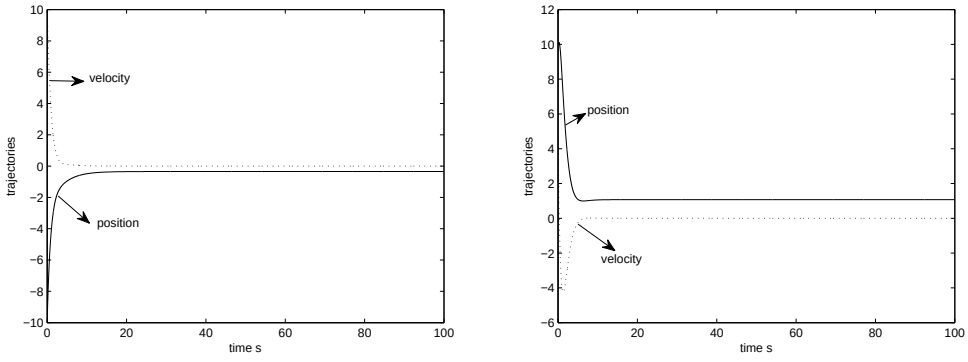

(a) (b)

Figure 6.3: Simulation results of the numerical example. (a) For the case of CCW hysteretic actuator in the positive feedback interconnection with the initial condition $x(0) = [-10\ 10]^T$; (b)For the case of CW hysteretic actuator in the negative feedback interconnection with the initial condition $x(0) = [10\ 5]^T$.

$L = \begin{bmatrix} 1 & 0 & -2 & -3 \end{bmatrix}$ and $w = 0$. Hence the controller $\mathbf{C}$ can stabilize the closed-loop system with negative feedback interconnection. According to Theorem 4.3.1 the closed-loop system converges to the largest invariant set in $\{(x, y_\Phi) | Lx + wy_\Phi = 0\} = \{(x, y_\Phi) | \begin{bmatrix} 1 & 0 & -2 & -3 \end{bmatrix} x = 0\}$. This implies that the velocity of the mass-damper-spring system converges to zero and the position of the mass-damper-spring system converges to a constant. The simulation results are shown in Figure 6.3(b) with the initial condition $x(0) = [10\ 5]^T$.

6.2 PID Control of a Hysteretic Second-order System

In this section, we focus on a second-order hysteretic system where two cases are considered:

Case 1 the hysteresis system has CW I/O behavior. An example to this problem is position control of a (micro-)vehicle where we manipulate the rotation of the wheels in order to exert forces to the vehicle's body via friction forces;

Case 2 the hysteresis system has CCW I/O behavior. An example to this problem is the piezo-actuated stage, where the velocity of the stage is controlled by a piezo-actuator. It is well known that a piezo-actuator exhibits CCW hysteresis from input voltage to output displacement;

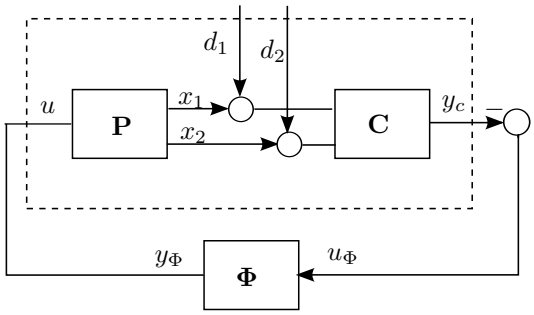

Figure 6.4: Negative feedback interconnection with a linear system $\mathbf{P}$, a controller $\mathbf{C}$ and a Duhem hysteresis operator $\mathbf{\Phi}$.

6.2.1 Hysteresis System with CW I/O Behavior

Consider a feedback interconnection of a second-order single-input single-output (SISO) linear system with a PID and a hysteretic actuator as shown in Figure 6.4, where $\mathbf{P}$ represents the linear plant, $\mathbf{C}$ is the PID controller and $\mathbf{\Phi}$ represents the Duhem hysteresis operator. In Figure 6.4, the measurement noise is represented by the disturbance d_1 and d_2. The disturbance d_1 and d_2 can also be regarded as the estimation error which could result from the application of a state observer for the plant $\mathbf{P}$.

The closed-loop system as shown in Figure 6.4, is given by

$$\begin{aligned}
\mathbf{P}: \quad & \dot{x} = Ax + Bu, \\
\mathbf{C}: \quad & \dot{z} = x_1 + d_1, \\
& y_c = k_i z + \begin{bmatrix} k_p & k_d \end{bmatrix} x - k_p d_1 - k_d d_2, \\
\mathbf{\Phi}: \quad & \dot{y}_\Phi = f_1(y_\Phi, u_\Phi)\dot{u}_{\Phi+} + f_2(y_\Phi, u_\Phi)\dot{u}_{\Phi-}, \\
& u_\Phi = -y_c, \; u = y_\Phi,
\end{aligned} \tag{6.6}$$

where $A \in \mathbb{R}^{2\times 2}$, $B \in \mathbb{R}^{2\times 1}$, $C \in \mathbb{R}^{1\times 2}$ and $x = \begin{bmatrix} x_1 & x_2 \end{bmatrix}^T$. For the PID controller $\mathbf{C}$, z is the state of the integrator, $k_p > 0$, $k_i > 0$ and $k_d > 0$ are the controller gains. For the Duhem hysteresis operator $\mathbf{\Phi}$, the functions f_1 and f_2 are assumed to be locally Lipschitz.

Theorem 6.2.1 *Consider system* (6.6) *with* $d_1 = 0$ *and* $d_2 = 0$. *Assume that the Duhem hysteresis operator* $\mathbf{\Phi}$ *satisfies all the hypotheses of Theorem 4.3.1. If there exists* $Q = Q^T >$

0, L, $k_p > 0$, $k_i > 0$ *and* $k_d > 0$ *such that the following inequalities*

$$A^T Q + QA + L^T L \leq 0 \tag{6.7}$$

$$QB - A^T \begin{bmatrix} k_p & k_d \end{bmatrix}^T - \begin{bmatrix} k_i \\ 0 \end{bmatrix} = L^T w \tag{6.8}$$

$$2 \begin{bmatrix} k_p & k_d \end{bmatrix} B = w^2 + v \tag{6.9}$$

hold for some $w \in \mathbb{R}$, $v > 0$ *and the tuple* (A, L) *is observable, then for every initial condition* $(x_0, z_0) \in \mathbb{R}^3$ *and every admissible* $y_{\Phi_0} \in \mathbb{R}$, *the state trajectories of the closed-loop system* (6.6) *are bounded and converge to* $\mathcal{A} := \{(x, z, y_\Phi) \in \mathbb{R}^4 | x = 0, y_\Phi = 0\}$, *i.e. the closed-loop system is globally asymptotic stable with respect to* $\mathcal{A}$ *(*$\mathcal{A}$*-GAS).*

Note that $v > 0$ in (6.9) will be used later to show the dissipativity property for robustness analysis.

Proof: By assumption, the Duhem operator $\mathbf{\Phi}$ is CW and there exists a function $H_{\circlearrowleft_1} : \mathbb{R}^2 \to \mathbb{R}_+$ such that

$$\dot{H}_{\circlearrowleft_1}(y_\Phi(t), u_\Phi(t)) \leq y_\Phi(t) \dot{u}_\Phi(t). \tag{6.10}$$

Using $V_G(x) = \frac{1}{2} x^T Q x$, (6.6) and (6.7)-(6.9), we have

$$\begin{aligned}
\dot{V}_G(x) &= \frac{1}{2} x^T (A^T Q + QA) x + x^T QBu \\
&= \dot{y}_c u + \frac{1}{2} x^T (A^T Q + QA) x + x^T QBu - \dot{y}_c u \\
&= \dot{y}_c u + \frac{1}{2} x^T (A^T Q + QA) x + x^T \left(QB - \begin{bmatrix} k_i \\ 0 \end{bmatrix} \right) u \\
&\quad - x^T A^T \begin{bmatrix} k_p & k_d \end{bmatrix}^T u - \begin{bmatrix} k_p & k_d \end{bmatrix} B u^2, \\
&\leq \dot{y}_c u - \frac{1}{2} x^T L^T L x + x^T L^T w u - \frac{1}{2} w^2 u^2 - \frac{1}{2} v u^2, \\
&\leq \dot{y}_c u - \frac{1}{2} (Lx - wu)^T (Lx - wu) - \frac{1}{2} v u^2.
\end{aligned}$$

Based on Definition 2.3.3, it can be easily checked that the linear system is CCW.

Now using $V_{cl}(x, z, y_\Phi) = V_G(x) + H_{\circlearrowleft_1}(y_\Phi, -k_i z - \begin{bmatrix} k_p & k_d \end{bmatrix} x)$ as the Lyapunov function of the closed-loop system (6.6) and substituting the interconnection conditions $u_\Phi = -y_c$ and $u = y_\Phi$, we obtain

$$\begin{aligned}
\dot{V}_{cl} &= \dot{V}_G + \dot{H}_{\circlearrowleft_1}, \\
&\leq \dot{y}_c u - \frac{1}{2} (Lx - wu)^T (Lx - wu) + y_\Phi \dot{u}_\Phi, \\
&= -\frac{1}{2} (Lx - wu)^T (Lx - wu) - \frac{1}{2} v u^2.
\end{aligned}$$

Since V_G is proper in x, this inequality implies that x is bounded. Moreover, using Proposition 4.3.5, we also have the boundedness of y_Φ. Based on LaSalle's invariance principle and the compactness of (x, y_Φ), the trajectories converge to the largest invariant set $\mathbf{O}$ contained in $M := \{(x, y_\Phi) \in \mathbb{R}^3 | Lx - wy_\Phi = 0, y_\Phi = 0\}$ as $t \to \infty$.

Since $y_\Phi = 0$ and $Lx = 0$ in the invariant set $\mathbf{O}$ in M, the linear system $\mathbf{P}$ (in the invariant set $\mathbf{O}$) satisfies $LAx = 0$. By the observability of (A, L), $Lx = 0$ and $LAx = 0$ imply that $x = 0$. Thus, it follows that $y_\Phi = 0$ and $x = 0$ in $\mathbf{O}$ and we conclude that (6.6) is GAS with respect to $\mathcal{A} := \{(x, z, y_\Phi) \in \mathbb{R}^4 | x = 0, y_\Phi = 0\}$. □

To illustrate Theorem 6.2.1, consider the following force-actuated mass-damper-spring system with PID controller and a hysteretic actuator

$$\begin{aligned}
\begin{bmatrix} \dot{x}_1 \\ \dot{x}_2 \end{bmatrix} &= \begin{bmatrix} 0 & 1 \\ -\frac{k}{m} & -\frac{b}{m} \end{bmatrix} \begin{bmatrix} x_1 \\ x_2 \end{bmatrix} + \begin{bmatrix} 0 \\ \frac{1}{m} \end{bmatrix} u \\
\dot{z} &= x_1 \\
y_c &= k_i z + k_p x_1 + k_d x_2 \\
y_\Phi &= \Phi(u_\Phi) \\
u_\Phi &= -y_c, u = y_\Phi
\end{aligned} \tag{6.11}$$

where x_1 is the displacement, x_2 is the velocity, z is the state of the integrator, $k > 0$ is the spring constant, $b > 0$ is the damping constant and $m > 0$ is the mass.

Corollary 6.2.2 *Assume that for the Duhem hysteresis operator* $\mathbf{\Phi}$ *there exists* $H_{\circlearrowleft} : \mathbb{R}^2 \to \mathbb{R}_+$ *such that for every* $u_\Phi \in AC(\mathbb{R}_+)$ *and for every admissible* $y_{\Phi_0} \in \mathbb{R}$, (6.10) *holds with* $y_\Phi := \Phi(u_\Phi, y_{\Phi_0})$. *If* $k_i \geq \frac{kk_d}{2m}$ *and* $k_p \geq \frac{mk_i}{b} + \frac{b}{2m}k_d$, *then the closed-loop system* (6.11) *satisfies* (6.7), (6.8) *and* (6.9) *with* $L = \begin{bmatrix} k\sqrt{\frac{k_d}{m}} & b\sqrt{\frac{k_d}{m}} \end{bmatrix}$, $w = \sqrt{\frac{k_d}{m}}$, $v = \frac{k_d}{m}$ *and*

$$Q = \begin{bmatrix} bk_i + kk_p - \frac{bk}{m}k_d & mk_i \\ mk_i & mk_p \end{bmatrix}.$$

In other words, (6.11) *is* $\mathcal{A}$*-GAS.*

Robustness Analysis

In the next case, we study the robustness of the closed-loop system (6.6) by adding disturbances d_1 and d_2 to the measurement of the plant's state. This is related to the case where d_1 and d_2 are regarded as the state estimation error due to the application

of a state observer. In [49, 2], a notion of *integral* input-to-state stability is introduced for the stability analysis of nonlinear systems given a bounded-energy input signal. It is shown in [2] that a system is integral input-to-state stable (*i*ISS) if the system is (a) 0-GAS and (b) dissipative with supply rate σ. In [23] it is shown that for a class of dissipative systems, the *i*ISS gain is equal to the supply rate σ. Here, we study the robustness of system (6.6) by applying the modified concept of *i*ISS, where instead of discussing the *i*ISS with respect to the origin, we are interested in the *i*ISS property with respect to a set $\mathcal{A}$ ($\mathcal{A}$-*i*ISS). The definitions of $iISS$ and $\mathcal{A}$-*i*ISS are given in Chapter 2.

Lemma 6.2.3 *Consider the system in* (6.6) *with* $d_1, d_2 \in C^1(\mathbb{R}_+)$ *s.t.* $\dot{d}_1, \dot{d}_2 \in AC(\mathbb{R}_+)$. *Assume that the hypotheses of Theorem 6.2.1 hold. Then there exists a* $\mu > 0$, *such that* (6.6) *is dissipative with supply rate* $\sigma(d_1, \dot{d}_1, \dot{d}_2) = \mu \left\| \begin{smallmatrix} d_1 \\ \dot{d}_1 \\ \dot{d}_2 \end{smallmatrix} \right\|^2$.

Proof: Let $V_{cl} = V_G + H_{\circlearrowleft_1}$ be the Lyapunov function for the closed-loop system, where V_G and $H_{\circlearrowleft_1}$ have the same descriptions as in the proof of Theorem 6.2.1. Then we have

$$\begin{aligned}
\dot{V}_{cl} &= \dot{V}_G + \dot{H}_{\circlearrowleft_1}, \\
&\leq \dot{y}_c u - \frac{1}{2}(Lx - wu)^T(Lx - wu) + y_\Phi \dot{u}_\Phi - \frac{1}{2}vu^2, \\
&= -\frac{1}{2}(Lx - wu)^T(Lx - wu) + k_p y_\Phi \dot{d}_1 + k_d y_\Phi \dot{d}_2 + k_i y_\Phi d_1 - \frac{1}{2}vu^2
\end{aligned}$$

where the last equality is obtained since $u_\Phi = -y_c + k_p d_1 + k_d d_2$. Using Young's inequality and $u = y_\Phi$, we have

$$\begin{aligned}
\dot{V}_{cl} &\leq \frac{k_i \eta}{2} d_1^2 + \frac{1}{2\eta} y_\Phi^2 + \frac{k_d \epsilon}{2} \dot{d}_2{}^2 + \frac{1}{2\epsilon} y_\Phi^2 + \frac{k_p \delta}{2} \dot{d}_1{}^2 + \frac{1}{2\delta} y_\Phi^2 - \frac{1}{2} v y_\Phi^2, \\
&= \frac{k_i \eta}{2} d_1^2 + \frac{k_p \delta}{2} \dot{d}_1{}^2 + \frac{k_d \epsilon}{2} \dot{d}_2{}^2 - \frac{1}{2}(v - \frac{1}{\epsilon} - \frac{1}{\delta} - \frac{1}{\eta}) y_\Phi^2
\end{aligned}$$

where ϵ and δ are arbitrary positive constants. Since $v > 0$, we can take ϵ and δ such that

$$\frac{1}{\epsilon} + \frac{1}{\delta} + \frac{1}{\eta} \leq v \tag{6.12}$$

holds. This implies that system (6.6) is dissipative with respect to σ where $\sigma(d_1, \dot{d}_1, \dot{d}_2) = \mu \left\| \begin{smallmatrix} d_1 \\ \dot{d}_1 \\ \dot{d}_2 \end{smallmatrix} \right\|^2$ and $\mu = \max\{\frac{k_i \eta}{2}, \frac{k_d \delta}{2}, \frac{k_d \epsilon}{2}\}$. □

Theorem 6.2.4 *Consider the system in* (6.6) *with* $d_1, d_2 \in C^1(\mathbb{R}_+)$ *s.t.* $\dot{d}_1, \dot{d}_2 \in AC(\mathbb{R}_+)$. *Assume that the hypotheses in Theorem 6.2.1 hold and additionally,* (6.12) *is satisfied with* $\epsilon, \delta > 0$. *Assume that the functions* f_1 *and* f_2 *of the Duhem operator* Φ *satisfy*

(B) *For every compact set* $K \in \mathbb{R}$, *there exists* $c > 0$ *such that*

$$\|f_1(\nu, \xi)\| \leq c, \ \|f_2(\nu, \xi)\| \leq c \quad \forall \nu \in K, \xi \in \mathbb{R}. \tag{6.13}$$

Then (6.6) *is iISS with respect to* $\mathcal{A}$ *($\mathcal{A}$-iISS), with iISS gain* $\gamma\left(\left\| \begin{smallmatrix} d_1 \\ \dot{d}_1 \\ \dot{d}_2 \end{smallmatrix} \right\|\right) = \mu \left\| \begin{smallmatrix} d_1 \\ \dot{d}_1 \\ \dot{d}_2 \end{smallmatrix} \right\|^2$, *where* $\mu > 0$.

Proof: The proof of Theorem 6.2.4 follows the same arguments as in the proof of Theorem 6.2.1 in [23]. Firstly, the arguments in [49] which use the converse Lyapunov theorem for GAS system are replaced by the similar arguments using the converse Lyapunov theorem for $\mathcal{A}$-GAS system as discussed in [55].

Notice that the system (6.1) with $d_1 = 0$ and $d_2 = 0$ can be written explicitly as

$$\begin{bmatrix} \dot{z} \\ \dot{x} \\ \dot{y}_\Phi \end{bmatrix} = \begin{bmatrix} x_1 \\ Ax + By_\Phi \\ f_1(y_\Phi, u_\Phi)(-([\,k_i \ \ 0\,] + [\,k_p \ \ k_d\,]A)x - [\,k_p \ \ k_d\,]By_\Phi)_+ \\ +f_2(y_\Phi, u_\Phi)(-([\,k_i \ \ 0\,] + [\,k_p \ \ k_d\,]A)x - [\,k_p \ \ k_d\,]By_\Phi)_- \end{bmatrix}, \tag{6.14}$$

where $u_\Phi = -k_i z - [\,k_p \ \ k_d\,]\, x$. It can be checked that the RHS of equation (6.14) is locally Lipschitz. Let us write (6.14) by $\dot{\zeta} = f(\zeta)$ where $\zeta = [\,x^T \ z \ y_\Phi\,]^T$. Based on the converse Lyapunov theorem [55, Corollary 2], Theorem 6.2.1 implies that there exists a smooth Lyapunov function $V_G : \mathbb{R}^4 \to \mathbb{R}_+$ such that

- there exist $\mathcal{K}_\infty$ functions α_1 and α_2 such that

$$\alpha_1(\|\zeta\|_{\mathcal{A}}) \leq V_G(\zeta) \leq \alpha_2(\|\zeta\|_{\mathcal{A}}) \qquad \forall \zeta \in \mathbb{R}^4.$$

- there exists a continuous, positive definite function α_3 such that

$$\frac{\mathrm{d}V_G(\zeta)}{\mathrm{d}\zeta} f(\zeta) \leq -\alpha_3(\|\zeta\|_{\mathcal{A}}) \qquad \forall \zeta \in \mathbb{R}^4.$$

With the disturbance d_1 and d_2, the system (6.6) can be written as

$$\dot{\zeta} = f(\zeta, d_1, d_2, \dot{d}_1, \dot{d}_2) = \begin{bmatrix} x_1 + d_1 \\ Ax + By_\Phi \\ f_1(y_\Phi, u_\Phi)(-([\,k_i \ \ 0\,] + [\,k_p \ \ k_d\,]A)x \\ -[\,k_p \ \ k_d\,]By_\Phi - [\,k_p \ \ k_d\,]\begin{bmatrix} \dot{d}_1 \\ \dot{d}_2 \end{bmatrix})_+ \\ +f_2(y_\Phi, u_\Phi)(-([\,k_i \ \ 0\,] + [\,k_p \ \ k_d\,]A)x \\ -[\,k_p \ \ k_d\,]By_\Phi - [\,k_p \ \ k_d\,]\begin{bmatrix} \dot{d}_1 \\ \dot{d}_2 \end{bmatrix})_- \end{bmatrix},$$

$u_\Phi = -k_i z - \begin{bmatrix} k_p & k_d \end{bmatrix} x - \begin{bmatrix} k_p & k_d \end{bmatrix} \begin{bmatrix} d_1 \\ d_2 \end{bmatrix}$. Using Assumption (**B**), we have that for every $\mathbb{B}_l^{\mathcal{A}} = \left\{ \begin{bmatrix} z \\ x \\ y_\Phi \end{bmatrix} \middle| \left\| \begin{matrix} x \\ y_\Phi \end{matrix} \right\| \leq l \right\}$, there exists $c > 0$ such that

$$\|f(\zeta, d_1, d_2, \dot{d}_1, \dot{d}_2)\| \leq c \left(1 + \mu \left\| \begin{matrix} d_1 \\ \dot{d}_1 \\ \dot{d}_2 \end{matrix} \right\|^2 \right) \quad \forall (\zeta, d_1, d_2, \dot{d}_1, \dot{d}_2) \in \mathbb{B}_l^{\mathcal{A}} \times \mathbb{R}^4. \tag{6.15}$$

By replacing the compact set $K \subset \mathbb{R}^n$ in [23, Assumption (**A**)] and in the rest of the proof in [23] by $\mathbb{B}_l^{\mathcal{A}}$, we can obtain the same lemmas as given in [23, Lemma 3.2, Lemma 3.3 and Lemma 3.4], see, in Appendix .1. This together with the converse Lyapunov function for $\mathcal{A}$-GAS system, we can obtain the $\mathcal{A}$-*i*ISS Lyapunov function similar to the proof of [23, Theorem 3.1]. □

Numerical Example

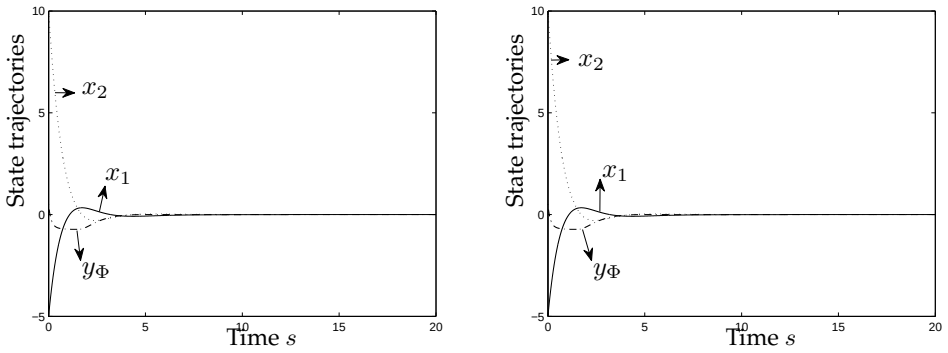

(a) (b)

Figure 6.5: The state trajectories of the closed-loop system (6.16) with $x_{10} = -5$, $x_{20} = 10$, $y_{\Phi 0} = 0.5$. (a) without disturbance d_1 and d_2; (b) with disturbance $d_1 = d_2 = \frac{1}{1+t^2}$.

To illustrate the above results, we simulate the force-actuated mass-damper-spring system as given in (6.11) in MATLAB. In the simulation setup, we consider $m = 1$, $k = 1$ and $b = 2$. The friction force is modeled by the Dahl hysteresis model

as described in Chapter 3 with $F_c = 0.75$, $\rho = 1.5$ and $r = 1$. Then (6.11) becomes

$$\begin{aligned}
\begin{bmatrix} \dot{x}_1 \\ \dot{x}_2 \end{bmatrix} &= \begin{bmatrix} 0 & 1 \\ -1 & -2 \end{bmatrix} \begin{bmatrix} x_1 \\ x_2 \end{bmatrix} + \begin{bmatrix} 0 \\ 1 \end{bmatrix} u \\
\dot{z} &= x_1 \\
y_c &= k_i z + k_p x_1 + k_d x_2 \\
\dot{y}_\Phi &= 1.5(1 - \frac{y_\Phi}{0.75})\dot{u}_{\Phi+} + 1.5(1 + \frac{y_\Phi}{0.75})\dot{u}_{\Phi-} \\
u_\Phi &= -y_c, u = y_\Phi
\end{aligned} \tag{6.16}$$

The control parameters are chosen as $k_p = 1$, $k_i = 1/2$ and $k_d = 1/4$ where it can be easily checked that by taking

$$Q = \begin{bmatrix} \frac{3}{2} & \frac{1}{2} \\ \frac{1}{2} & 1 \end{bmatrix},$$

inequalities (6.7)-(6.9) are satisfied.

We remark that the Dahl model given in (6.16) satisfies Assumption (**B**) in Theorem 6.2.4.

First, let us consider the case when there is no disturbance in the system. Given the initial condition $x_{10} = -5$, $x_{20} = 10$ and $y_{\Phi 0} = 0.5$, Figure 6.5(a) shows that the state trajectories converge to the invariant set $\mathcal{A} := \{(x_1, x_2, z, y_\Phi) | x_1 = 0, x_2 = 0, y_\Phi = 0\}$ in agreement with Theorem 6.2.1.

For the next case, we add the disturbance $d_1 = d_2 = \frac{1}{1+t^2}$ as in (6.1). The simulation results are shown in Figure 6.5(b), which shows that all state trajectories converge to $\mathcal{A}$. This is a consequence of the $\mathcal{A}$-*i*ISS property of the closed-loop system.

6.2.2 Hysteresis System with CCW I/O Behavior

As a different case study, we consider hysteretic actuators with CCW I/O behavior (for example piezo-actuator). Consider a feedback interconnection of a mass-damper-spring system with a PD controller and a hysteretic actuator as shown in Figure 6.6, where **P** represents the linear plant, **C** is the PD controller and **Φ** represents the CCW Duhem hysteresis operator. In Figure 6.6, the exogeneous disturbance signal is represented by d. The closed-loop system as shown in Figure 6.6, is

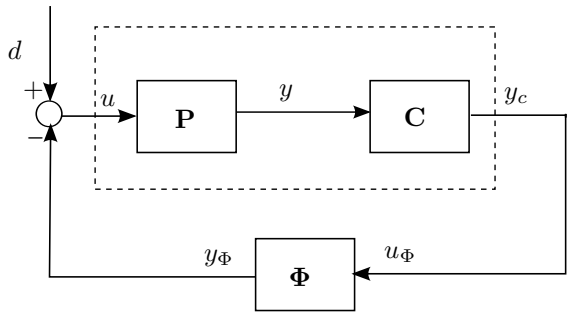

Figure 6.6: Negative feedback interconnection with a linear system $\mathbf{P}$, a controller $\mathbf{C}$ and a Duhem hysteresis operator $\mathbf{\Phi}$.

given by

$$\left.\begin{array}{ll} \mathbf{P}: & \dot{x} = \begin{bmatrix} 0 & 1 \\ -\frac{k}{m} & -\frac{b}{m} \end{bmatrix} x + \begin{bmatrix} 0 \\ \frac{1}{m} \end{bmatrix} u, \\ & y = \begin{bmatrix} c_1 & c_2 \end{bmatrix} x \\ \mathbf{C}: & y_c = k_p y + k_d \dot{y}, \\ \mathbf{\Phi}: & \dot{y}_\Phi = f_1(y_\Phi, u_\Phi)\dot{u}_{\Phi+} + f_2(y_\Phi, u_\Phi)\dot{u}_{\Phi-}, \\ & u_\Phi = y_c,\ u = d - y_\Phi, \end{array}\right\} \tag{6.17}$$

where $x = \begin{bmatrix} x_1 & x_2 \end{bmatrix}^T$ with x_1 be the position and x_2 be the velocity, and c_1, c_2 are the measurement gains of the position and velocity, respectively. For the PD controller $\mathbf{C}$, $k_p > 0$ and $k_d > 0$ are the controller gains. For the Duhem hysteresis operator $\mathbf{\Phi}$, the functions f_1 and f_2 are assumed to be locally Lipschitz.

First, we consider the case where $d = 0$, i.e. there is no input disturbance in the closed-loop system. Let $\mathbf{G}$ denote the cascaded system of $\mathbf{P}$ and $\mathbf{C}$, then we have

$$\mathbf{G}: \left\{\begin{array}{ll} \dot{x} & = Ax + Bu, \\ y_c & = Cx + Du, \end{array}\right. \tag{6.18}$$

where

$$A = \begin{bmatrix} 0 & 1 \\ -\frac{k}{m} & -\frac{b}{m} \end{bmatrix}, \quad B = \begin{bmatrix} 0 \\ \frac{1}{m} \end{bmatrix},$$
$$C = \begin{bmatrix} k_p c_1 - \frac{k_d c_2 k}{m} & k_p c_2 + k_d c_1 - \frac{k_d c_2 b}{m} \end{bmatrix}, \quad D = \frac{k_d c_2}{m}.$$

Theorem 6.2.5 *Consider the closed-loop system in* (6.17) *with* $d = 0$. *Assume that the Duhem hysteresis operator* $\mathbf{\Phi}$ *satisfies all the assumptions in Theorem 4.2.1. If there exists* $Q = Q^T > 0$, $L = [\, l_1 \; l_2 \,]$, w ,$k_p > 0$ *and* $k_d > 0$ *such that the following inequalities hold.*

$$\begin{bmatrix} Q & C^T \\ C & D \end{bmatrix} > 0 \tag{6.19}$$

$$A^T Q + QA + L^T L \leq 0 \tag{6.20}$$

$$QB + A^T C^T = L^T w \tag{6.21}$$

$$2CB = -w^2, \tag{6.22}$$

and $-\frac{b}{m} + \frac{l_2}{wm} < 0$, *then for every initial conditions* $x_0 \in \mathbb{R}^2$ *and every admissible* $y_{\Phi_0} \in \mathbb{R}$, *the state trajectories of the closed-loop system* (6.17) *are bounded and converge to* $\mathcal{A} := \{(x_1, x_2, y_\Phi) \in \mathbb{R}^3 | x_2 = 0\}$, *i.e. the closed-loop system is globally asymptotic stable with respect to* $\mathcal{A}$ *(*$\mathcal{A}$*-GAS).*

Proof:

By the assumption of the theorem, the Duhem operator $\mathbf{\Phi}$ is CCW and there exists a function $H_{\circlearrowleft_1} : \mathbb{R}^2 \to \mathbb{R}_+$ such that

$$\dot{H}_{\circlearrowleft_1}(y_\Phi(t), u_\Phi(t)) \leq \dot{y}_\Phi(t) u_\Phi(t). \tag{6.23}$$

Using $V_G = \frac{1}{2} x^T Q x + (y_c - Du)u + \frac{D}{2} u^2$ as the Lyapunov function for the linear systems $\mathbf{G}$, and (6.20)-(6.22), we have

$$\begin{aligned} \dot{V}_G &= \frac{1}{2} x^T (A^T Q + QA) x + x^T QBu + x^T A^T C^T u + uCBu + y_c \dot{u} \\ &\leq y_c \dot{u} - \frac{1}{2} (Lx - wu)^2. \end{aligned}$$

Based on Definition 2.3.6, it can be easily checked that $\mathbf{G}$ is CW.

Now take $V_{cl}(x, y_\Phi) = V_G + H_{\circlearrowleft_1}(y_\Phi, y_c)$ as the Lyapunov function of the closed-loop system (6.17) and substituting the interconnection conditions $u_\Phi = -y_c$ and $u = y_\Phi$, we obtain

$$\begin{aligned} \dot{V}_{cl} &= \dot{V}_G + \dot{H}_{\circlearrowleft_1}, \\ &\leq y_c \dot{u} - \frac{1}{2} (Lx - wu)^2 + \dot{y}_\Phi u_\Phi, \\ &= -\frac{1}{2} (Lx - wu)^2. \end{aligned}$$

Using (6.19), it can be checked that V_G is proper in x and y_Φ. Based on LaSalle's invariance principle and the compactness of (x, y_Φ), the trajectories converge to the largest invariant set $\mathbf{O}$ contained in $\mathcal{M} := \{(x, y_\Phi) \in \mathbb{R}^3 | Lx - w y_\Phi = 0\}$ as $t \to \infty$.

In the invariant set $\mathbf{O}$ in $\mathcal{M}$, $y_\Phi = -\frac{L}{w}x$, i.e., $u = \frac{L}{w}x$. Substituting $u = \frac{L}{w}x$ in $\mathbf{P}$, we have

$$\dot{x} = \begin{bmatrix} 0 & 1 \\ -\frac{k}{m} + \frac{l_1}{wm} & -\frac{b}{m} + \frac{l_2}{wm} \end{bmatrix} x \tag{6.24}$$

From (6.22), we have that $w = \pm\frac{\sqrt{2k_dc_2b-2m(k_pc_2+k_dc_1)}}{m}$. Using (6.20) and (6.21), it can be computed that l_1 has a unique solution $l_1 = \frac{k\sqrt{2k_dc_2b-2m(k_pc_2+k_dc_1)}}{m}$ if $w = \frac{\sqrt{2k_dc_2b-2m(k_pc_2+k_dc_1)}}{m}$ or $l_1 = -\frac{k\sqrt{2k_dc_2b-2m(k_pc_2+k_dc_1)}}{m}$ if $w = -\frac{\sqrt{2k_dc_2b-2m(k_pc_2+k_dc_1)}}{m}$. Substituting these w and l_1 into (6.24), we get

$$\dot{x} = \begin{bmatrix} 0 & 1 \\ 0 & -\frac{b}{m} + \frac{l_2}{wm} \end{bmatrix} x \tag{6.25}$$

holds which implies that $x_2 = 0$ in the invariant set $\mathbf{O}$. By LaSalle's principle, this implies that $x_2(t) \to 0$ as $t \to \infty$ if $-\frac{b}{m} + \frac{l_2}{wm} < 0$. Hence, the closed-loop system is GAS with respect to $\mathcal{A} := \{(x_1, x_2, y_\Phi) \in \mathbb{R}^3 | x_2 = 0\}$. □

Remark 6.2.6 *The conditions given in* (6.19)-(6.22) *can provide the interval of control parameters such that the closed-loop system is $\mathcal{A}$-GAS. For instance, if $k_p \leq \frac{k_dc_2k}{c_1m}$, $k_p \leq \frac{k_dc_2b-k_dc_1m}{c_2m}$ and $k_p > k_d\frac{b^3c_2-b^2c_1m-kc_1m^2}{b^2c_2m+kc_2m^2-bc_1m^2}$ then the closed-loop system* (6.17) *satisfies* (6.19)-(6.22) *with $L = [\,\frac{\sqrt{2q}k}{m}\ 0\,]$, $w = \frac{\sqrt{2q}}{m}$ and*

$$Q = \begin{bmatrix} \frac{k_dc_2k^2}{m} - k_pc_1k & \frac{qk}{m} \\ \frac{qk}{m} & k_dc_2k - k_pc_1m - \frac{qb}{m} \end{bmatrix}$$

where $q = (k_dc_2b - k_pc_2m - k_dc_1m)$.

Robustness Analysis

Now let us proceed our analysis with $d \neq 0$, i.e., we study the robustness of the closed-loop system (6.17) by adding disturbances d to the input of the plant. In this case the robustness of the closed-loop system is also based on the concept of $\mathcal{A}$-*i*ISS.

Lemma 6.2.7 *Consider the closed-loop system in* (6.17) *with $d \in C^1(\mathbb{R}_+)$ s.t. $\dot{d} \in AC(\mathbb{R}_+)$. Assume that the Duhem hysteresis operator satisfies the hypotheses given in Theorem 6.2.5. If there exists $Q = Q^T > 0$, $L = [\,l_1\ l_2\,]$, w, $k_p > 0$ and $k_d > 0$ such that the following*

inequalities hold.

$$\begin{bmatrix} Q & C^T \\ C & D \end{bmatrix} > 0 \tag{6.26}$$

$$A^TQ + QA + L^TL + \epsilon_1 I \leq 0 \tag{6.27}$$

$$QB + A^TC^T = L^Tw \tag{6.28}$$

$$2CB = -w^2 - \epsilon_2, \tag{6.29}$$

for some positive constants ϵ_1 and ϵ_2. Suppose $-\frac{b}{m} + \frac{l_2}{wm} < 0$, then there exists $\mu > 0$ such that the closed-loop system is dissipative with respect to the supply function $\sigma(d, \dot{d}) = \mu \left\| \begin{smallmatrix} d \\ \dot{d} \end{smallmatrix} \right\|^2$.

Proof: Let $V_{cl} = V_G + H_{\circlearrowleft_1}$ be the Lyapunov function for the closed-loop system, where V_G and $H_{\circlearrowleft_1}$ have the same descriptions as in the proof of Theorem 6.2.5. Then using (6.26)- (6.29) we have

$$\begin{aligned}
\dot{V}_{cl} &= \dot{V}_G + \dot{H}_{\circlearrowleft_1}, \\
&\leq y_c\dot{u} - \frac{1}{2}(Lx - wu)^T(Lx - wu) + \dot{y}_\Phi u_\Phi - \frac{1}{2}\epsilon_1 x^Tx - \frac{1}{2}\epsilon_2 u^2, \\
&= -\frac{1}{2}(Lx - wu)^T(Lx - wu) + y_c\dot{d} - \frac{1}{2}\epsilon_1 x^Tx - \frac{1}{2}\epsilon_2 u^2
\end{aligned}$$

where the last equality is obtained since $u = d - y_\Phi$. Using Young's inequality, $u = y_\Phi$ and $\epsilon_3 > 0$, we have

$$\begin{aligned}
\dot{V}_{cl} &\leq \frac{\eta}{2}\dot{d}^2 + \frac{1}{2\eta}y_c^2 - \frac{1}{2}\epsilon_1 x^Tx - \frac{1}{2}\epsilon_2 u^2 \\
&\leq \frac{\eta}{2}\dot{d}^2 + \frac{1}{2\eta}D^2u^2 + \frac{1}{2\eta}x^TC^TCx - \frac{1}{2}\epsilon_1 x^Tx - \frac{1}{2}\epsilon_2 u^2 \\
&\leq \frac{\eta}{2}\dot{d}^2 + \frac{\eta}{2}d^2
\end{aligned}$$

where the last inequality is obtained since η is an arbitrary positive constant. This implies that system (6.17) is dissipative with respect to σ where $\sigma(d, \dot{d}) = \mu \left\| \begin{smallmatrix} d \\ \dot{d} \end{smallmatrix} \right\|^2$ and $\mu := \eta/2$. □

Theorem 6.2.8 *Consider the closed-loop system in* (6.17) *with $d \in C^1(\mathbb{R}_+)$ s.t. $\dot{d} \in AC(\mathbb{R}_+)$. Assume that the hypotheses in Lemma 6.2.7 hold. Then* (6.17) *is iISS with respect to $\mathcal{A}$ ($\mathcal{A}$-iISS), with iISS gain $\gamma\left(\left\| \begin{smallmatrix} d \\ \dot{d} \end{smallmatrix} \right\|\right) = \mu \left\| \begin{smallmatrix} d \\ \dot{d} \end{smallmatrix} \right\|^2$, where $\mu > 0$.*

Proof: The proof of the Theorem 6.2.8 is similar to the proof of Theorem 3.1 in [23]. First of all, consider the system (6.17) with $d = 0$ which has the following form

$$\begin{bmatrix} \dot{x} \\ \dot{y}_\Phi = Ax - By_\Phi \\ \frac{f_1(y_\Phi,u_\Phi)}{1+Df_1(y_\Phi,u_\Phi)}(CAx - CBy_\Phi)_+ \\ +\frac{f_2(y_\Phi,u_\Phi)}{1+Df_2(y_\Phi,u_\Phi)}(CAx - CBy_\Phi)_- \end{bmatrix}, \tag{6.30}$$

where $u = -y_\Phi$. It can be checked that the RHS of equation (6.30) is locally Lipschitz. Let us write (6.30) as $\dot{\zeta} = f(\zeta)$ where $\zeta = \begin{bmatrix} x^T & y_\Phi \end{bmatrix}^T$. Based on the converse Lyapunov theorem [55, Corollary 2], Theorem 6.2.5 implies that there exists a smooth Lyapunov function $V_G : \mathbb{R}^3 \to \mathbb{R}_+$ such that

- there exist $\mathcal{K}_\infty$ functions α_1 and α_2 such that

$$\alpha_1(\|\zeta\|_{\mathcal{A}}) \leq V_G(\zeta) \leq \alpha_2(\|\zeta\|_{\mathcal{A}}) \qquad \forall \zeta \in \mathbb{R}^3.$$

- there exists a continuous, positive definite function α_3 such that

$$\frac{\mathrm{d}V_G(\zeta)}{\mathrm{d}\zeta} f(\zeta) \leq -\alpha_3(\|\zeta\|_{\mathcal{A}}) \qquad \forall \zeta \in \mathbb{R}^3.$$

In the case when the input disturbance $d \neq 0$, the system (6.17) can be written as $\dot{\zeta} = f(\zeta, d, \dot{d})$ where

$$f(\zeta, d, \dot{d}) = \begin{bmatrix} Ax + B(d - y_\Phi) \\ \frac{f_1(y_\Phi,u_\Phi)}{1+Df_1(y_\Phi,u_\Phi)}(CAx + CB(d - y_\Phi) + D\dot{d})_+ \\ +\frac{f_2(y_\Phi,u_\Phi)}{1+Df_2(y_\Phi,u_\Phi)}(CAx + CB(d - y_\Phi) + D\dot{d})_- \end{bmatrix},$$

$u = d - y_\Phi$. Since $f_1(y_\Phi, u_\Phi) \geq 0$ and $f_2(y_\Phi, u_\Phi) \geq 0$ according to the assumptions of Theorem 4.2.1, then

$$\frac{f_1(y_\Phi, u_\Phi)}{1 + Df_1(y_\Phi, u_\Phi)} \in [0, 1],$$
$$\frac{f_2(y_\Phi, u_\Phi)}{1 + Df_1(y_\Phi, u_\Phi)} \in [0, 1].$$

Hence, we have that for every $\mathbb{B}_l^{\mathcal{A}} = \left\{ \begin{bmatrix} x \\ y_\Phi \end{bmatrix} \middle| \left\| \begin{matrix} x \\ y_\Phi \end{matrix} \right\| \leq l \right\}$, there exists a $c > 0$ such that

$$\|f(\zeta, d, \dot{d})\| \leq c \left(1 + \mu \left\| \begin{matrix} d \\ \dot{d} \end{matrix} \right\|^2\right), \ \forall (\zeta, d, \dot{d}) \in \mathbb{B}_l^{\mathcal{A}} \times \mathbb{R}^2. \tag{6.31}$$

The rest of the proof can use the same arguments as in [23] where the compact set $K \subset \mathbb{R}^n$ in [23] is replaced by $\mathbb{B}_l^{\mathcal{A}}$. It can be checked that the same lemmas as given in [23, Lemma 3.2, Lemma 3.3 and Lemma 3.4] (see, in Appendix .1) can also be obtained in this case. Applying the Lemmas and the converse Lyapunov function for $\mathcal{A}$-GAS system, we can obtain the $\mathcal{A}$-*i*ISS Lyapunov function similar to the proof of [23, Theorem 3.1]. □

Numerical Example

To illustrate the above results, we provide a numerical example of system (6.17), a typical application of such system is the piezo-actuated stage. For the mass-damper-spring system, we set $m = 1$, $b = 2$ and $k = 4$. The hysteretic actuator is represented by the Bouc-Wen model as introduced in Subsection 3.2.4, with the parameters $k_x = 1.2117 \times 10^{-7}$, $k_w = -5.08 \times 10^{-6}$, $n = 1.27$, $\rho = 8.93 \times 10^{-3}$ and $\sigma = 0.74$. The control parameters for the PD controller can then be obtained based on the parameters of the linear plant. It can be checked that with $k_p = \frac{3}{2}$, $k_d = 2$, $L = [\,4\ 0\,]$ and $w = 1$, the matrix

$$Q = \begin{bmatrix} 26 & 2 \\ 2 & 5.5 \end{bmatrix}$$

satisfies the conditions as given in (6.19)-(6.22).

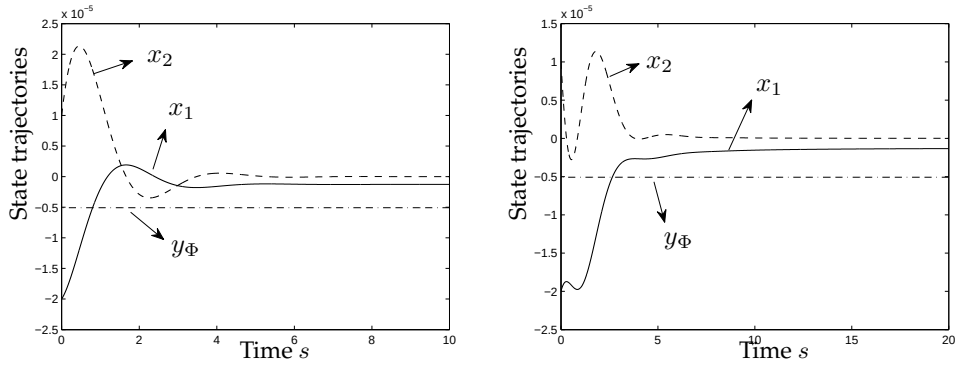

(a) (b)

Figure 6.7: The state trajectories of the closed-loop system (6.17) with $x_{10} = 1$, $x_{20} = -1$, $y_{\Phi 0} = 0.5$. (a) without disturbance d ; (b) with disturbance $d = \frac{10^{-4}}{t^2+1}$.

First, let us consider the case when there is no disturbance in the system. Given the initial condition $x_{10} = -2 \times 10^{-5}$, $x_{20} = 10^{-5}$ and $y_{\Phi 0} = -5.08 \times 10^{-6}$, Figure 6.7(a) shows that the state trajectories converge to the invariant set $\mathcal{A} := \{(x_1, x_2, z, y_\Phi) | x_2 = 0\}$ in agreement with Theorem 6.2.5.

For the next case, we add a disturbance signal $d(t) = \frac{10^{-4}}{t^2+1}$, which satisfies $d, \dot{d} \in L^2$, to the input of the linear plant. The simulation result is shown in Figure 6.7(b), which shows that all state trajectories converge to $\mathcal{A} := \{(x_1, x_2, z, y_\Phi) | x_2 = 0\}$. This is a consequence of the $\mathcal{A}$-*i*ISS property of the closed-loop system.

6.3 Application to Set-point Velocity Tracking

Micro/nano positioning mechanisms are commonly used to drive stages to follow a desired pattern/trajectory. For example, in the atomic force microscopy, the sample is placed on a stage which is driven by a piezo-actuator and a fixed cantilever is placed on top of the sample. Then the stage moves in a raster pattern (move back and forth at a constant speed) where the roughness of the sample is measured through the deflection of the cantilever by a laser sensor. However, without a proper velocity tracking, the quality of the measurement degrade [34].

In this section, we apply our results of Section 6.2 in an experiment using a piezo-actuated stage. The control goal is to design a PD controller such that the stage will track a constant speed, similar to the raster scanning scenario.

6.3.1 Experimental Results

Consider again the closed-loop system (6.17) with $d = 0$. Let $\bar{x}_2 = \bar{v}$ denote the desired constant velocity and the corresponding steady-state displacement is then given by $\bar{x}_1 = \bar{v}t$ (up to a constant) with $t \in \mathbb{R}_+$. It follows from the state equations of the closed-loop system in (6.17) that in the steady-state, $\bar{y}_\Phi = -k\bar{v}t - b\bar{v}$ (up to a constant). Denote $\bar{\zeta} = \begin{bmatrix} \bar{x}_1 & \bar{x}_2 & \bar{y}_\Phi \end{bmatrix}^T$, $e = \begin{bmatrix} e_1 & e_2 & e_\Phi \end{bmatrix}^T$, where $e_1 = x_1 - \bar{x}_1$, $e_2 = x_2 - \bar{x_2}$ and $e_\Phi = y_\Phi - \bar{y}_\Phi$. Let $\tilde{u}_\Phi = u_\Phi - \bar{u}_\Phi$ where $\bar{u}_\Phi$ satisfies $-k_w + k_x \bar{u}_\Phi = \bar{y}_\Phi$. It can be computed that, in the neighborhood of $(e_\Phi, \tilde{u}_\Phi) = (0, 0)$, the operator $e_\Phi = \tilde{\Phi}(\tilde{u}_\Phi)$ can be approximated by a Duhem operator. Hence the error dynamics can be described by

$$f(e) = \begin{bmatrix} e_2 \\ -\frac{k}{m}e_1 - \frac{b}{m}e_2 - \frac{1}{m}e_\Phi \\ f_1(e_\Phi, \tilde{u}_\Phi)(\dot{\tilde{u}}_\Phi)_+ + f_2(e_\Phi, \tilde{u}_\Phi)(\dot{\tilde{u}}_\Phi)_- \end{bmatrix}, \tag{6.32}$$

Applying Theorem 6.2.5, we can obtain that the error system (6.32) is locally asymptotically stable with respect to $\mathcal{A} := \{(e_1, e_2, e_\Phi) \in \mathbb{R}^3 | e_2 = 0\}$, in other words,

the velocity tracking is achieved. We remark that in the original coordinates, the applied control input is given by $u_\Phi = \tilde{u}_\Phi + \bar{u}_\Phi$ where $\tilde{u}_\Phi := k_p(y - \bar{v}t - \bar{v}) + k_d(\dot{y} - \bar{v})$ is the output of the PD controller. The control parameters can then be obtained dependent on the parameters of the linear plant.

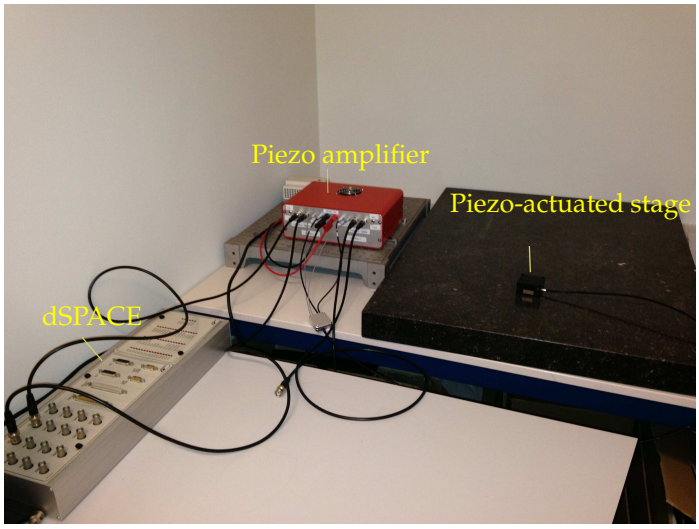

Figure 6.8: The experiment setup: piezo-actuated stage, piezo-amplifier and Dspace.

Figure 6.8 illustrates the experiment setup of the piezo-actuated stage, where the piezo-actuated stage P611.2S from Physik Instrumente (PI) is used combined with the piezo amplifier E610.S0 from Physik Instrumente (PI). The piezo-actuated stage P611.2S is a 2-Axis piezo system and the travel range of this stage is $100 \times 100\mu m$. Note that, in our experiment, only one axis is used. The displacement of the stage is measured by a strain gauge sensor with a resolution of 2 nanometer. The input voltage is controlled by a PC computer where the MATLAB Real-Time Workshop is used. The DS1104 PPC control board is used as the real-time controller and the control algorithm is implemented in Simulink/MATLAB. The control scheme is described in Figure 6.9.

The piezo-actuated stage contains two parts: a hysteretic actuator and a positioning mechanism which can be considered as a mass-damper-spring system. The system modeling of the piezo-actuated stage is shown in Figure 6.10.

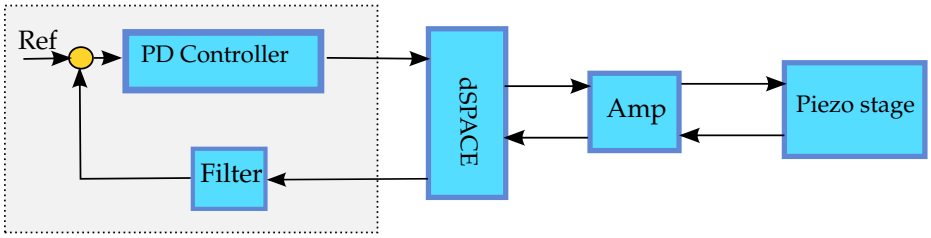

Figure 6.9: The control scheme of the piezo-actuated satge.

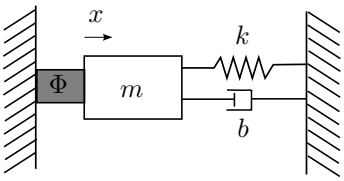

Figure 6.10: The system modeling of the piezo-actuated stage.

The system equation of the piezo-actuated stage are given by

$$\begin{aligned} \mathbf{P}: \dot{x} &= \begin{bmatrix} 0 & 1 \\ -\frac{k}{m} & -\frac{b}{m} \end{bmatrix} x + \begin{bmatrix} 0 \\ \frac{1}{m} \end{bmatrix} u, \\ y &= \begin{bmatrix} 1 & 0 \end{bmatrix} x \\ \mathbf{\Phi}: \dot{y}_\Phi &= f_1(y_\Phi, u_\Phi)\dot{u}_{\Phi+} + f_2(y_\Phi, u_\Phi)\dot{u}_{\Phi-}, \end{aligned} \tag{6.33}$$

where $x = [\, x_1 \; x_2 \,]^T$, x_1 denotes the displacement and x_2 denotes the velocity. The hysteresis system $\mathbf{\Phi}$ is represented by the Bouc-Wen model as introduced in (3.22) in Chapter 3 with

$$\begin{cases} f_1(\gamma, \upsilon) & = k_x + k_w\rho - k_w\rho\sigma|\frac{\gamma - k_x\upsilon}{k_w}|^{n-1}\frac{\gamma - k_x\upsilon}{k_w} - k_w\rho(1-\sigma)|\frac{\gamma - k_x\upsilon}{k_w}|^n \\ f_2(\gamma, \upsilon) & = k_x + k_w\rho + k_w\rho\sigma|\frac{\gamma - k_x\upsilon}{k_w}|^{n-1}\frac{\gamma - k_x\upsilon}{k_w} - k_w\rho(1-\sigma)|\frac{\gamma - k_x\upsilon}{k_w}|^n. \end{cases} \tag{6.34}$$

Since the hysteretic actuator and the mass-damper-spring system are coupled, i.e., no measurements on the output of the hysteretic actuator are available. This coupling can be clearly observed from the figures. The changes of the input-output map of the piezo-actuated stage for different input frequencies in Figure 6.11 indicates that the input-output response of the piezo-actuated stage is frequency dependent, i.e., when the input frequency is low the linear dynamics fade out and the hysteresis dominates the system behavior. When the input frequency is high the linear dynamics dominate the system behavior.

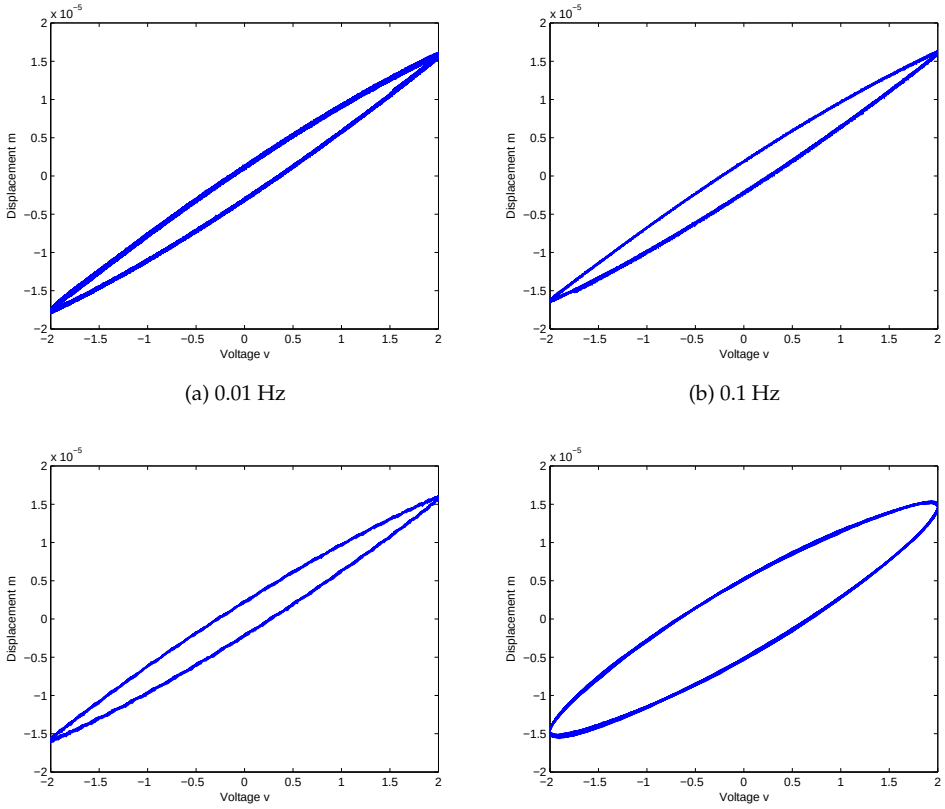

(a) 0.01 Hz (b) 0.1 Hz

(c) 1 Hz (d) 10 Hz

Figure 6.11: The input-output response of the piezo-actuated stage with different input frequency.

The identification process is separated into two parts: the identification of the Bouc-Wen model and the identification of the mass-damper-spring system.

First of all, we identify the hysteresis system by applying low frequent input signals, in which case the linear plant can be considered as a DC gain, which is approximately $\frac{1}{k}$. Then the parameters of the Bouc-Wen model become $\bar{k}_x = \frac{k_x}{k}$ and $\bar{k}_w = \frac{k_w}{k}$ in (6.34). To identify parameters of the Bouc-Wen model (6.34), we first determine the initial parameters of the Bouc-Wen model based on the limit cycle approach as proposed in [16].

- Excite the piezo-actuated stage with a wave signal v and wait till the output

y_Φ reach a steady state $\bar{y}_\Phi$.

- Choose a nonzero constant q_1 and excite the piezo-actuated stage with a wave signal $v_1 = v + q_1$ and wait till the output y_{Φ_1} reach a steady state $\bar{y}_{\Phi_1}$.
- Determine $\bar{k}_x$ by using $\bar{k}_x = \frac{\bar{y}_{\Phi_1}(v+q_1) - \bar{y}_\Phi(v)}{q_1}$.
- Compute $\theta(v) = \bar{y}_\Phi(v) - \bar{k}_x v$.
- Determine v_* such that $\theta(v_*) = 0$.
- Compute a by using $a = \left(\frac{\mathrm{d}\theta(v)}{\mathrm{d}v}\right)_{v=v_*}$.
- Choose two constant v_{*_1} and v_{*_2} such that $v_{*_2} > v_{*_1} > v_*$. Then compute

$$n = \frac{\log\left(\frac{(\frac{\mathrm{d}\theta(v)}{\mathrm{d}v})_{v=v_{*_2}} - a}{(\frac{\mathrm{d}\theta(v)}{\mathrm{d}v})_{v=v_{*_1}} - a}\right)}{\log\left(\frac{\theta(v_{*_2})}{\theta(v_{*_1})}\right)}$$

$$\varpi = \frac{a - (\frac{\mathrm{d}\theta(v)}{\mathrm{d}v})_{v=v_{*_2}}}{\theta(v_{*_2})^n}$$

- Compute $\bar{k}_w = \sqrt[n]{\frac{a}{\varpi}}$ and $\rho = \frac{a}{\bar{k}_w}$.
- Compute σ by using

$$\sigma = \frac{1}{2}\left(\frac{\frac{\frac{1}{\bar{k}_w}(\frac{\mathrm{d}\theta(v)}{\mathrm{d}v})_{v=v_{*_3}} - 1}{\rho}}{(-\frac{\theta(v_{*_3})}{\bar{k}_w})^n} + 1\right).$$

The obtained initial parameters for the Bouc-Wen model are $\bar{k}_x = 1.2381 \times 10^{-5}$, $\bar{k}_w = -1.038 \times 10^{-6}$, $\sigma = 12.31$, $n = 1$ and $\rho = 4.43$. Then an optimal nonlinear least square algorithm (lsqcurvefit) in MATLAB is used to estimate the real parameters of the Bouc-Wen model. Based on these two steps, the identified parameters for the Bouc-Wen model (6.34) are: $\bar{k}_x = 0.2379$, $\bar{k}_w = -0.0723$, $\rho = 2.57$, $\sigma = 3.53$ and $n = 1.46$. The identification results are shown in Figure 6.12, where a triangular input signal with amplitude 2 and frequency 0.01Hz is applied to the model and the setup.

Based on the parameters of the Bouc-Wen model, we continue to identify the mass-damper-spring system. In this case, a sinus input signal with amplitude 1.5 and frequency 10Hz is applied to the setup. To determine the parameters, we use the nonlinear least square optimization toolbox (lsqcurvefit). The obtained parameters

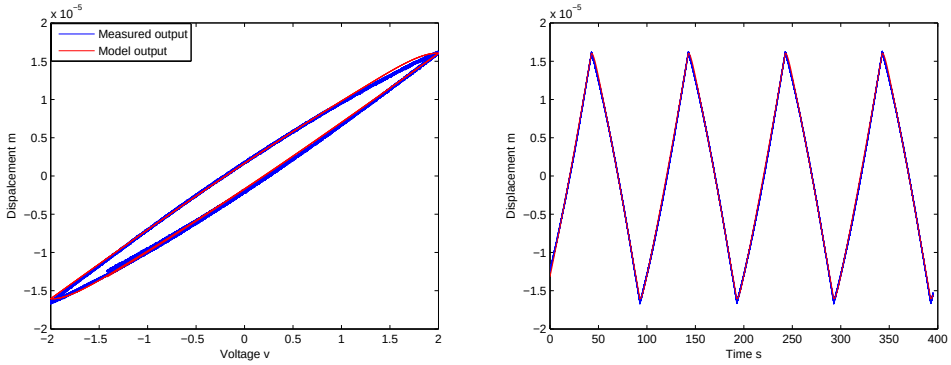

(a) (b)

Figure 6.12: The identification results of the Bouc-Wen model, where the red line indicates the model output and the blue line is the measured output.

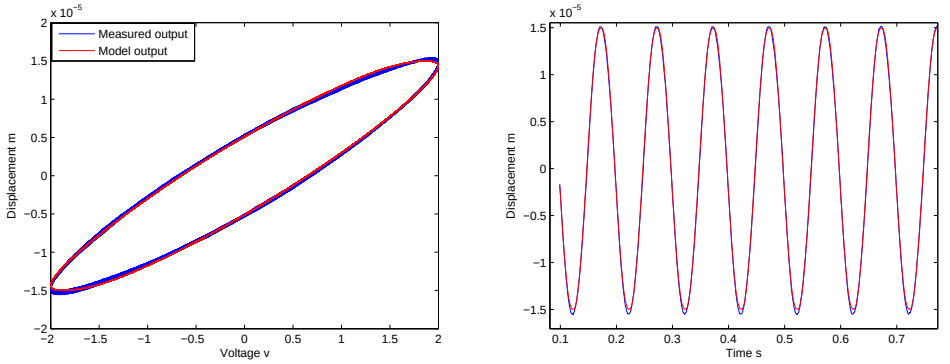

(a) (b) zoom in

Figure 6.13: The identification results of the piezo-actuated stage, where the red line indicates the model output and the blue line is the measured output.

are $m = 0.0352$, $b = 80.0543$ and $k = 2.5541 \times 10^4$. The identification results are shown in Figure 6.13.

To validate the identified parameters, we apply a mixed frequency sinus signal to the identified model obtained above and the real setup. Denote y_{Φ_r} the measured output sequence, y_{Φ_m} the model output sequence and N the length of the output sequence. Then the average estimation error e is quantified as $e = \frac{\sqrt{(y_{\Phi_r} - y_{\Phi_m})^2}}{N}$,

which is equal to 1.0107×10^{-9}. The comparison results are shown in Figure 6.14 which indicates that the model fits the system well.

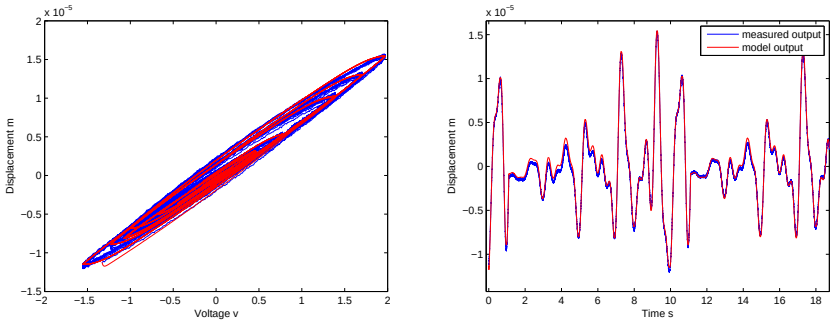

(a) Comparison between the model output and the measured output in input-output plane

(b) Comparison between the model output and the measured output in time (zoom in)

Figure 6.14: Identification results for the piezo-actuated stage, where the red line is the output of the model and the blue line is the measured output from the setup.

Based on the identified parameters, it can be checked that with $k_p = 2000$, $k_d = 1$, $L = \begin{bmatrix} 3.1981 \times 10^6 & 0 \end{bmatrix}$ and $w = 125.215$, we can obtain the matrix Q

$$Q = \begin{bmatrix} 1.85 \times 10^{10} & 7.04 \times 10^6 \\ 7.04 \times 10^6 & 3.4 \times 10^3 \end{bmatrix},$$

which satisfies the conditions given in (6.19)-(6.22). The simulation result of tracking a constant velocity $\bar{v} = 5\mu$m/s is shown in Figure 6.15(a). The experimental result is shown in Figure 6.15(b) where we use constant reference velocity of $\bar{v} = 5\mu$m/s. The experimental result indicate that the stage tracks asymptotically the reference velocity 5μm/s in agreement with Theorem 6.2.5.

To show the robustness of the controlled system, an input disturbance is introduced to the setup by using a DC motor (LSC30/2 from Maxon Motor) as shown in Figure 6.16. The motor rotates at a constant speed where a flexible flap is attached to the motor so that a periodic disturbance force can be introduced to the stage. In the experiment, the motor is turned on for a short period of time when the controlled system reaches its steady state in order to simulate bounded energy disturbance signal. The disturbance force that is introduced to the system is given in Figure 6.17(a).

The simulation results are shown in Figure 6.17(c), and the experimental results are shown in Figure 6.17(d), where we use constant reference velocity 2μm/s. The experimental results show the robustness of the closed-loop system as presented earlier in Theorem 6.2.8.

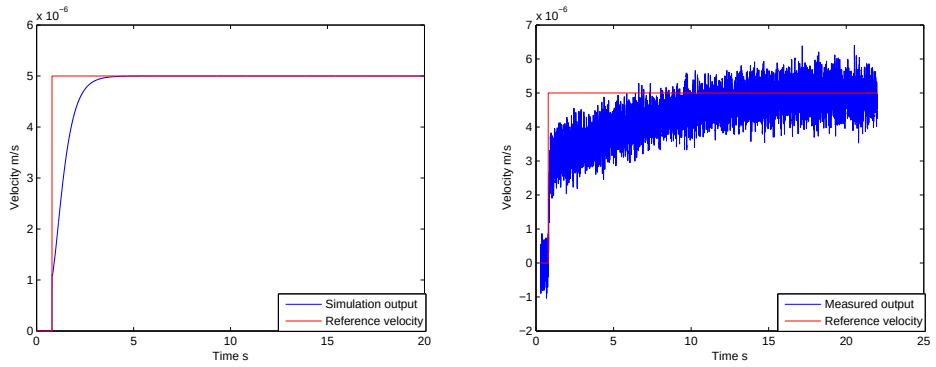

(a) Simulation results

(b) Experiment results

Figure 6.15: (a) Simulation results of the piezo-actuated stage system for tracking a constant velocity 5μm/s; (b) Experimental results of the piezo-actuated stage system for tracking a constant velocity 5μm/s.

6.4 Concluding Remarks

In this chapter, a controller design methodology has been given based on the absolute stability results presented in Chapter 5. Firstly, a general linear controller design algorithm is proposed, where the proposed controller can guarantee the stability of the closed-loop system, so that the state trajectories converge to an invariant set. Secondly, we provide a simple control design for two cases: a second-order system with a CW hysteretic actuator and a second-order system with a CCW hysteretic actuator. For both cases, sufficient conditions on the control parameters are presented such that the controlled system is GAS with respect to an invariant set. Furthermore, the robustness analysis of the closed-loop system is shown based on the concept of *i*ISS. Finally, a PD controller is designed for a piezo-actuated stage such that the stage can track a constant velocity.

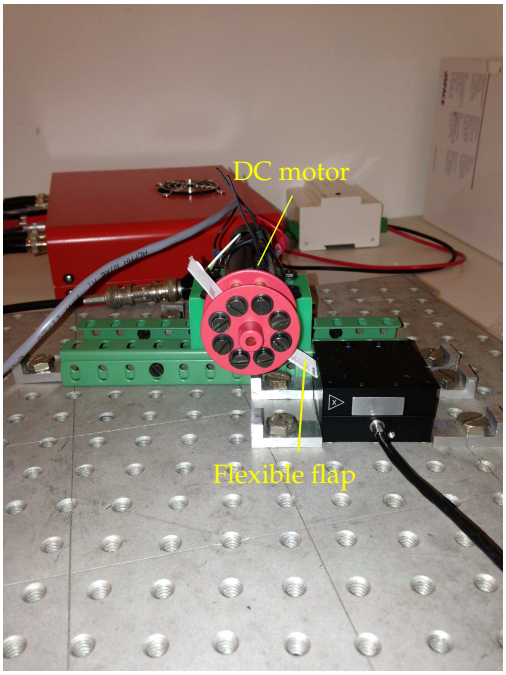

Figure 6.16: Experimental setup with disturbance generator.

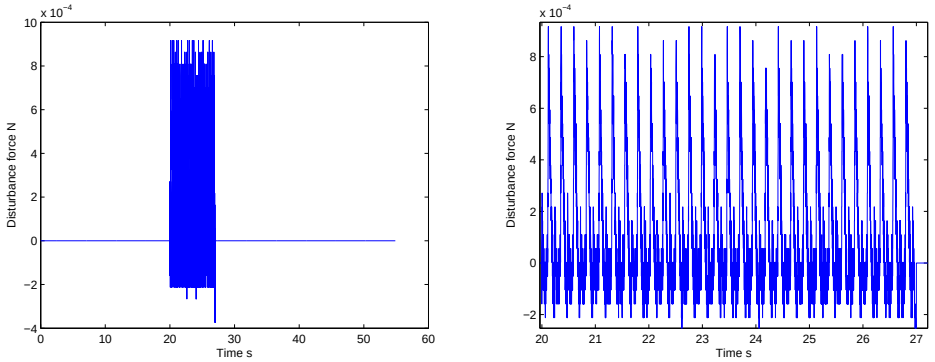

(a) Disturbance force

(b) Disturbance force (zoom in)

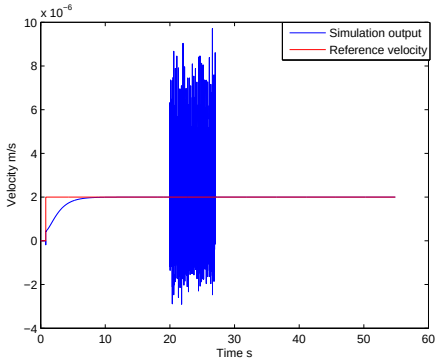

(c) Simulation results

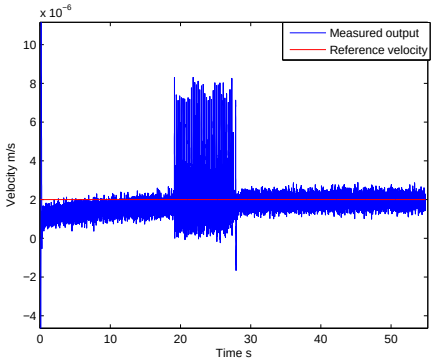

(d) Experiment results

Figure 6.17: (a) and (b) Disturbance force applied to the system; (c) Simulation results of the piezo-actuated stage system for tracking a constant velocity 2μm/s with input disturbance; (d) Experimental results of the piezo-actuated stage system for tracking a constant velocity 2μm/s with input disturbance.

Chapter 7

Conclusions and Future Research

7.1 Conclusions

This thesis exploits a natural input-output (I/O) property of hysteresis operator, in the stability analysis, as well as, the controller design for such systems. Two classes of Duhem hysteresis operator are considered: the Duhem hysteresis operator with CCW I/O behavior and the Duhem hysteresis operator with CW I/O behavior.

The first part of this work is to study these I/O properties by providing sufficient conditions for CCW and CW Duhem operator. In particular, explicit storage functions are proposed such that they satisfy the CCW or CW dissipation inequality. Furthermore, the relation between the proposed storage function and the available storage function from the classical dissipativity theory is also discussed.

The second part of this work addresses the stability analysis and controller design for systems with hysteresis nonlinearity. Using the results from the first part, I investigate the absolute stability of a feedback interconnection between a linear system and a Duhem hysteresis operator. For solving this absolute stability problem, sufficient conditions are given based on the counter-clockwise (CCW) or clockwise (CW) input-output property of the linear system and the Duhem operator. Consequently, a linear controller design algorithm is proposed which can guarantee the stability of the closed-loop system, i.e. the state trajectories are converging to an invariant set.

Furthermore, two case-studies have been studied for a second-order linear plant with a hysteretic actuator controlled by a proportional, integral and derivative (PID) controller. Using the CCW and CW properties of the hysteresis system and the linear system, sufficient conditions on the control parameters can be given such that the states of the linear plant and the hysteresis system converge to zero. The robustness of the closed-loop system with respect to the measurement noise is also investigated, using the *integral* input-to-state stability (*i*ISS) concept.

Finally, experiments on a piezo-actuated stage has been conducted to validate our stability and control design approach.

7.2 Future work

This thesis has addressed the stability analysis and controller design for systems with Duhem type hysteresis nonlinearity. There remains a number of open problems with regards to the analysis of hysteretic systems. In the following, I list few of these problems that can extend the results in this thesis.

- For stability analysis, this thesis mainly focuses on the feedback interconnection between a linear system and a Duhem hysteresis nonlinearity. In Section 5.5, the absolute stability analysis of a feedback interconnection between a nonlinear system and a Duhem hysteresis nonlinearity has been briefly introduced. The extensive investigation for feedback interconnection between a nonlinear system and a Duhem nonlinearity can be studied further.

- For the controller design approach, the interval of the control parameters are determined in a particular way so that the cascaded system of the linear system and the controller exhibits CCW or CW behavior. It is of interest to investigate how conservative this interval is.

- This work mainly focuses on the symmetric and rate-independent hysteresis. Since in some applications, hysteresis phenomena can be asymmetric and rate-dependent, an extension of this work is to establish results for asymmetric Duhem hysteresis operator [41, 24] and for rate-dependent one [35, 38].

- In Section 6.2.2, a case-study of CCW hysteretic actuator has been discussed, where a PID controller is applied to achieve set-point velocity tracking. We think that the stability analysis framework as discussed in Chapter 5 can be used to design a PID controller for position tracking using a CCW hysteresis operator. So far, we are unable to provide a rigorous proof for such claim despite the fact that it has been confirmed by simulation results.

- Another extension of this work is on how to generalize the construction of the storage functions for general hysteresis operator, for example, multi-dimensional hysteresis operator, such as, the hysteresis exhibited by a magnetorheological damper [10] which has two input signals: voltage and displacement, and the general semilinear Duhem operator as introduced in [35].

Appendices

.1 Reference lemmas

Consider a nonlinear system with input u, of the form

$$\dot{x} = f(x,u), \quad x(0) = x^0 \in \mathbb{R}^n, \quad f(0,0) = 0, \tag{1}$$

where $f : \mathbb{R}^n \times \mathbb{R}^m \to \mathbb{R}^n$ is locally Lipschitz.

Theorem .1.1 *[23, Theorem 3.1] Assume that* (1) *is* $0-GAS$ *and dissipative with supply function* $\sigma \in \mathcal{K}$. *Assume further that* f *and* σ *are such that the following holds.*

(C) *For each compact set* $K \subset \mathbb{R}^n$ *there exists* $c > 0$ *such that*

$$\|f(\xi,\nu)\| \leq c(1+\sigma(\|\nu\|)) \quad \forall (\xi,\nu) \in K \times \mathbb{R}^m.$$

Then (1) *is iISS with iISS gain* $\gamma = \sigma$.

Lemma .1.2 *[23, Lemma 3.2] Let* $f : \mathbb{R}^n \times \mathbb{R}^m \to \mathbb{R}^n$ *be continuous. Then, for each compact set* K, *there exists a function* $\rho_K \in \mathcal{K}_\infty$ *such that*

$$\|f(\xi,\nu) - f(\xi,0)\| \leq \rho_K(\|\nu\|) \quad \forall (\xi,\nu) \in K \times \mathbb{R}^m.$$

Lemma .1.3 *[23, Lemma 3.3] Let* $f : \mathbb{R}^n \times \mathbb{R}^m \to \mathbb{R}^n$ *be continuous and* $\sigma \in \mathcal{K}$. *Assume that (***C***) holds. Let* $w : \mathbb{R}^n \to \mathbb{R}_+$ *be continuous and such that, for some* $\alpha \in \mathcal{K}_\infty$

$$\alpha(\|\xi\|) \leq w(\xi) \quad \forall \xi \in \mathbb{R}^n.$$

Then, for every continuous function $\theta : (0,\infty) \to (0,\infty)$, *there exist a continuous function* $\delta : (0,\infty) \to (0,\infty)$ *such that*

$$\|f(\xi,\nu) - f(\xi,0)\| \leq \theta(w(\xi)) + \delta(w(\xi))\sigma(\|\nu\|), \quad \forall \xi \in \mathbb{R}^n \setminus 0 \quad \forall \nu \in \mathbb{R}^n.$$

Lemma .1.4 *[23, Lemma 3.4] Let* $f : \mathbb{R}^n \times \mathbb{R}^m \to \mathbb{R}^n$ *be locally Lipschitz with* $f(0,0) = 0$ *and* $\sigma \in \mathcal{K}$. *Assume (***C***) holds and (1) is* 0*-GAS. For every* $\epsilon > 0$, *there exists a continuous positive definite function* $\alpha : \mathbb{R}_+ \to \mathbb{R}_+$ *and a* C^1 *function* $W : \mathbb{R}^n \to \mathbb{R}_+$ *such that* $W(0) = 0$, $W(x) > 0$ *for* $x \neq 0$ *and, for all* $(\xi,\nu) \in \mathbb{R}^n \times \mathbb{R}^m$

$$\langle W(\xi), f(\xi,\nu)\rangle \leq -\alpha(\|\xi\|) + \epsilon\sigma(\|\nu\|).$$

Bibliography

[1] D. Angeli. Systems with Counterclockwise Input-Output Dynamics. *IEEE Transactions on Automatic Control*, 51(7):1130–1143, 2006.

[2] D. Angeli, E. D. Sontag, and Y. Wang. A Characterization of Integral Input to State Stability. *IEEE Transactions on Automatic Control*, 45(6):1082–1097, 2000.

[3] G. Bertotti and I. D. Mayergoyz. *The Science of Hysteresis: Mathematical Modeling and Applications*. Academic Press, San Diego, 2006.

[4] M. Brokate and J. Sprekels. *Hysteresis and Phase Transitions*. Springer Verlag, New York, 1996.

[5] L. O. Chua and S. C. Bass. A Generalized Hysteresis Model. *IEEE Trans. Circuit Theory*, 19(1):36–48, 1972.

[6] B. D. Coleman and M. L. Hodgdon. A Constitutive Relation for Rate-independent Hysteresis in Ferromagnetically Soft Materials. *International Journal of Engineering Science*, 24(6):897–919, 1986.

[7] P. Dahl. Solid Friction Damping of Mechanical Vibrations. *AIAA J.*, 14(2):1675–1682, 1976.

[8] D. Damjanovic. Hysteresis in Piezoelectric and Ferroelectric Materials. *The Science of Hysteresis*, 3, 2005.

[9] C. Canudas de Wit, H. Olsson, K. J. Astrom, and P. Lischinsky. A New Model for Control of System with Friction. *IEEE Transactions on Automatic Control*, 40(3):419–425, 1995.

[10] S. J. Dyke, B. F. Spencer, M. K. Sain, and J. D. Carlson. Modeling and Control of Magnetorheological Dampers for Seismic Response Reduction. *Smart Material*, 5(5):565–575, 1996.

[11] J. W. Ewing. Exiperimental Researches in Magnetism. *Transactions of the Royal Society of London*, 176:523–640, 1885.

[12] P. Ge and M. Jouaneh. Modeling Hysteresis in Piezoceramic Actuators. *Precision Eng.*, 17(3):211–221, 1995.

[13] R.B. Gorbet and K.A. Morris. Generalized Dissipation in Hysteretic Systems. In *Proc. IEEE Conf. Dec. Contr.*, Tampa, 1998.

[14] R.B. Gorbet, K.A. Morris, and D.W.L.Wang. Passivity-Based Stability and Control of Hysteresis in Smart Actuators. *IEEE Transaction on Control Systems Technology*, 9(1):5–16, 2001.

[15] P. Hartman. *Ordinary Differential Equations*. Birkhauser, 1982.

[16] F. Ikhouane and O. G. Bellmunt. A Limit Cycle Approach for the Parametric Identification of Hysteretic Systems. *System and Control Letters*, 57(8):663–669, 2008.

[17] F. Ikhouane and J. Rodellar. A Linear Control for Hysteretic System. *IEEE Transactions on Automatic Control*, 51(2):340–344, 2006.

[18] F. Ikhouane and J. Rodellar. *Systems with Hysteresis: Analysis, Identification and Control using the Bouc-Wen model*. Wiley, 2007.

[19] M. A. Janaideh, S. Rakheja, and C. Y. Su. An Analytical Generalized Prandtl-Ishlinskii Model Inversion for Hysteresis Compensation in Micropositioning Control. *IEEE Transactions on Mechatronics*, 16(4):734–744, 2011.

[20] B. Jayawardhana, H. Logemann, and E.P. Ryan. PID Control of Second-order Systems with Hysteresis. *International Journal of Control*, 81(8):1331–1342, 2008.

[21] B. Jayawardhana, Ruiyue Ouyang, and V. Andrieu. Dissipativity of General Duhem Hysteresis Models. In *Proc. IEEE Conf. Dec. Contr.*, Orlando, 2011.

[22] B. Jayawardhana, Ruiyue Ouyang, and V. Andrieu. Stability of Systems with Duhem Hysteresis Operator: Dissipativity Approach. *Automatica*, 48(10):2657–2662, 2012.

[23] B. Jayawardhana, E.P. Ryan, and Andrew R. Teel. Bounded-Energy-Input Convergent-State Property of Dissipative Nonlinear Systems: An iISS Approach. *IEEE Transactions on Automatic Contro*, 55(1):159–164, 2010.

[24] H. Jiang, H. Ji, J. Qiu, and Y. Chen. A Modified Prandtl-Ishlinskii Model for Modeling Asymmetric Hysteresis of Piezoelectric Actuators. *IEEE Tansactions on Automatic Control*, 57(5):1200–1210, 2010.

[25] D. C. Jiles and D. L. Atherton. Theory of Ferromagnetic Hysteresis. *Journal of Magnetism and Magnetic Material*, 61(1-2):48–60, 1986.

[26] T. Kamada, T. Fujita, T. Hatayama, T. Arikabe, N. Murai, S. Aizawa, and K. Tohyama. Active Vibration Control of Frame Structures with Smart Structures using Piezoelectric Actuators. *Journal of Smart Material and Structures*, 6(4):448–456, 1997.

[27] H.K. Khalil. *Nonlinear Systems*. Prentice-Hall 3rd edition, New Jersey, 2002.

[28] C. J. Lin and S. R. Yang. Precise Positioning of Piezo-actuated Stages using Hysteresis-observer based Control. *Mechatronics*, 16(7):417–426, 2006.

[29] H. Logemann and E. P. Ryan. Systems with Hysteresis in the Feedback Loop: Existence, Regularity and Asymptotic Behaviour of Solutions. *ESAIM Control, Optimiz. and Calculus of Variations*, 9:169–196, 2003.

[30] H. Logemann and E. P. Ryan. Asymptotic Behaviour of Nonlinear Systems. *American Mathematical Monthly*, 111(10):864–889, 2004.

[31] H. Logemann, E. P. Ryan, and I. Shvartsman. Integral Control of Infinite-dimensional Systems in the Presence of Hysteresis: an Input-Output Approach. *ESAIM-Control, Optimisation and Calculus of Variations*, 13(3):458–483, 2007.

[32] J. W. Macki, P. Nistri, and P. Zecca. Mathematical Models for Hysteresis. *SIAM*, 35(1):94–123, 1993.

[33] I. Mayergoyz. *Mathematical Models of Hysteresis and Their Applications*. Academic Press, Boston, 2003.

[34] B. Mokaberi and A. G. Requicha. Compensation of Scanner Creep and Hysteresis for AFM Nanomanipulation. *IEEE Transactions on Automation Science and Engineering*, 5(2):197–206, 2008.

[35] J. Oh and D. S. Bernstein. Semilinear Duhem Model for Rate-independent and Rate-dependent Hysteresis. *IEEE Trans. Automat. Contr.*, 50(5):631–645, 2005.

[36] R. Ouyang, V. Andrieu, and B. Jayawardhana. On the Characterization of the Duhem Hysteresis Operator with Clockwise Input-Output Dynamics. *System and Control Letters*, 62(3):286–293, 2013.

[37] R. Ouyang and B. Jayawardhana. Absolute Stability Analysis for Linear Systems with Duhem Hysteresis Operator. *submitted*.

[38] A. K. Padthe, B. Drincic, J. Oh, D. D. Rizos, S. D. Fassois, and D. S. Bernstein. Duhem Modeling of Friction-Induced Hysteresiss. *IEEE Control System Magazine*, 28(5):90–107, 2008.

[39] A. K. Padthe, J. Oh, and D. S. Bernstein. Counterclockwise Dynamics of a Rate-independent Semilinear Duhem Model. In *Proc. IEEE Conf. Dec. Contr.*, Seville, 2005.

[40] I. R. Petersen and A. Lanzon. Feedback Control of Negative-imaginary System. *IEEE Control System Magazine*, 30(5):54–72, 2010.

[41] L. Riccardi, D. Naso, B. Turchiano, H. Janocha, and D. K. Palagachev. On PID Control of Dynamic Systems with Hysteresis Using a Prandtl-Ishlinskii Model. In *Proc. IEEE American Control Conference*, Montreal, 2012.

[42] R.Ouyang and B. Jayawardhana. Stability Analysis and Controller Design for a System with Hysteresis. In *Proc. IEEE American Control Conference*, Montreal, 2012.

[43] R.Ouyang, B. Jayawardhana, and V. Andrieu. On the Robustness of Hysteretic Second-order Systems with PID: iISS Approach. In *Proc. IEEE Conference on Decision and Control*, Maui, 2012.

[44] R.V.Iyer and X. Tan. Control of Hysteretic Systems through Inverse Compensation. *IEEE Control Systems Magazine*, 29(1):83–99, 2009.

[45] C. Sakai, H. Ohmori, and A. Sano. Modeling of MR Damper with Hysteresis for Adaptive Vibration Control. In *Proc. IEEE Conf. Dec. Contr.*, Maui, 2003.

[46] J. P. La Salle. *The Stability of Dynamical Systems*. SIAM, Philadelphia, 1976.

[47] G. Song, J. Zhao, X. Zhou, and J. A. D. Abreu-Garcia. Tracking Control of a Piezoceramic Actuator with Hysteresis Compensation Using Inverse Preisach Model. *IEEE Transaction On Mechatronics*, 10(2):198–209, 2005.

[48] Z. Song, A. Lanzon, S. Patra, and I. Petersen. A Negative-Imaginary Lemma without Minimality Assumptions and Robust State-Feedbakc Synthesis for Uncertain Negative-Imaginary Systems. *System and Control Letters*, 61(12):1269–1276, 2012.

[49] E. D. Sontag. Comments on Integral Variants of ISS. *System and Control Letters*, 34(1):93–100, 1998.

[50] J. Stewart. *Calculus*. Thomson Brooks/Cole, 1999.

[51] J. Takacs. Mathematical Proof of the Definition of Anhysteretic State. *Physical B*, 372:57–60, 2006.

[52] G. Tao and P. V. Kokotovic. Adaptive Control of Systems with Unknown Output Backlash. *IEEE Transaction On Automatic Control*, 40(2):326–330, 1995.

[53] S. Tarbouriech and C. Prieur. Stability Analysis for systems with Backlash and Saturated Actuator. *Nonlinear Control System*, 7(1):669–674, 2007.

[54] S. Tarbouriech, C. Prieur, and I. Queinnec. Stability Analysis for Linear systems with Input Backlash through Sufficient LMI Conditions. *Automatica*, 46(11):1911–1915, 2010.

[55] A. R. Teel and L. Praly. A Smooth Lyapunov Function from A Class-KL Estimate Involving two Positive Semidefinite functions. *ESAIM: Contr., Opt. and Cal. of Variations*, 5:313–367, 2000.

[56] H.L. Trentelman and J.C.Willems. Every Storage Functions is a State Function. *Systems and Control Letters*, 32:249–259, 1997.

[57] S. Valadkhan, K. Morris, and A. Khajepour. Stability and Robust Position Control of Hysteretic Systems. *International Journal of Robust and Nonlinear Control*, 20(4):460–471, 2009.

[58] P.J. van Bree, C.M.M. van Lierop, and P.P.J. van den Bosch. Control-oriented Hysteresis Models for Magnetic Electron Lenses. *IEEE Trans. Magnet.*, 45(11):5235–5238, 2009.

[59] A.J. van der Schaft. *$\mathcal{L}_2$-Gain and Passivity Techniques in Nonlinear Control*. Springer-Verlag, London, 2000.

[60] A.J. van der Schaft. Positive Feedback Interconnection of Hamiltonian Systems. In *Proc. IEEE Conf. Dec. Contr.*, Orlando, 2011.

[61] A. Visintin. *Differential Models of Hysteresis*. Springer-Verlag, New York, 1994.

[62] J. C. Willems. Dissipative Dynamical Systems. Part I: General Theory. Part II: Linear Systems with Quadratic Supply Rates. *Arch. Rat. Mech. Anal.*, 45(5):321–393, 1972.

[63] J. Zhou, C. Zhang, and C. Wen. Robust Adaptive Output Control of Uncertain Nonlinear Plants with Unknown Backlash Nonlinearity. *IEEE Transaction On Automatic Control*, 52(3):503–509, 2007.

Summary

Hysteresis is a nonlinear phenomenon that presents in many physical systems, such as piezo-actuator, magneto-rheological damper, ferromagnetic material and friction-induced mechanical systems. The existence of hysteresis in physical systems has been shown to affect the performance and even the stability of the system. Therefore, a proper handling by a controller is needed for a system contains hysteresis.

To describe the hysteresis phenomenon in different systems, many mathematical models have been proposed. This thesis focuses on one class of hysteresis model, namely, the **Duhem hysteresis operator**, which has been successfully used to represent the hysteresis phenomena in many physical systems.

In the first part of this thesis, two dissipativity properties of the Duhem hysteresis operator are investigated: the Duhem hysteresis operator with counterclockwise input-output behavior **(CCW I/O behavior)** and the Duhem hysteresis operator with clockwise input-output behavior **(CW I/O behavior)**. We have provided sufficient conditions on the Duhem operator such that it is CCW (or CW). In particular, we show the dissipativity property of the CCW (or CW) Duhem hysteresis operator by constructing an explicit storage function satisfying the CCW (or CW) dissipation inequality. Moreover, the relations between the constructed storage functions to the available storage functions used in the classical dissipation theory have also been discussed.

Based on the dissipativity property of the Duhem hysteresis operator and motivated by real applications, we investigate the stability of a feedback interconnection between a linear system and a Duhem hysteresis operator. For solving this absolute stability problem, sufficient conditions have been presented based on the counterclockwise (CCW) or clockwise (CW) input-output property of the linear system and the Duhem operator. Furthermore, we have also extended the results to the case where the Duhem operator is feedback interconnected to a nonlinear system.

As an application to the absolute stability analysis, we study the control design for a linear system interconnected with a hysteretic actuator (or sensor). Furthermore, we have studied the robustness property of a second-order linear plant controlled by a proportional, integral and derivative (PID) controller with a hysteretic actuator. The hysteretic actuator is modeled by a Duhem model which exhibits: (i) clockwise (CW) input-output (I/O) dynamics (such as the Dahl model, LuGre model and Maxwell-Slip model, which have been used to describe hysteresis phenomena in mechanical friction); (ii) counter-clockwise(CCW) input-output (I/O) dynamics(such as the Jiles-Atherton model, Coleman model and Bouc-Wen model which have been used to describe the hysteresis phenomena in piezo-actuator). Based on our absolute stability results, we provide sufficient conditions on the controller gains that depend on the plant parameters such that the closed-loop system is globally asymptotic stable with respect to a set. The robustness of the closed-loop system with respect to the measurement noise is also given, using the *integral* input-to-state stability (*i*ISS) concept.

Finally, experiments on a piezo-actuated stage has been conducted to validate our stability and controller design approach which are presented in the first six chapters.

Samenvatting

Hysterese is een niet-lineair verschijnsel dat in veel fysische systemenaanwezig is, waaronder piëzo-actuatoren, magnetisch-reologische dempers, ferromagnetisch materiaal en mechanische systemen onderhevig aan wrijving. Het is aangetoond dat de aanwezigheid van hysterese in fysische systemen invloed heeft op de prestatie en zelfs de stabiliteit van het systeem. Daarom is een adequate aanpak met behulp van een regelaar nodig voor een systeem met hysterese.

Om het hysterese verschijnsel te beschrijven in verschillende soorten systemen, zijn vele wiskundige modellen voorgesteld. Dit proefschrift richt zich op een specifieke klasse onder de hysterese modellen, de zogenaamde Duhem hysterese operator, welke succesvol is gebruikt om hysterese te beschrijven in veel fysische systemen.

In het eerste deel van dit proefschrift worden twee dissipativiteits eigenschappen van de Duhem hysterese operator bestudeerd: de Duhem hysterese operator met tegenwijzerzin ingang-uitgang gedrag (TWZ I/U gedrag) en de Duhem hysterese operator met wijzerzin ingang-uitgang gedrag (WZ I/U gedrag). We hebben een voldoende voorwaarde verstrekt voor de Duhem operator wanneer hij TWZ (of WZ) is. In het bijzonder laten we de dissipativiteits eigenschap van de TWZ (of WZ) Duhem hysterese operator zien, door een expliciete opslagfunctie te construeren die aan de TWZ (of WZ) dissipatie ongelijkheid voldoet. Bovendien worden de relaties tussen de construeerde opslagfuncties en de beschikbare opslagfuncties uit klassieke dissipatie theorie besproken.

Op basis van de dissipativiteits eigenschap van de Duhem hysterese operator en gemotiveerd door reële toepassingen onderzoeken we de stabiliteit van een terugkoppelingsverbinding tussen een lineair systeem en een Duhem hysterese operator. Voor de oplossing van dit absolute stabiliteit probleem worden voldoende voorwaarden gepresenteerd op basis van de tegenwijzerzin (TWZ) of wijzerzin (WZ)

ingang-uitgang eigenschap van het lineaire systeem en de Duhem operator. Bovendien hebben we de resultaten uitgebreid voor het geval waar de Duhem operator via terugkoppeling is verbonden met een niet-lineair systeem.

Als een mogelijke toepassing van deze absolute stabiliteit analyse, bestuderen we het regelaar ontwerp voor een lineair systeem verbonden met een hysterese actuator (of sensor). Daarnaast hebben we de robuustheid van een tweede orde lineaire installatie, aangestuurd door een proportionele, integrerende, differentiërende (PID) regelaar met een hysteretische actuator bestudeerd. De hysteretische actuator is gemodelleerd als een Duhem model met: (i) wijzerzin (WZ) ingang-uitgang (I/U) dynamica (zoals het Dahl model, LuGre model en Maxwell-Slip model, welke gebruikt worden voor het beschrijven van hysterese verschijnselen ten gevolge van mechanische wrijving); of (ii) tegenwijzerzin (TWZ) ingang-uitgang (I/U) dynamica (zoals het Jiles-Atherton model, Coleman model en Bouc-Wen model, welke gebruikt worden om de hysterese verschijnselen in piëzo-actuatoren te beschrijven). Op basis van onze absolute stabiliteit resultaten, verstrekken we voldoende voorwaarden voor de regelaar constanten, die afhangen van de installatie parameters, zodanig dat het gesloten lus systeem globaal asymptotisch stabiel is ten aanzien van een verzameling. De robuustheid van het gesloten lus systeem ten aanzien van meet ruis is ook gegeven, gebruik makend van het integraal ingang-naar-toestand stabiliteit (iITS) concept.

Tot slot zijn er experimenten uitgevoerd met een piëzo-aangestuurd platform om onze stabiliteit en regelaar ontwerp methode, die gepresenteerd is in de eerste zes hoofdstukken, te valideren.